

Mining S-PLUS for Metal-Poor Stars in the Milky Way

2 VINICIUS M. PLACCO ,¹ FELIPE ALMEIDA-FERNANDES ,^{1,2} ANKE ARENTSEN ,³ YOUNG SUN LEE,⁴
3 WILLIAM SCHOENELL ,⁵ TIAGO RIBEIRO,⁶ ANTONIO KANAAN,⁷ AND CLÁUDIA MENDES DE OLIVEIRA²

4 ¹ NSF's NOIRLab, 950 N. Cherry Ave., Tucson, AZ 85719, USA

5 ² Departamento de Astronomia, Instituto de Astronomia, Geofísica e Ciências Atmosféricas da USP, Cidade
6 Universitária, 05508-900, São Paulo, SP, Brazil

7 ³ Université de Strasbourg, CNRS, Observatoire Astronomique de Strasbourg, UMR 7550, F-67000 Strasbourg, France

8 ⁴ Department of Astronomy and Space Science, Chungnam National University, Daejeon 34134, South Korea

9 ⁵ GMTO Corporation 465 N. Halstead Street, Suite 250 Pasadena, CA 91107, USA

10 ⁶ Rubin Observatory Project Office, 950 N. Cherry Ave., Tucson, AZ 85719, USA

11 ⁷ Departamento de Física, Universidade Federal de Santa Catarina, Florianópolis, SC 88040-900, Brazil

ABSTRACT

This work presents the medium-resolution ($R \sim 1,500$) spectroscopic follow-up of 516 low-metallicity star candidates from the Southern Photometric Local Universe Survey (S-PLUS). The objects were selected from narrow-band photometry, taking advantage of the metallicity-sensitive S-PLUS colors. The follow-up observations were conducted with the Blanco and Gemini South telescopes, using the COSMOS and GMOS spectrographs, respectively. The stellar atmospheric parameters (T_{eff} , $\log g$, and $[\text{Fe}/\text{H}]$), as well as carbon and α -element abundances, were calculated for the program stars in order to assess the efficacy of the color selection. Results show that $92^{+2}_{-3}\%$ of the observed stars have $[\text{Fe}/\text{H}] \leq -1.0$, $83^{+3}_{-4}\%$ have $[\text{Fe}/\text{H}] \leq -2.0$, and $15^{+3}_{-3}\%$ have $[\text{Fe}/\text{H}] \leq -3.0$, including two ultra metal-poor stars ($[\text{Fe}/\text{H}] \leq -4.0$). The sample also includes 68 Carbon-Enhanced Metal-Poor (CEMP) stars, with 4 stars belonging to Group-III. Based on the calculated metallicities, further S-PLUS color cuts are proposed, which can increase the fractions of stars with $[\text{Fe}/\text{H}] \leq -1.0$ and ≤ -2.0 to 98% and 88%, respectively. Such high success rates enable targeted high-resolution spectroscopic follow-up efforts, as well as provide selection criteria for fiber-fed multiplex spectroscopic surveys.

Keywords: Narrow band photometry (1088), Metallicity (1031), Stellar atmospheres (1584), Chemical abundances (224)

1. INTRODUCTION

There is a wealth of information contained in the catalogs of stars (Allende Prieto 2016), which are simply the difference in integrated fluxes on two given photometric bandpasses. The first determinations of effective temperatures from photometry date back to the early 20th century (Greaves et al. 1929) and since then extensive work has been conducted to characterize and calibrate temperature scales in optical (Bessell 1979) and near-infrared (Alonso et al. 1996, 1999; Casagrande et al. 2010) systems, just to mention a few. The same applies

³⁹ to estimating the metallicity ($[\text{Fe}/\text{H}]^{\text{1}}$) of stellar sources ⁴⁰ from photometry. Many studies in the literature relied ⁴¹ on the calibration of the ultra-violet excess for stellar ⁴² sources, which is heavily dependent on the metallicity ⁴³ (Wallerstein 1964; Schuster & Nissen 1989; Bonifacio ⁴⁴ et al. 2000), but there are others that take advantage ⁴⁵ of infrared colors, depending on the stellar population ⁴⁶ (e.g. cold brown dwarfs - Leggett et al. 2010).

⁴⁷ More recently, large-scale surveys have taken these ⁴⁸ photometric parameter determination strategies to the ⁴⁹ next level by building databases with millions of ⁵⁰ spectroscopically-observed objects. Two such examples

Corresponding author: Vinicius M. Placco
vinicius.placco@noirlab.edu

¹ $[\text{A}/\text{B}] = \log(N_A/N_B)_{\star} - \log(N_A/N_B)_{\odot}$, where N is the number density of atoms of a given element in the star (\star) and the Sun (\odot), respectively.

are the Sloan Digital Sky Survey (SDSS; York et al. 2000) in the northern hemisphere and the SkyMapper Sky Survey (SMSS; Wolf et al. 2018) in the southern hemisphere. Both of these surveys conducted separate sub-surveys aiming to perform medium-resolution ($R \sim 1,500$) spectroscopic follow-up of stars in the Milky Way Galaxy: the Sloan Extension for Galactic Understanding and Exploration (SEGUE-1; Yanny et al. 2009) and SEGUE-2 (Rockosi et al. 2022), and the AAOmega Evolution of Galactic Structure (AEGIS; Keller et al. 2007; Yoon et al. 2018, among others). These not only served as the basis for a number of statistical studies of stellar populations in the Milky Way (Ivezić et al. 2012), but also as prime datasets for high-resolution spectroscopic follow-up and calibration of photometric parameter determinations.

The SDSS makes use of the Sloan Photometric System, which comprises of five colors ($u'/g'/r'/i'/z'$) that cover the region between 3,000 Å and 11,000 Å into five essentially nonoverlapping passbands (Fukugita et al. 1996). Ivezić et al. (2008) were able to determine temperatures (with typical uncertainties of ~ 100 K) and metallicities (with uncertainties of 0.2 dex or better for $-2.0 \leq [\text{Fe}/\text{H}] \leq -0.5$) for over 2 million F/G stars in the Milky Way. One of the limitations on the low-metallicity end is due to the broadness of the u filter, which loses its metallicity sensitivity, hampering efforts to extend the determinations to $[\text{Fe}/\text{H}] \leq -2.5$. In two follow-up studies from the work of Ivezić et al. (2008), An et al. (2013) and An et al. (2015) re-determined the photometric metallicities and the metallicity distribution functions (MDFs) in the Galactic halo from SDSS photometry. These efforts relied on improved photometry from the Stripe 82 region of SDSS and were able to increase the metallicity range of the photometric estimates down to $[\text{Fe}/\text{H}] \sim -2.5$.

The SkyMapper filter set design was optimized for stellar astrophysics, in particular the study of stellar populations in the Milky Way (Keller et al. 2007). It is composed of six filters: $u/v/g/r/i/z$ (Bessell et al. 2011). The u ($\lambda_{\text{cen}} = 349$ nm) and v ($\lambda_{\text{cen}} = 384$ nm) filters are a two-filter version of the SDSS u' , providing additional photometric sensitivity. The SkyMapper Data Release 1 (DR1; Wolf et al. 2018) has been extensively used to determine photometric stellar atmospheric parameters and select low-metallicity stars for spectroscopic follow-up. Casagrande et al. (2019), using the SkyMapper DR1, were able to determine temperatures and metallicities with uncertainties better than ~ 100 K and ~ 0.2 dex for $[\text{Fe}/\text{H}] \geq -2.0$, respectively. A similar study by Huang et al. (2019), limited to red giant stars, were able to reach slightly lower uncertainties (~ 80 K

and ~ 0.18 dex), however with the parameter space still limited to $[\text{Fe}/\text{H}] \geq -2.0$, with only a few objects with metallicities below this threshold. Chiti et al. (2021a) extended the low-metallicity limit to $[\text{Fe}/\text{H}] < -2.5$ with $\sigma \sim 0.31$ dex, with the goal of constructing the photometric MDF of the Milky Way (Chiti et al. 2021b). In terms of spectroscopic follow-up, Da Costa et al. (2019) presents 2,618 candidates selected to have photometric $[\text{Fe}/\text{H}] < -2.0$ from their metallicity-sensitive diagram. Results show that over 40% of the observed stars have $[\text{Fe}/\text{H}] \leq -2.75$.

The Pristine Survey (Starkenburg et al. 2017) has been successfully using narrow-band photometry on the metallicity sensitive Ca II H and K absorption features (in addition to SDSS broad-band g and i) to search for low-metallicity stars in the Galaxy from the Northern hemisphere. The ~ 100 Å wide narrow-band filter has a larger predictive power than the broader band counterparts of SDSS and SkyMapper and is able to successfully predict metallicities in the $[\text{Fe}/\text{H}] \sim -3.0$ regime (Youakim et al. 2017). The results of a three-year medium-resolution spectroscopic follow-up campaign show that $\sim 70\%$ of the 1,007 stars observed have $[\text{Fe}/\text{H}] < -2.0$ and $\sim 9\%$ have $[\text{Fe}/\text{H}] < -3.0$ (Aguado et al. 2019)².

The Javalambre Photometric Local Universe Survey (J-PLUS; Cenarro et al. 2019) and the Southern Photometric Local Universe Survey (S-PLUS; Mendes de Oliveira et al. 2019) have a unique 12 broad- and narrow-band filter set, consisting of four SDSS (g, r, i, z), one modified SDSS u , and seven narrow-band filters. The narrow-band filters were designed to probe very specific regions in the optical wavelength regime and accommodate a wide variety of science cases, from high-precision photometric redshifts (Molino et al. 2019) to the identification of low-metallicity stars in the Galactic halo (Galarza et al. 2022). The names and key absorption features sampled by the narrow-band filters are: $J0378 - [\text{O II}]$; $J0395 - \text{Ca II H+K}$; $J0410 - \text{H}\delta$; $J0430 - G$ band; $J0515 - \text{Mg } b$ triplet; $J0660 - \text{H}\alpha$; and $J0861 - \text{Ca}$ triplet. It is worth pointing out that the $J0395$ filter shares a similar central wavelength and width as the Pristine narrow-band filter. However, J-PLUS and S-PLUS have the advantage of also performing narrow band photometry in the Mg b triplet ($J0515$) and Ca ($J0861$) triplet regions, which are also useful for metallicity and surface gravity determinations (Majew-

² The Pristine Survey has individual photometric metallicities to compare to the spectroscopic determinations. For the work of Aguado et al. 2019, 23% of the stars with photometric $[\text{Fe}/\text{H}] < -3.0$ also have spectroscopic $[\text{Fe}/\text{H}] < -3.0$.

ski et al. 2000). Whitten et al. (2019) used J-PLUS photometry to predict T_{eff} and [Fe/H] using artificial neural networks and reached uncertainties of ~ 91 K and ~ 0.25 dex for stars in the $-3.0 \lesssim [\text{Fe}/\text{H}] \leq -0.5$. In a follow-up study using S-PLUS, Whitten et al. (2021) were able to estimate the first photometric carbon abundances for a sample of over 50,000 stars, with uncertainties better than ~ 0.35 dex. Finally, Galarza et al. (2022) used J-PLUS photometry to predict stellar atmospheric parameters from machine learning techniques, reaching a success rate of 64% in identifying stars with $[\text{Fe}/\text{H}] < -2.5$, confirmed by medium-resolution spectroscopic follow-up.

The possibility of accurately determining stellar atmospheric parameters and chemical abundances for large datasets drawn from photometry, and especially for a wide range of metallicities, is fundamental in the context of studying low-metallicity stars. Very Metal-Poor (VMP - $[\text{Fe}/\text{H}] < -2.0$; Beers & Christlieb 2005) stars are the “local” observational probes that allow astronomers to address questions at cosmological scales (Bromm & Larson 2004). The research that was once limited to individual stars (Carney & Peterson 1981) has been expanded to much larger samples, allowing the investigation of relations such as the carbon-enhancement observed in metal-poor stars (Lucatello et al. 2006; Aoki et al. 2007), the possible origins of the subclasses within this group (Masseron et al. 2010), their role in the chemical evolution of the early universe (Woosley & Weaver 1995; Heger & Woosley 2002; Meynet et al. 2006; Norris et al. 2013; Frebel & Norris 2015), and the connection between the Galactic halo and low-mass dwarf galaxies accreted within the context of hierarchical assembly (Yuan et al. 2020; Limberg et al. 2021a; Shank et al. 2022, among others). Growing statistics on VMP stars narrow error bars and broadens our understanding of the early stages of the chemical evolution of the Universe.

This article reports on the medium-resolution ($R \sim 1,500$) spectroscopic follow-up of low-metallicity star candidates selected from the S-PLUS Data Release 3 (DR3). The main goal is to assess whether the metallicity-sensitive S-PLUS colors are effective in selecting metal-poor stars for spectroscopic follow-up. Section 2 describes the medium-resolution spectroscopic observations, followed by the estimates of the stellar atmospheric parameters and abundances in Section 3. In Section 4 we analyze the sensitivity of the narrow-band photometry to the stellar parameters, the effectiveness of the S-PLUS color selection for low-metallicity stars, the distribution of carbon and α -element abundances, and further improvements in the color selection. Our

conclusions and prospects for future work are provided in Section 5.

2. TARGET SELECTION AND OBSERVATIONS

2.1. The S-PLUS Data Release 3

For this work, the S-PLUS Data Release 3 (DR3; Buzzo et al., in prep) was used. The data structure in this data release, as well as the photometric extraction and calibration process, are the same as the S-PLUS Data Release 2 (DR2; Almeida-Fernandes et al. 2022). The only difference is the addition of observations in the South Galactic Hemisphere for DR3. At the time the candidates for this work were selected, the catalogs were only available internally to the collaboration and are now publicly available through the S-PLUS Cloud³ service.

The first step in the data selection was to apply a series of restrictions in the DR3 database, mostly related to the quality of the photometry, probability of being a stellar source, and a color range suitable to study low-metallicity stars. Then, metal-poor star candidates were chosen for the medium-resolution spectroscopic campaign, based on their location on a metallicity-dependent color-color diagram, as described below. The following restrictions were applied to the DR3 database:

- $\text{CLASS_STAR} \geq 0.95$: sources having a high probability of being a star;
- $\text{gSDSS} \leq 17.5$: brightness limit for spectroscopic follow-up within reasonable exposure times;
- $\text{nDet_magPStotal} = 12$: only sources with all twelve magnitudes measured;
- $(\text{gSDSS}-\text{iSDSS}) \in [0.2:1.6]$: color window to remove possible contamination from white dwarfs and A-type stars on the blue end and objects cooler than $T_{\text{eff}} \sim 4000$ K on the red end;
- $(\text{J0410}-\text{J0861}) \in [0.3:3.5]$: same as above using a narrow-band color;
- **Total:** 820,829 stars.

The S-PLUS magnitudes used throughout this work are the 3-arcsec aperture corrected values, labelled PStotal . The left panel of Figure 1 shows the density of the selected stars in a color-color diagram. The color $(\text{J0395}-\text{J0660})-2 \times (\text{g}-\text{i})$ was chosen based on the work of Starkenburg et al. (2017) for the Pristine Survey, which is proven to have a strong [Fe/H] dependency. The g filter was replaced with J0660 as a temperature sensitive feature and the $-2 \times (\text{g}-\text{i})$ was

³ <https://splus.cloud/>

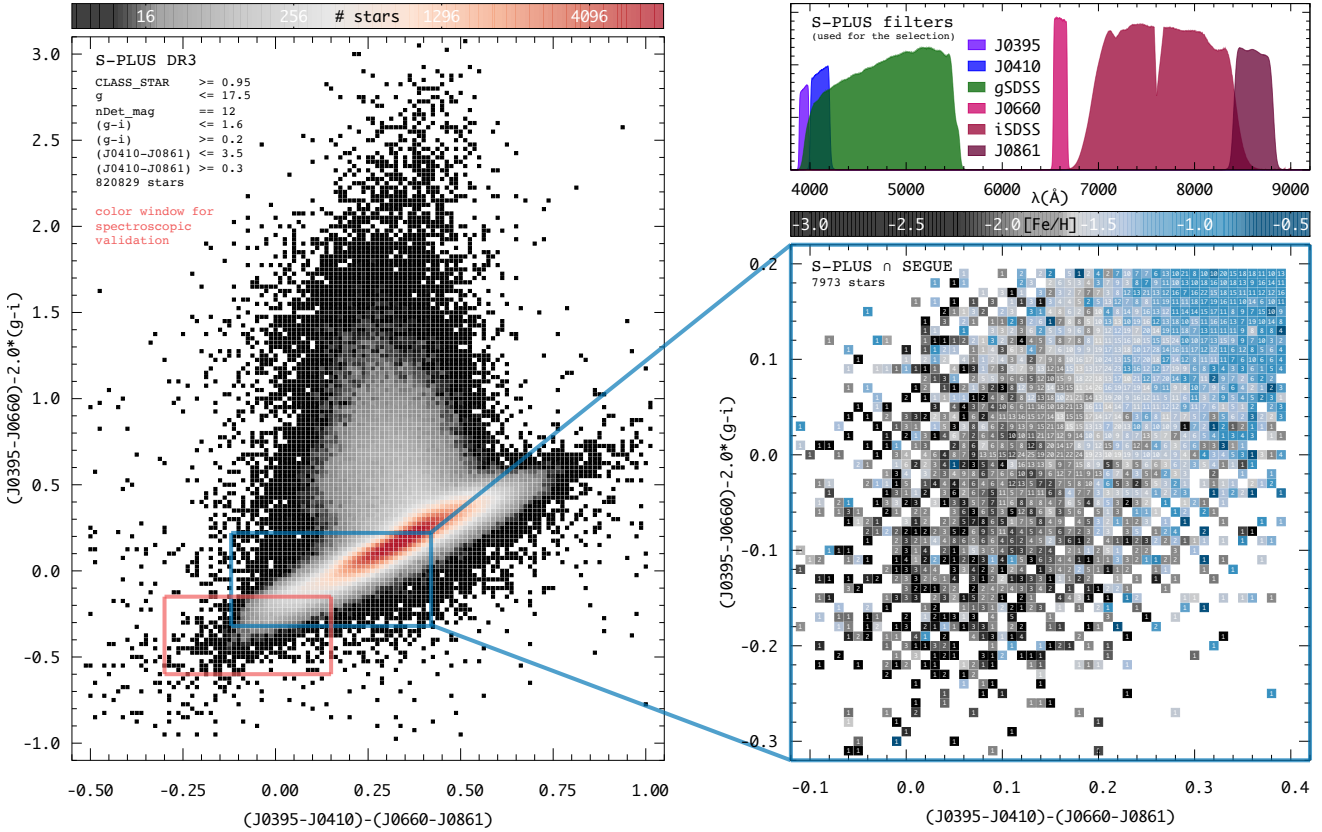


Figure 1. Left panel: stellar density for the selected S-PLUS DR3 sample in a color-color diagram. The red box outlines the color window for the spectroscopic follow-up (see text for details). The inset (bottom right panel) shows the cross-match with the SDSS/SEGUE spectroscopic database, color-coded by the average metallicity in each bin. The number of stars in each bin is also shown. Top right panel: S-PLUS transmission curves for the six narrow-band and broad band filters used in this selection.

used to re-shape the color-color diagram. In the x-axis, both Starkenburg et al. (2017) and Da Costa et al. (2019) employ the $(g-i)_0$ color. Due to the dependency of the Ca II K line strength with temperature, there is a color range, roughly $(g-i)_0 \lesssim 0.3$, where the metallicity-dependent color difference between a star with $[Fe/H] = -2.0$ and -4.0 becomes smaller than the typical uncertainties in the photometry. In an attempt to address this degeneracy, this work employs the $(J0395-J0410)-(J0660-J0861)$ combination, that uses the filters centered on H δ and H α and provides better temperature sensitivity. This temperature-dependent metallicity color index should increase the success rate of finding metal-poor stars. The transmission curves for the six S-PLUS filters used in this selection are shown in the top right panel of Figure 1.

The catalog generated from the S-PLUS DR3 selection above was cross-matched with the SDSS/SEGUE spectroscopic database. From that cross-match, sources with $CLASS == QSO$, $\sigma_{Teff} > 200$ K, and $S/N < 20$ were excluded. The lower right panel of Figure 1 shows a section of the color-color diagram, with each 0.01×0.01 bin colored by its average $[Fe/H]$ value from the spectroscopic data.

Also shown in each bin are the number of stars used to calculate the average. The metallicity dependency is very evident in both axes and allows for an improved selection of potential metal-poor stars for spectroscopic follow-up.

Figure 2 further explores this color space. Each panel shows a different metallicity regime, color coded by the fraction of stars in each 0.05×0.05 bin. The number of stars in each bin is also shown. As an example, the bin centered on $(0.0, -0.1)$ has 1 star with $[Fe/H] > -1.0$ ($\sim 2\%$), 19 stars with $-2.0 < [Fe/H] \leq -1.0$ ($\sim 46\%$), and 21 stars with $[Fe/H] \leq -2.0$ ($\sim 52\%$). For the spectroscopic follow-up, from the right panel, a cut was made where most bins have at least a 50% fraction of $[Fe/H] \leq -2.0$ star. Limits were also placed on the blue end of each color, to avoid sources with potentially spurious colors. The final color window for the selection of targets for the spectroscopic follow-up was defined as: $(J0395-J0410)-(J0660-J0861) \in [-0.30 : 0.15]$ and $(J0395-J0660)-2 \times (g-i) \in [-0.60 : -0.15]$ (see red-colored box in the left panel of Figure 1). Within this window, targets were chosen based on their bright-

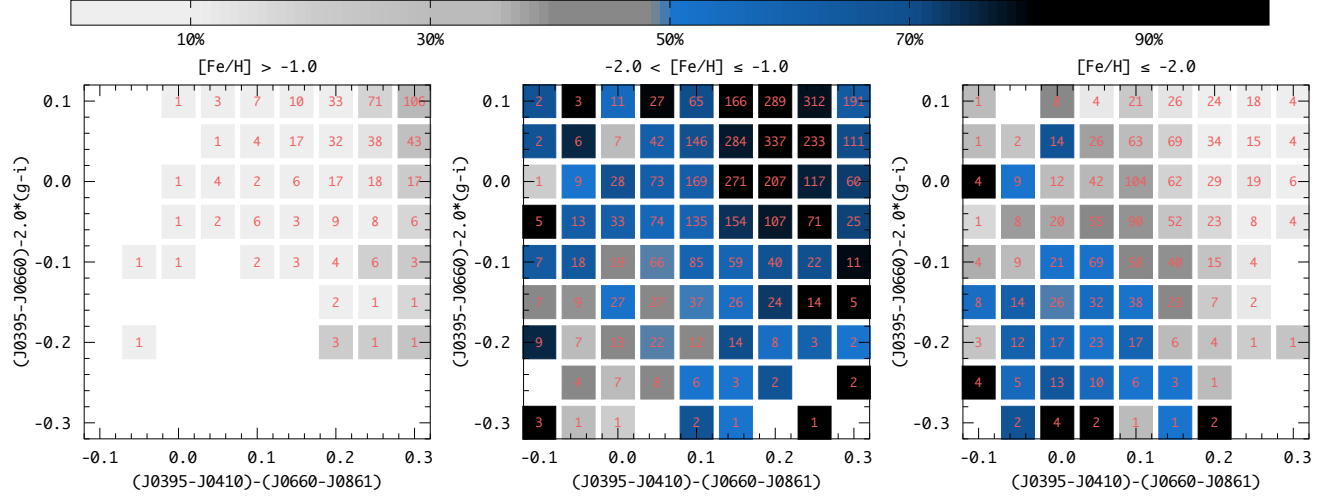


Figure 2. Color-color diagram for three different $[Fe/H]$ regimes. The bins in each panel are color-coded by the fraction of stars with an average metallicity in a given range. The number of stars in each bin is also shown.

ness and observability at a given telescope. Details are provided in the next section.

2.2. Medium-Resolution Spectroscopy

The spectroscopic follow-up campaign was conducted in semesters 2019A, 2019B, 2020A, 2021A, and 2022A. Data were collected for 516 metal-poor star candidates, selected from their S-PLUS photometry, described above. The stars were observed with two different telescope/instrument setups: Blanco/COSMOS and Gemini South/GMOS-S.

The distribution (in Galactic coordinates) of the observed stars is shown in the top panel of Figure 3, color-coded by telescope. The point size is proportional to the g magnitude of each target. The dust map traces the Galactic plane and was constructed from the Schlegel et al. (1998) reddening values. Also shown (gray solid line) is the celestial equator. The apparent grouping of the stars is due to the S-PLUS observing strategy, which started with the STRIPE82 (equatorial) region (DR1), then moving towards halo fields at lower southern declinations (DR2 and DR3). Note that most of the faint targets were observed with the Gemini telescope, due to its larger aperture. Table 1 lists the name, coordinates, and observing details for each star. The bottom panels of Figure 3 show the magnitude distribution of the observed targets in all the 12 S-PLUS filters. Each panel displays the transmission curve for the filters with their central wavelength (in Å). Table 2 lists all the magnitude values (and errors) for the observed stars, taken from the S-PLUS DR3 catalog.

For consistency in the spectroscopic observations, grating/slit combinations were chosen to yield a resolving power $R \sim 1,200 - 1,800$, and exposure times were set to reach a signal-to-noise ratio of at least $S/N \sim 30$.

per pixel at the Ca II K line (3933.3\AA). Calibration frames included arc-lamp exposures, bias frames, and quartz flats. Specific details of each instrument and data reduction are given below.

CTIO Blanco Telescope—A total of 384 stars were observed with the Víctor M. Blanco 4-meter Telescope, located at the Cerro Tololo Inter American Observatory, using the COSMOS (Cerro Tololo Ohio State Multi-Object Spectrograph; Martini et al. 2014) instrument. Observations were conducted in remote visitor mode in October 2019, December 2020, January 2021, and April 2022 (2019B-0069, 2020A-0032, and 2022A-210002). The exposure times ranged from 90 to 1800 seconds, with a total of 57.96 hours on target. The setup included a $600\text{ }1\text{ mm}^{-1}$ grating (blue setting) and a $1''.5$ slit, resulting in a wavelength coverage in the range $[3600:6300]\text{\AA}$ at resolving power $R \sim 1,800$. All tasks related to spectral reduction, extraction, and wavelength calibration were performed using standard IRAF⁴ packages.

Gemini South Telescope—132 stars were observed with the 8.1 m Gemini South telescope and the GMOS (Gemini Multi-Object Spectrographs; Davies et al. 1997; Gielen et al. 2016) instrument. Observations were conducted in the “Poor Weather” queue mode in April-June 2019, June-July 2021, and April-May 2022 (GS-2019A-Q-408, GS-2021A-Q-419, and GS-2022A-Q-406). The exposure times ranged from 210 to 1800 seconds, with a total of 43.80 hours on target. The $B600\text{ }1\text{ mm}^{-1}$ grating (G5323) and a $1''.5$ slit were used with a 2×2 binning, resulting in a wavelength coverage in the range

⁴ <https://iraf-community.github.io/>.

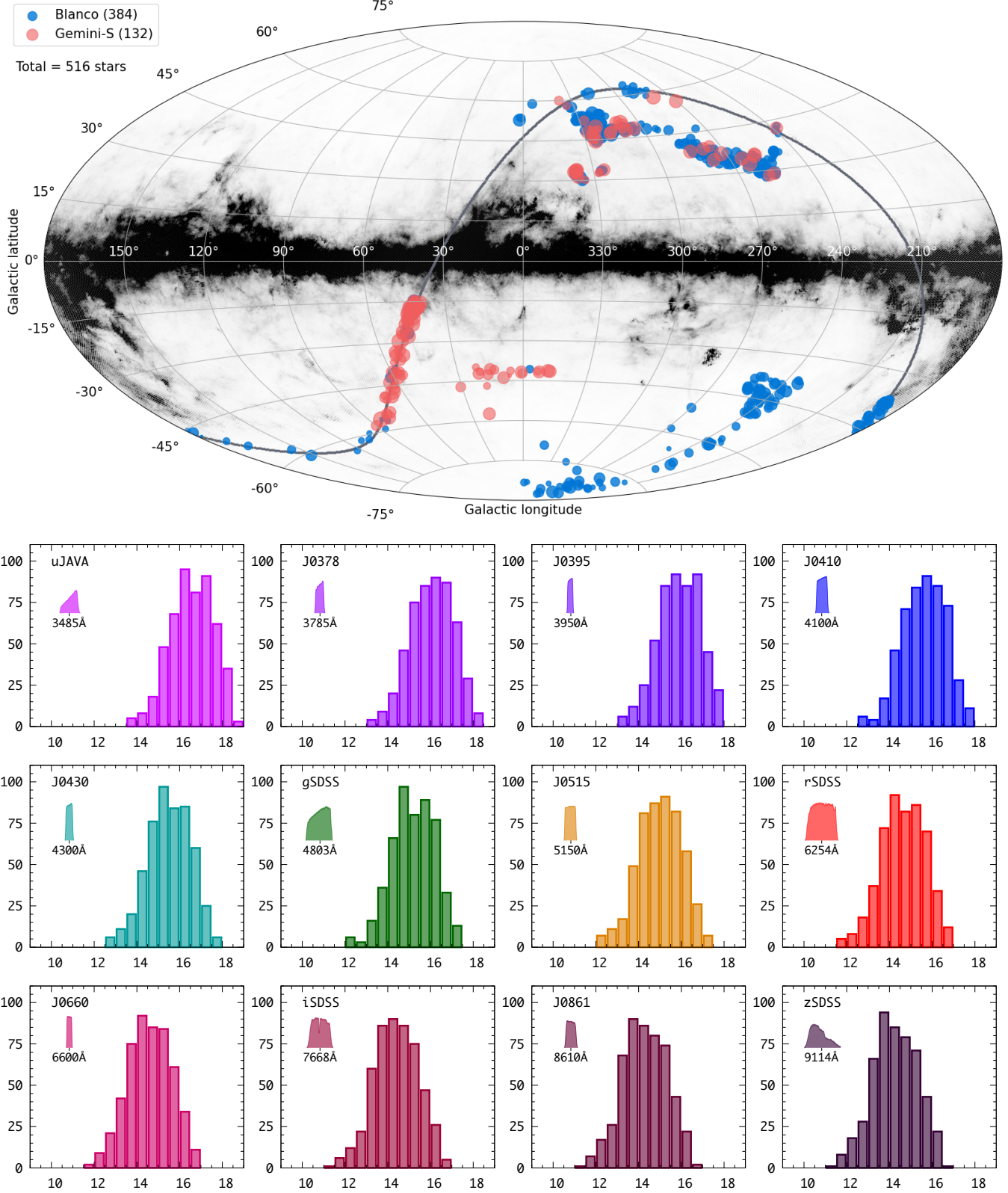


Figure 3. Top: Galactic coordinates for the stars observed in this work, color-coded by telescope. The point size is proportional to the g magnitude. The gray line traces the celestial equator. The dust map uses reddening values from Schlegel et al. (1998). Bottom: Magnitude distribution of the observed stars in the 12-filter system of S-PLUS. Each panel also shows the name, transmission curve, and central wavelength (in Å) for the filters.

[3200:5800] Å at resolving power $R \sim 1,200$. The complete data reduction was performed using the DRAGONS⁵ software package (Labrie et al. 2019).

360 3. STELLAR PARAMETERS AND CHEMICAL 361 ABUNDANCES

362 The determinations of stellar atmospheric parameters
363 (T_{eff} , $\log g$, and $[\text{Fe}/\text{H}]$), carbonicity ($[\text{C}/\text{Fe}]$), and α -
364 to-iron ratios ($[\alpha/\text{Fe}]$) for the stars observed as part of
365 spectroscopic follow-up were made using the n-SSPP
366 (Beers et al. 2014, 2017), which is a modified version
367 of the SEGUE Stellar Parameter Pipeline (SSPP; Lee
368 et al. 2008a,b, 2011, 2013). The software uses photomet-
369 ric and spectroscopic information to calculate the atmo-
370 spheric parameters based on spectral line indices, pho-
371 tometric calibrations, and synthetic spectra matching.
372 The $[\text{C}/\text{Fe}]$ and $[\alpha/\text{Fe}]$ are estimated from the strength
373 of the CH G-band molecular feature at ~ 4300 Å and
374 the Mg I triplet at 5150–5200 Å, respectively. The n-
375 SSPP was able to estimate T_{eff} , $\log g$, and $[\text{Fe}/\text{H}]$ for
376 all the 492 stars observed as part of this work. The
377 $[\text{C}/\text{Fe}]$ and $[\alpha/\text{Fe}]$ abundance ratios were estimated for
378 450⁶ and 479 stars, respectively. The average uncertain-
379 ties for this sample are 70 K for T_{eff} , 0.24 dex for $\log g$,
380 0.11 dex for $[\text{Fe}/\text{H}]$, and 0.21 dex for $[\text{C}/\text{Fe}]$ and $[\alpha/\text{Fe}]$.

381 The adopted atmospheric parameters and abundance
382 ratios for the sample are listed in Table 3. Also in-
383 cluded in the table are the corrections for carbon abun-
384 dances, based on the stellar-evolution models presented
385 in Placco et al. (2014), the final $[\text{C}/\text{Fe}]$, and $A(\text{C})$ ⁷, the
386 latter two including the corrections. Figure 4 shows the
387 $\log g$ vs. T_{eff} diagram for the sample, compared with
388 the YY isochrones for different metallicities (12 Gyr,
389 0.8 M_{\odot} , $[\alpha/\text{Fe}] = +0.4$; Demarque et al. 2004). The
390 point sizes are inversely proportional to the $[\text{Fe}/\text{H}]$ val-
391 ues and typical uncertainties are also shown. Based on
392 the color selection from the S-PLUS filters, it is expected
393 that the majority of the stars ($\sim 78\%$) have tempera-
394 tures in the [4700:5700] K range. There is an overall
395 agreement between observations and the isochrones for
396 $[\text{Fe}/\text{H}] = -2.0$ and -3.0 , apart from a small systematic
397 offset of $\sim 50 - 100$ K for the spectroscopic tempera-
398 tures. In addition, it is evident that the majority of the
399 higher metallicity stars (smaller symbols, in particular

⁵ <https://github.com/GeminiDRSoftware/DRAGONS>.

⁶ Most stars without carbon abundance determinations were ob-
served with CTIO/Blanco. There was an artifact at the exact
same position as the CH band head that affected some of the
spectra and prevented reliable spectral fits by the n-SSPP.

⁷ $A(\text{C}) = \log(N_{\text{C}}/N_{\text{H}}) + 12$

400 $[\text{Fe}/\text{H}] \geq -1.0$, have $T_{\text{eff}} \geq 5700$ K. This will be further
401 discussed in Section 4.4.

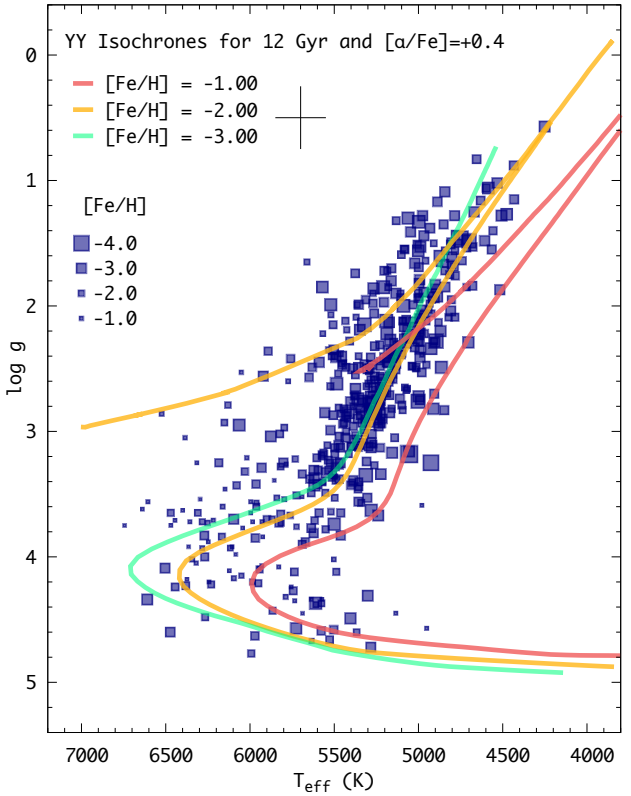


Figure 4. Surface gravity vs. T_{eff} diagram for the program stars, using the parameters calculated by the n-SSPP, listed in Table 3. The point size is inversely proportional to the metallicity. Also shown are the YY Isochrones (12 Gyr, 0.8 M_{\odot} , $[\alpha/\text{Fe}] = +0.4$; Demarque et al. 2004) for $[\text{Fe}/\text{H}] = -1.0$, -2.0 , and -3.0 , and horizontal-branch tracks from Dotter et al. (2008).

402 Figure 5 shows example spectra for the 100 most
403 metal-poor stars observed with Blanco (left panel) and
404 Gemini-South (right panel), which have both $[\text{C}/\text{Fe}]$ and
405 $[\alpha/\text{Fe}]$ determined by the n-SSPP. Also shown are the
406 adopted parameters for each target (see Section 3 for de-
407 tails). The absorption features of interest for the calcu-
408 lation of each parameter are identified on the top of the
409 panels. The shaded regions correspond to the specific
410 atmospheric parameter or chemical abundance probed
411 by the S-PLUS filters outlined on the bottom of the pan-
412 els. The spectra are sorted by $[\text{Fe}/\text{H}]$. Despite the vari-
413 ation in T_{eff} , it is possible to note the overall decrease in
414 the strength of the Ca II features as the metallicity de-
415 creases, as well as the increase in T_{eff} , $A(\text{C})$, and $[\alpha/\text{Fe}]$
416 as their associated absorption features strengthen.

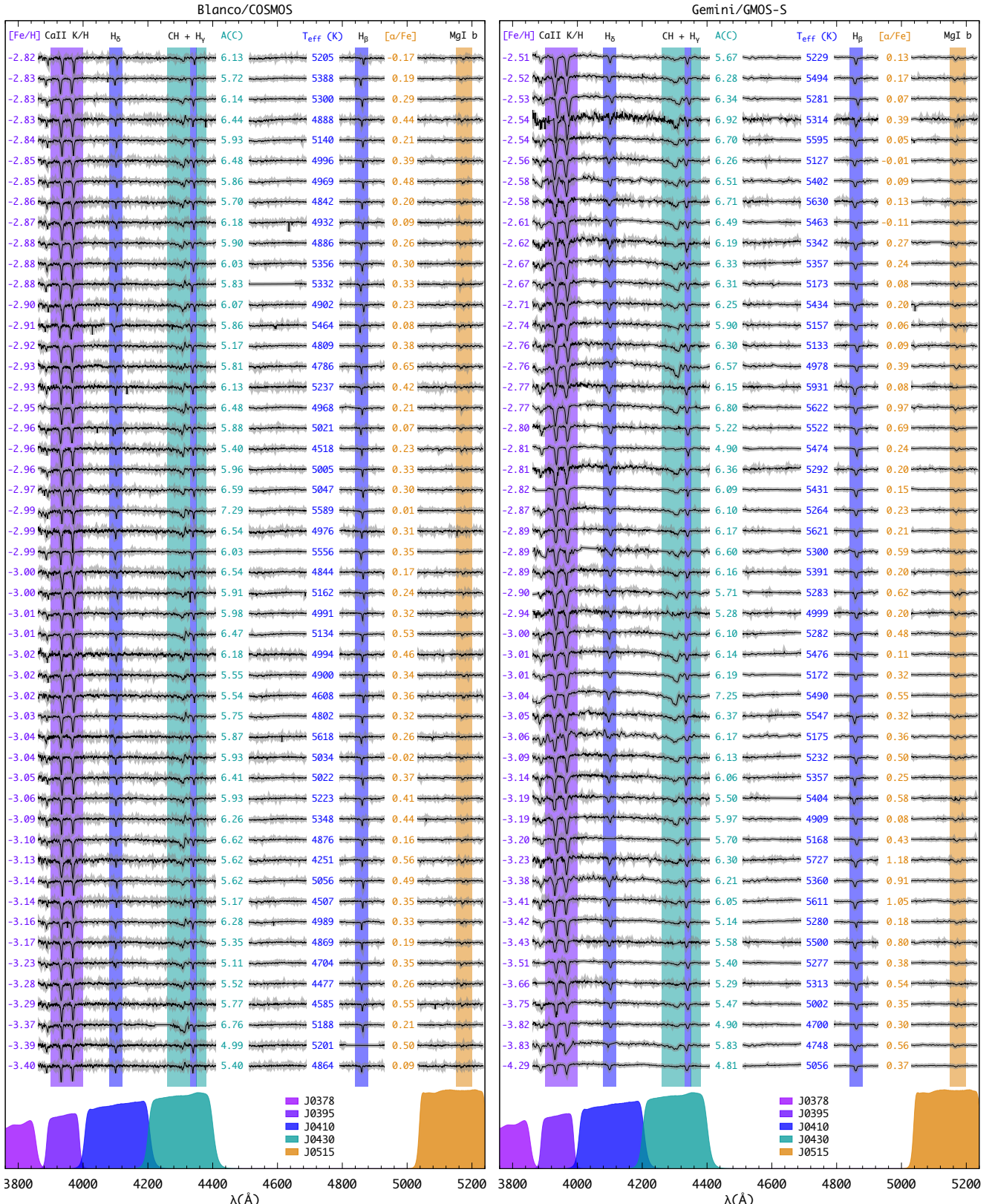


Figure 5. Example spectra for 100 program stars observed with Blanco (left panel) and Gemini-South (right panel), sorted by decreasing metallicity. The shaded areas highlight absorption features of interest for the determination of the stellar parameters and chemical abundances (see text for details). Also shown are the values calculated by the n-SSPP, as well as the S-PLUS filters that probe such features, with the exception of H_γ and H_β.

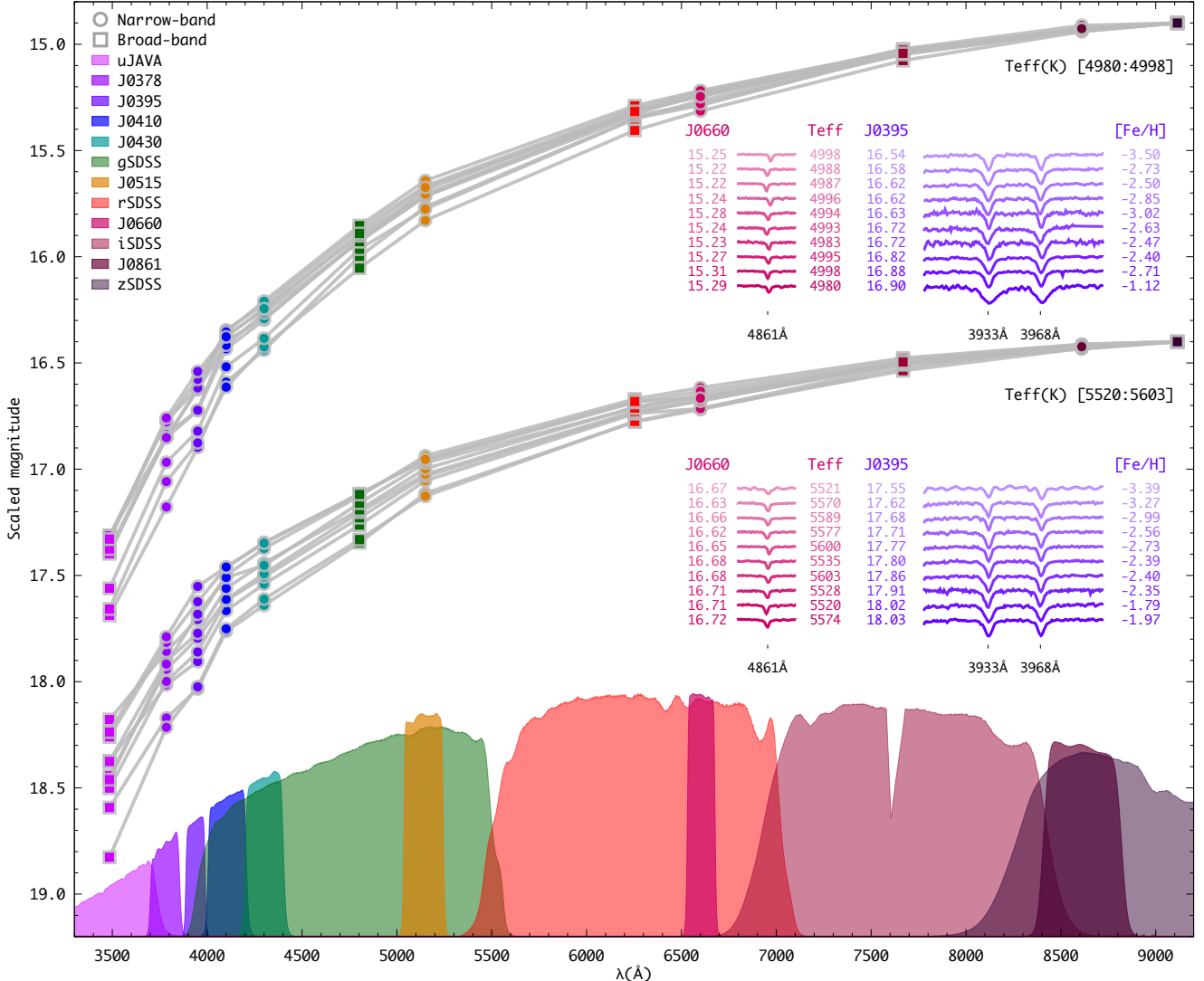


Figure 6. Spectral energy distribution (SED) for 20 selected program stars from Blanco and Gemini. Magnitudes were scaled to $z\text{SDSS}=14.9$ (top) and 16.4 (bottom). The temperature range for each set is displayed right below the SEDs. The insets show the observed spectra around the $\text{H}\beta$ and Ca II HK absorption features, sorted by their J0395 scaled magnitude. Also shown are the T_{eff} and $[\text{Fe}/\text{H}]$ for each star and the S-PLUS transmission curves. See text for further details.

417

4. ANALYSIS AND DISCUSSION

418

4.1. $[\text{Fe}/\text{H}]$ sensitivity from narrow-band photometry

419

As described in Section 2, the S-PLUS colors using the narrow-band J0395 filter are effective in separating different metallicity regimes (see also Figure 2). Hence, for a given temperature, the difference between the J0395 and J0660 magnitudes should decrease as a function of $[\text{Fe}/\text{H}]$ ⁸. An attempt to illustrate and quantify this effect is shown in Figure 6. There are two sets of Spec-

420 tral Energy Distributions (SED) with ten stars each, in
421 two narrow temperature intervals. The magnitudes were
422 scaled to an arbitrary $z\text{SDSS}$ value in order to preserve
423 their color indices and allow for a star-to-star compari-
424 son of the sensitivity of the other magnitudes to changes
425 in stellar parameters. The insets show sections of the ob-
426 served spectra (sorted by their J0395 scaled magnitude)
427 around the Ca II HK and $\text{H}\beta$ features, as well as their
428 respective parameters ($[\text{Fe}/\text{H}]$ and T_{eff}) and scaled mag-
429 nitudes (J0395 and J0660). Assuming that the three
430 bluest filters carry most of the metallicity information,
431 it is possible to qualitatively see the larger variation in
432 magnitudes, as compared with the magnitudes from the
433 redder filters. Under the assumption that (most) of this

⁸ As an example, for two stars with the same $T_{\text{eff}}/\log g$ and at the same distance, the one with the lowest metallicity would be brighter in J0395.

440 variation is due to changes in metallicity, it is expected
 441 that the sorted J0395 magnitudes would naturally result
 442 in a [Fe/H] sequence.

443 For the SEDs on the top set, all T_{eff} values are within
 444 18 K, which translates into a 0.09 mag ($\sim 0.5\%$) varia-
 445 tion in the J0660 flux. As expected, there is an increase
 446 of the J0395 magnitude with [Fe/H]. The two extremes
 447 of the [Fe/H] scale have a 0.36 magnitude difference in
 448 J0395, which roughly translates into a 2.0 dex varia-
 449 tion in [Fe/H]. At this temperature range, the above
 450 variation in the Ca II HK region flux is well above the
 451 typical magnitude uncertainties from S-PLUS, making
 452 it possible to have a good metallicity discriminant.

453 To a certain degree, the same applies to the bottom set
 454 of SEDs, which has an average T_{eff} about 500 K warmer
 455 than the top set, with a somewhat larger dispersion of
 456 83 K. These warmer temperatures result in weaker ab-
 457 sorption features when compared to the cooler set for a
 458 given [Fe/H], but are still larger than the typical uncer-
 459 tainties in the measured flux. For this group, the varia-
 460 tion in the J0660 magnitude is very small (0.05 mag),
 461 while the difference between the extremes in J0395
 462 (0.48 mag) still translates into a 1.5 dex range in terms
 463 of [Fe/H].

464 4.2. Effectiveness of S-PLUS color selection

465 One of the main goals of this work is to improve
 466 the success rate of finding low-metallicity stars from
 467 photometry, taking advantage of the metallicity sen-
 468 sitivity of the S-PLUS narrow-band filters. Figure 7
 469 shows the color-color diagram for the S-PLUS DR3 data,
 470 the cross-match between S-PLUS and SDSS/SEGUE
 471 (color-coded by metallicity range), and the 492 stars
 472 observed in this work. The point size is inversely
 473 proportional to [Fe/H]. The selection window for
 474 the spectroscopic follow-up, as defined in Section 2 is
 475 $(J0395-J0410)-(J0660-J0861) \in [-0.30:0.15]$ and
 476 $(J0395-J0660)-2 \times (g-i) \in [-0.60:-0.15]$. Also
 477 shown in the figure is SPLUS J2104–0049, the first
 478 ultra metal-poor star identified in S-PLUS, with
 479 $[\text{Fe}/\text{H}] = -4.03^9$ (Placco et al. 2021).

480 There is, as expected, a strong correlation between
 481 metallicity and the position of a star in this color-
 482 color diagram. However, that does not imply a di-
 483 rect translation between these colors and [Fe/H], as ev-
 484 idenced by the stars with smaller points (higher met-
 485 licities) present towards negative colors. However, these
 486 higher-metallicity stars can be filtered-out by another
 487 color combination (see Section 4.4 below for further de-

⁹ The n-SSPP estimated $[\text{Fe}/\text{H}] = -4.29$ from the Gemini/GMOS medium-resolution spectrum.

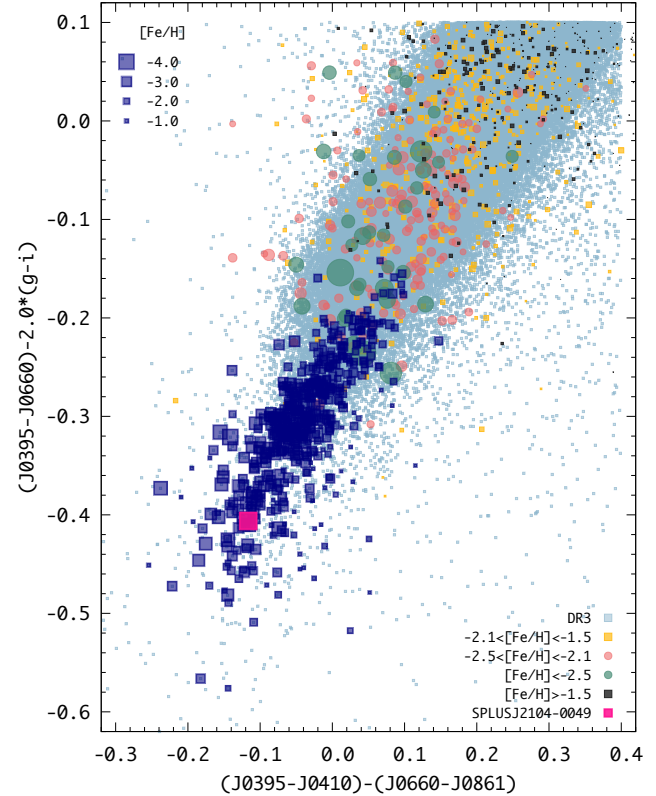


Figure 7. S-PLUS color-color diagram for DR3 (light blue filled squares), SDSS/SEGUE cross-match, and the stars observed in this work (dark blue filled squares). The point size is inversely proportional to the metallicity. Also shown is SPLUS J2104–0049, an ultra metal-poor star identified in S-PLUS.

488 tails. What still holds true, as set forth by Figure 2,
 489 is the fact that the fraction of stars with $[\text{Fe}/\text{H}] \leq -2.0$
 490 increases for decreasing $(J0395-J0660)-2 \times (g-i)$ and
 491 $(J0395-J0410)-(J0660-J0861)$.

492 A different procedure to assess the efficiency of the
 493 color selection is by looking at the MDF of the ob-
 494 served stars and compare it with previous attempts of
 495 following-up low-metallicity star candidates. The top
 496 panel of Figure 8 shows the MDF of the stars observed in
 497 this work, compared with data from Placco et al. (2018),
 498 Placco et al. (2019), and Limberg et al. (2021b)¹⁰ in the
 499 middle panels. The total number of stars and fractions
 500 for different metallicity ranges are also shown for each
 501 sample. The bottom panel shows the cumulative distri-

¹⁰ Even though these three efforts have followed-up data selected from different approaches, both had the goal of maximizing the number of observed stars with $[\text{Fe}/\text{H}] \leq -2.0$. A comparison could also be made with the work of Aguado et al. (2019), Da Costa et al. (2019), and Galarza et al. (2022). However, these studies used photometric metallicities for their target selection, as opposed to the color-color diagrams employed by this work.

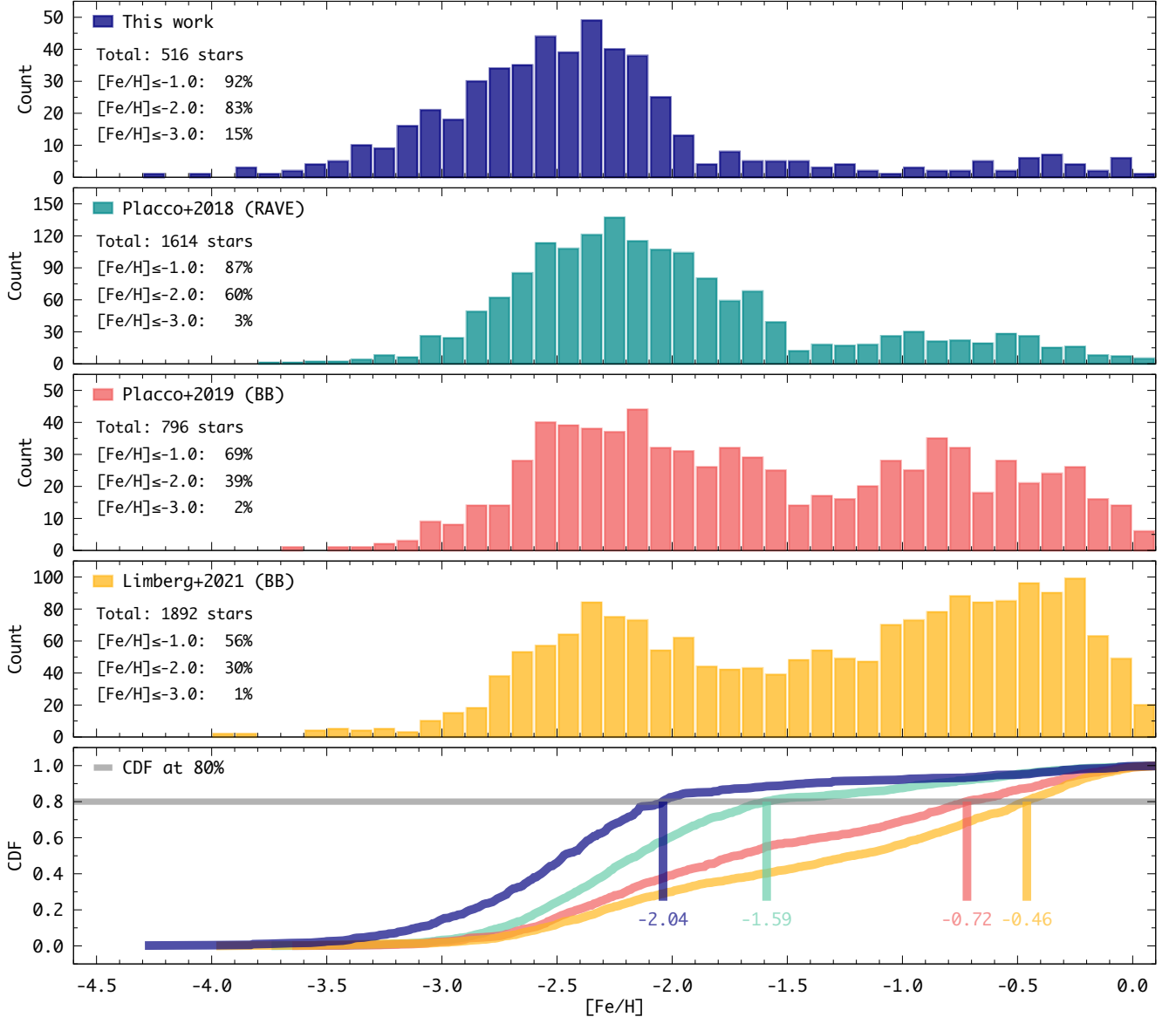


Figure 8. Metallicity histogram for the program stars (top panel), compared with the distributions from Placco et al. (2018), Placco et al. (2019), and Limberg et al. (2021b) (middle panels). Each panel shows the total number of stars and the fractions for different metallicity regimes. The bottom panel shows the cumulative distribution functions (CDF) for the three samples, marking the $[\text{Fe}/\text{H}]$ value for which they reach 80%.

bution function (CDF) for the three samples, indicating the 80th percentile value for $[\text{Fe}/\text{H}]$. It is possible to see that the S-PLUS color selection is far superior than the previous efforts in selecting low-metallicity star candidates. The success rate for $[\text{Fe}/\text{H}] \leq -2.0$ is $83^{+3\%}_{-4\%}{}^{+11\%}_{-11\%}$, as compared to 60% in Placco et al. (2018), 39% in Placco et al. (2019), and 30% in Limberg et al. (2021b). Finally, the fraction of stars with $[\text{Fe}/\text{H}] \leq -3.0$ (15%)

is higher than the fraction of stars with $[\text{Fe}/\text{H}] > -1.5$ (11%), which confirms the effectiveness of the S-PLUS color window in selecting low-metallicity stars.

4.3. Carbon and α -element abundances

The carbon and α -element abundances calculated by the n-SSPP can provide further insight on the origin of the observed stars and serve as selection criteria for high-resolution spectroscopic follow-up. Even though the carbon abundances in the SEGUE sample were not used for the target selection in this work, the $(g-i)$ color (and, to some extent, also the J0395 and J0410

¹¹ Uncertainties in the fractions are represented by the Wilson score confidence intervals (Wilson 1927).

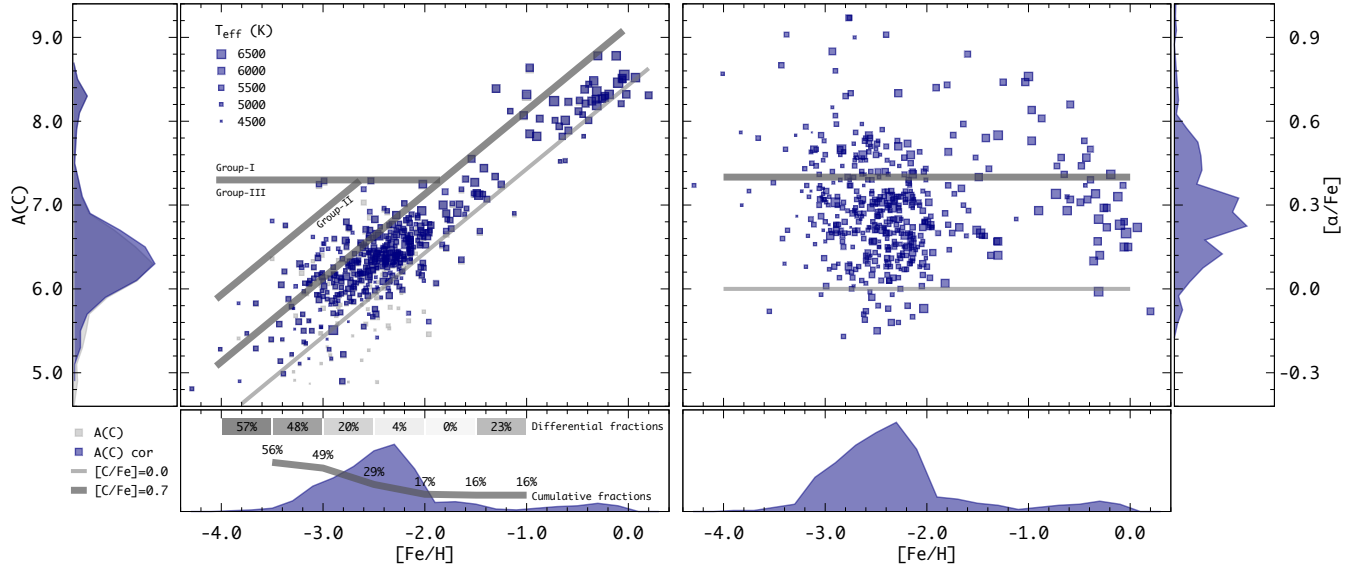


Figure 9. Absolute carbon, ($A(C)$), corrected as described in the text - left panel), and α -element abundance ratios, $[\alpha/Fe]$ (right panel), as a function of the metallicity calculated by the n-SSPP. The side and lower panels show the marginal distributions. The solid line in the lower left panel shows the cumulative CEMP fractions for the stars with $-3.5 \leq [Fe/H] \leq -1.0$ and the numbers of the top part of the panel are the differential fractions for 0.5 dex $[Fe/H]$ bins. Point sizes are proportional to T_{eff} .

521 magnitudes) can be affected by the presence of carbon
 522 molecular bands in the spectrum. As a consequence
 523 of the decreased emerging flux on the g band, a frac-
 524 tion of cool carbon-enhanced stars may fall outside the
 525 ($g-i$)¹² window defined in Section 2. Regardless, the
 526 abundances measured for the program stars allow for the
 527 calculation of the fractions of Carbon-Enhanced Metal-
 528 Poor (CEMP - $[C/\text{Fe}] \geq +0.7$; Aoki et al. 2007) stars as
 529 a function of the metallicity.

530 Figure 9 shows the distribution of $A(C)$ (left panel)
 531 and $[\alpha/\text{Fe}]$ (right panel) for the sample stars as a func-
 532 tion of the metallicity. The auxiliary panels show the
 533 marginal distributions. The lower left panel shows both
 534 the differential and cumulative CEMP fractions. Solid
 535 lines mark the solar values for the quantities, as well as
 536 the CEMP definition on the left panel and the average
 537 $[\alpha/\text{Fe}] = +0.4$ for the Galactic halo (Venn et al. 2004;
 538 Kobayashi et al. 2006) in the right panel. The point
 539 sizes are proportional to the temperature. The CEMP
 540 groups labeled are loosely defined based on the argu-
 541 ments presented in Yoon et al. (2016), which were built
 542 upon the work of Spite et al. (2013); Bonifacio et al.
 543 (2015); Hansen et al. (2015). The average α -element
 544 abundance for the sample ($[\alpha/\text{Fe}] = +0.29$) is somewhat
 545 lower than the typical value for stars with $[Fe/\text{H}] < -2.0$
 546 and there is no apparent trend with metallicities.

¹² As an example, the star SDSS J1327+3335, with $T_{\text{eff}}=4530$ K,
 $[Fe/\text{H}]=-3.38$, and $[C/\text{Fe}]=+2.18$, has $(g-i)=1.718$ (Yoon et al.
 2020).

547 Stars in the CEMP Group-I are believed to have ac-
 548 quired their carbon in a binary system from a now-
 549 evolved companion that went through its AGB phase
 550 (extrinsic enrichment; Placco et al. 2014). Members of
 551 Groups-II and III, on the other hand, carry in their at-
 552 mosphere the carbon signature inherited from its par-
 553 ent population (intrinsic enrichment; Placco et al. 2014).
 554 The distinction between Groups II and III lies on specific
 555 characteristics of the massive stars that polluted the gas
 556 clouds from which the subsequent low-mass stars were
 557 formed. For the sample presented in this work, there are
 558 68 CEMP stars, with 4 stars in Group-I, 60 in Group-II,
 559 and 4 in Group-III. Compared with the work of Yoon
 560 et al. (2016), the sample presented in this work has an
 561 exceptionally low number of Group-I stars, which should
 562 be the majority in the CEMP population. This may be
 563 partially¹³ a consequence of the ($g-i$) restriction men-
 564 tioned above and other S-PLUS color selections, which
 565 would exclude most of the higher metallicity and higher
 566 carbon abundance stars associated with the Group-I.

567 The cumulative CEMP fractions showed in the lower
 568 panel of Figure 9 are consistently lower for $[Fe/\text{H}] < -1.0$
 569 and < -2.0 when compared to other empirical estimates
 570 in the literature, derived from samples with similar spec-
 571 tral resolution (Placco et al. 2018; Yoon et al. 2018;

¹³ Arentsen et al. (2022) points out that, in general, low-metallicity star samples from medium-resolution spectroscopy show a lower than expected fraction of CEMP Group-I stars when compared to high-resolution samples.

Placco et al. 2019; Limberg et al. 2021b). This may be, once more, a consequence of the selection methods employed in this work. The same applies to the differential fractions. The fractions are in better agreement for the $[Fe/H] < -3.0$ regime, which could be due to the fact that Group-III stars dominate the CEMP population in this metallicity regime (see Arentsen et al. 2022, for a complete review of the CEMP fractions in the literature).

4.4. Further improvements in the color selection

Even though the S-PLUS color selections presented in this work are effective in selecting low-metallicity stars, additional restrictions can be made in order to decrease the number of stars with $[Fe/H] \geq -1.0$ for further spectroscopic follow-up and targeting. Further inspection of Figure 4 reveals that 42% of the stars with $T_{\text{eff}} \geq 5900$ K have $[Fe/H] \geq -1.0$, while only 3% of the stars with $T_{\text{eff}} < 5900$ K have $[Fe/H] \geq -1.0$.

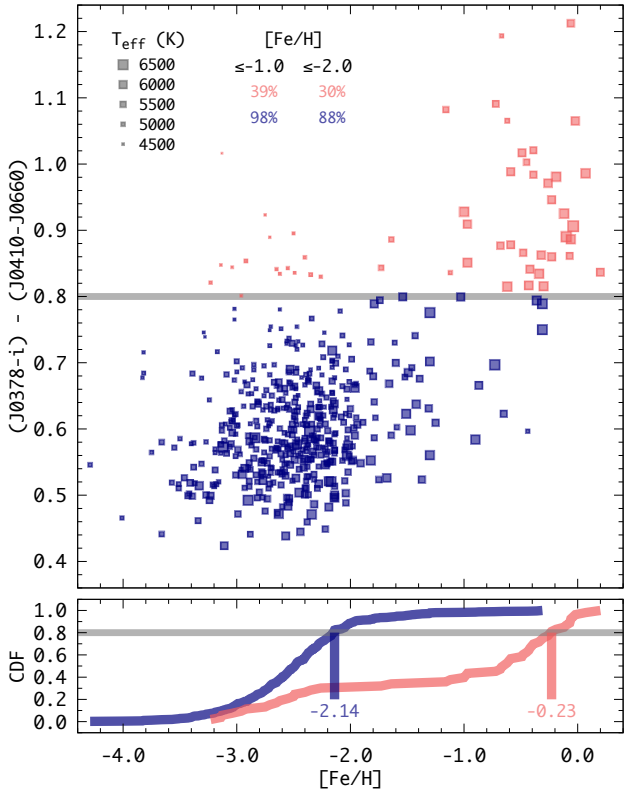


Figure 10. Top panel: $(J0378-i) - (J0410-J0660)$ as a function of the metallicity for the observed sample, with the gray line marking the proposed color cut. Also shown are the fractions of stars with $[Fe/H] \leq -1.0$ and ≤ -2.0 for the two subsamples. The point sizes are proportional to T_{eff} . Bottom panel: cumulative distribution functions (CDF) for the two subsamples, marking the $[Fe/H]$ value for which they reach 80%.

An exploratory analysis was conducted to search for an additional S-PLUS color combination that would help remove the higher metallicity stars for the continuation of the spectroscopic follow-up. One such candidate is $(J0378-i) - (J0410-J0660)$, which contains the metallicity-sensitive J0378 filter and the temperature-sensitive (J0410-J0660) color index. The top panel of Figure 10 shows the behavior of this color as a function of the metallicity. It is possible to see a very strong correlation between the two quantities, and a tentative cut was made at $(J0378-i) - (J0410-J0660) = 0.80$. The high color index subsample (red points) is dominated by the higher metallicity stars, with only 30% of the stars with $[Fe/H] \leq -1.0$ and 39% with $[Fe/H] \leq -2.0$. For the low color index subsample (blue points), the fractions are 98% for stars with $[Fe/H] \leq -1.0$ and 88% with $[Fe/H] \leq -2.0$. The bottom panel shows the CDFs for both subsamples, indicating the 80th percentile value for $[Fe/H]$.

This additional color restriction further improves the success rate for the identification of stars with $[Fe/H] \leq -2.0$ from the S-PLUS photometry. Even though there are low-metallicity stars with $(J0378-i) - (J0410-J0660) > 0.8$, their fraction is substantially smaller than for $(J0378-i) - (J0410-J0660) < 0.8$. The stars at the high color index subsample with $[Fe/H] \leq -2.0$ are all low-temperature ($T_{\text{eff}} \lesssim 4800$ K) and low-carbon ($[C/Fe] \leq 0.0$).

5. CONCLUSIONS

This work presented the medium-resolution spectroscopic follow-up of 516 low-metallicity star candidates selected from their S-PLUS photometry. By using metallicity-sensitive colors, the success rate found is 92 $^{+2}_{-3}\%$ for $[Fe/H] \leq -1.0$, 83 $^{+3}_{-4}\%$ for $[Fe/H] \leq -2.0$, and 15 $^{+3}_{-3}\%$ for $[Fe/H] \leq -3.0$, including two ultra metal-poor stars ($[Fe/H] \leq -4.0$). Based on the carbonicity determinations, there are 68 CEMP stars in the sample, including 60 Group-II and 4 Group-III. Most of these are already being followed-up with high-resolution spectroscopy in order to determine their chemical abundance pattern and further understand their origin. Based on the $[Fe/H]$ determined in this work, a further color restriction is proposed, which can potentially increase the fractions of stars with $[Fe/H] \leq -1.0$ and ≤ -2.0 to 98% and 88%, respectively.

The unpretentious color selection described in this work is not only extremely effective in providing targets for further spectroscopic studies, but also establishes a framework in which upcoming fiber-fed multiplex surveys can benefit from in terms of targeting. These surveys will continue to provide the individual pieces that

641 constitute the cosmic puzzle that is the chemical evolution
 642 of the universe.

643 The work of V.M.P. is supported by NOIRLab, which
 644 is managed by the Association of Universities for Re-
 645 search in Astronomy (AURA) under a cooperative
 646 agreement with the National Science Foundation. F.A.-
 647 F. acknowledges funding for this work from FAPESP
 648 grants 2018/20977-2 and 2021/09468-1. A.A. grate-
 649 fully acknowledges funding from the European Research
 650 Council (ERC) under the European Unions Horizon
 651 2020 research and innovation programme (grant agree-
 652 ment No. 834148). Y.S.L. acknowledges support from
 653 the National Research Foundation (NRF) of Korea grant
 654 funded by the Ministry of Science and ICT (NRF-
 655 2021R1A2C1008679). The S-PLUS project, including
 656 the T80-South robotic telescope and the S-PLUS sci-
 657 entific survey, was founded as a partnership between
 658 the Fundação de Amparo à Pesquisa do Estado de São
 659 Paulo (FAPESP), the Observatório Nacional (ON), the
 660 Federal University of Sergipe (UFS), and the Federal
 661 University of Santa Catarina (UFSC), with important
 662 financial and practical contributions from other col-
 663 laborating institutes in Brazil, Chile (Universidad de
 664 La Serena), and Spain (Centro de Estudios de Física
 665 del Cosmos de Aragón, CEFCa). We further acknowl-
 666 edge financial support from the São Paulo Research
 667 Foundation (FAPESP), the Brazilian National Research
 668 Council (CNPq), the Coordination for the Improvement
 669 of Higher Education Personnel (CAPES), the Carlos
 670 Chagas Filho Rio de Janeiro State Research Founda-
 671 tion (FAPERJ), and the Brazilian Innovation Agency
 672 (FINEP). The members of the S-PLUS collaboration are
 673 grateful for the contributions from CTIO staff in helping
 674 in the construction, commissioning and maintenance of
 675 the T80-South telescope and camera. We are also in-
 676 debted to Rene Laporte, INPE, and Keith Taylor for
 677 their important contributions to the project. From CE-
 678 FCA, we thank Antonio Marín-Franch for his invaluable
 679 contributions in the early phases of the project, David
 680 Cristóbal-Hornillos and his team for their help with the
 681 installation of the data reduction package JYPE version
 682 0.9.9, César Íñiguez for providing 2D measurements of
 683 the filter transmissions, and all other staff members for
 684 their support with various aspects of the project. Based
 685 on observations made at Cerro Tololo Inter-American
 686 Observatory at NSF's NOIRLab (NOIRLab Prop. IDs
 687 2019B-0069, 2020A-0032, 2022A-210002; PI: V. Placco),
 688 which is managed by the Association of Universities for

689 Research in Astronomy (AURA) under a cooperative
 690 agreement with the National Science Foundation. Based
 691 on observations obtained at the international Gem-
 692 ini Observatory (Program IDs: GS-2019A-Q-408, GS-
 693 2021A-Q-419, GS-2022A-Q-406), a program of NSF's
 694 NOIRLab, which is managed by the Association of Uni-
 695 versities for Research in Astronomy (AURA) under a co-
 696 operative agreement with the National Science Founda-
 697 tion. on behalf of the Gemini Observatory partnership:
 698 the National Science Foundation (United States), Na-
 699 tional Research Council (Canada), Agencia Nacional de
 700 Investigación y Desarrollo (Chile), Ministerio de Cien-
 701 cia, Tecnología e Innovación (Argentina), Ministério da
 702 Ciência, Tecnologia, Inovações e Comunicações (Brazil),
 703 and Korea Astronomy and Space Science Institute (Re-
 704 public of Korea). This research has made use of NASA's
 705 Astrophysics Data System Bibliographic Services; the
 706 arXiv pre-print server operated by Cornell University;
 707 the SIMBAD database hosted by the Strasbourg As-
 708 tronomical Data Center; and the online Q&A platform
 709 stackoverflow (<http://stackoverflow.com/>).

710 *Software:* awk (Aho et al. 1987), dustmaps (Green
 711 2018), DRAGONS (Labrie et al. 2019), gnuplot (Williams
 712 & Kelley 2015), IRAF (Tody 1986, 1993),
 713 matplotlib (Hunter 2007), n-SSPP (Beers et al. 2014),
 714 numpy (Oliphant 2006), pandas (McKinney 2010),
 715 sed (Mcmahon 1979), stilts (Taylor 2006).

716 *Facilities:* Blanco (COSMOS), Gemini:South
 717 (GMOS)

REFERENCES

- 718 Aguado, D. S., Youakim, K., González Hernández, J. I.,
 719 et al. 2019, MNRAS, 490, 2241,
 720 doi: [10.1093/mnras/stz2643](https://doi.org/10.1093/mnras/stz2643)
- 721 Aho, A. V., Kernighan, B. W., & Weinberger, P. J. 1987,
 722 The AWK Programming Language (Boston, MA, USA:
 723 Addison-Wesley Longman Publishing Co., Inc.)
- 724 Allende Prieto, C. 2016, A&A, 595, A129,
 725 doi: [10.1051/0004-6361/201628789](https://doi.org/10.1051/0004-6361/201628789)
- 726 Almeida-Fernandes, F., SamPedro, L., Herpich, F. R., et al.
 727 2022, MNRAS, 511, 4590, doi: [10.1093/mnras/stac284](https://doi.org/10.1093/mnras/stac284)
- 728 Alonso, A., Arribas, S., & Martínez-Roger, C. 1996, A&A,
 729 313, 873
- 730 Alonso, A., Arribas, S., & Martínez-Roger, C. 1999, A&AS,
 731 140, 261, doi: [10.1051/aas:1999521](https://doi.org/10.1051/aas:1999521)
- 732 An, D., Beers, T. C., Santucci, R. M., et al. 2015, ApJL,
 733 813, L28, doi: [10.1088/2041-8205/813/2/L28](https://doi.org/10.1088/2041-8205/813/2/L28)
- 734 An, D., Beers, T. C., Johnson, J. A., et al. 2013, ApJ, 763,
 735 65, doi: [10.1088/0004-637X/763/1/65](https://doi.org/10.1088/0004-637X/763/1/65)
- 736 Aoki, W., Beers, T. C., Christlieb, N., et al. 2007, ApJ,
 737 655, 492, doi: [10.1086/509817](https://doi.org/10.1086/509817)
- 738 Arentsen, A., Placco, V. M., Lee, Y. S., et al. 2022, A&A –
 739 in preparation
- 740 Beers, T. C., & Christlieb, N. 2005, ARA&A, 43, 531
- 741 Beers, T. C., Norris, J. E., Placco, V. M., et al. 2014, ApJ,
 742 794, 58, doi: [10.1088/0004-637X/794/1/58](https://doi.org/10.1088/0004-637X/794/1/58)
- 743 Beers, T. C., Placco, V. M., Carollo, D., et al. 2017, ApJ,
 744 835, 81, doi: [10.3847/1538-4357/835/1/81](https://doi.org/10.3847/1538-4357/835/1/81)
- 745 Bessell, M., Bloxham, G., Schmidt, B., et al. 2011, PASP,
 746 123, 789, doi: [10.1086/660849](https://doi.org/10.1086/660849)
- 747 Bessell, M. S. 1979, PASP, 91, 589, doi: [10.1086/130542](https://doi.org/10.1086/130542)
- 748 Bonifacio, P., Monai, S., & Beers, T. C. 2000, AJ, 120,
 749 2065, doi: [10.1086/301566](https://doi.org/10.1086/301566)
- 750 Bonifacio, P., Caffau, E., Spite, M., et al. 2015, A&A, 579,
 751 A28, doi: [10.1051/0004-6361/201425266](https://doi.org/10.1051/0004-6361/201425266)
- 752 Bromm, V., & Larson, R. B. 2004, ARA&A, 42, 79,
 753 doi: [10.1146/annurev.astro.42.053102.134034](https://doi.org/10.1146/annurev.astro.42.053102.134034)
- 754 Carney, B. W., & Peterson, R. C. 1981, ApJ, 245, 238,
 755 doi: [10.1086/158804](https://doi.org/10.1086/158804)
- 756 Casagrande, L., Ramírez, I., Meléndez, J., Bessell, M., &
 757 Asplund, M. 2010, A&A, 512, A54,
 758 doi: [10.1051/0004-6361/200913204](https://doi.org/10.1051/0004-6361/200913204)
- 759 Casagrande, L., Wolf, C., Mackey, A. D., et al. 2019,
 760 MNRAS, 482, 2770, doi: [10.1093/mnras/sty2878](https://doi.org/10.1093/mnras/sty2878)
- 761 Cenarro, A. J., Moles, M., Cristóbal-Hornillos, D., et al.
 762 2019, A&A, 622, A176,
 763 doi: [10.1051/0004-6361/201833036](https://doi.org/10.1051/0004-6361/201833036)
- 764 Chiti, A., Frebel, A., Mardini, M. K., et al. 2021a, ApJS,
 765 254, 31, doi: [10.3847/1538-4365/abf73d](https://doi.org/10.3847/1538-4365/abf73d)
- 766 Chiti, A., Mardini, M. K., Frebel, A., & Daniel, T. 2021b,
 767 ApJL, 911, L23, doi: [10.3847/2041-8213/abd629](https://doi.org/10.3847/2041-8213/abd629)
- 768 Da Costa, G. S., Bessell, M. S., Mackey, A. D., et al. 2019,
 769 MNRAS, 489, 5900, doi: [10.1093/mnras/stz2550](https://doi.org/10.1093/mnras/stz2550)
- 770 Davies, R. L., Allington-Smith, J. R., Bettess, P., et al.
 771 1997, in Proc. SPIE, Vol. 2871, Optical Telescopes of
 772 Today and Tomorrow, ed. A. L. Ardeberg, 1099–1106,
 773 doi: [10.1117/12.268996](https://doi.org/10.1117/12.268996)
- 774 Demarque, P., Woo, J.-H., Kim, Y.-C., & Yi, S. K. 2004,
 775 ApJS, 155, 667, doi: [10.1086/424966](https://doi.org/10.1086/424966)
- 776 Dotter, A., Chaboyer, B., Jevremović, D., et al. 2008,
 777 ApJS, 178, 89, doi: [10.1086/589654](https://doi.org/10.1086/589654)
- 778 Frebel, A., & Norris, J. E. 2015, ARA&A, 53, 631,
 779 doi: [10.1146/annurev-astro-082214-122423](https://doi.org/10.1146/annurev-astro-082214-122423)
- 780 Fukugita, M., Ichikawa, T., Gunn, J. E., et al. 1996, AJ,
 781 111, 1748, doi: [10.1086/117915](https://doi.org/10.1086/117915)
- 782 Galarza, C. A., Daflon, S., Placco, V. M., et al. 2022, A&A,
 783 657, A35, doi: [10.1051/0004-6361/202141717](https://doi.org/10.1051/0004-6361/202141717)
- 784 Gimeno, G., Roth, K., Chiboucas, K., et al. 2016, in
 785 Proc. SPIE, Vol. 9908, Ground-based and Airborne
 786 Instrumentation for Astronomy VI, 99082S,
 787 doi: [10.1117/12.2233883](https://doi.org/10.1117/12.2233883)
- 788 Greaves, W. M. H., Davidson, C., & Martin, E. 1929,
 789 MNRAS, 90, 104, doi: [10.1093/mnras/90.1.104](https://doi.org/10.1093/mnras/90.1.104)
- 790 Green, G. 2018, The Journal of Open Source Software, 3,
 791 695, doi: [10.21105/joss.00695](https://doi.org/10.21105/joss.00695)
- 792 Hansen, T., Hansen, C. J., Christlieb, N., et al. 2015, ApJ,
 793 807, 173, doi: [10.1088/0004-637X/807/2/173](https://doi.org/10.1088/0004-637X/807/2/173)
- 794 Heger, A., & Woosley, S. E. 2002, ApJ, 567, 532,
 795 doi: [10.1086/338487](https://doi.org/10.1086/338487)
- 796 Huang, Y., Chen, B. Q., Yuan, H. B., et al. 2019, ApJS,
 797 243, 7, doi: [10.3847/1538-4365/ab1f72](https://doi.org/10.3847/1538-4365/ab1f72)
- 798 Hunter, J. D. 2007, Computing in Science & Engineering, 9,
 799 90, doi: [10.1109/MCSE.2007.55](https://doi.org/10.1109/MCSE.2007.55)
- 800 Ivezić, Ž., Beers, T. C., & Jurić, M. 2012, ARA&A, 50, 251,
 801 doi: [10.1146/annurev-astro-081811-125504](https://doi.org/10.1146/annurev-astro-081811-125504)
- 802 Ivezić, Ž., Sesar, B., Jurić, M., et al. 2008, ApJ, 684, 287,
 803 doi: [10.1086/589678](https://doi.org/10.1086/589678)
- 804 Keller, S. C., Schmidt, B. P., Bessell, M. S., et al. 2007,
 805 PASA, 24, 1, doi: [10.1071/AS07001](https://doi.org/10.1071/AS07001)
- 806 Kobayashi, C., Umeda, H., Nomoto, K., Tominaga, N., &
 807 Ohkubo, T. 2006, ApJ, 653, 1145, doi: [10.1086/508914](https://doi.org/10.1086/508914)
- 808 Labrie, K., Anderson, K., Cárdenes, R., Simpson, C., &
 809 Turner, J. E. H. 2019, in Astronomical Society of the
 810 Pacific Conference Series, Vol. 523, Astronomical Data
 811 Analysis Software and Systems XXVII, ed. P. J. Teuben,
 812 M. W. Pound, B. A. Thomas, & E. M. Warner, 321
- 813 Lee, Y. S., Beers, T. C., Sivarani, T., et al. 2008a, AJ, 136,
 814 2022, doi: [10.1088/0004-6256/136/5/2022](https://doi.org/10.1088/0004-6256/136/5/2022)

- 815 —. 2008b, AJ, 136, 2050,
 816 doi: [10.1088/0004-6256/136/5/2050](https://doi.org/10.1088/0004-6256/136/5/2050)
- 817 Lee, Y. S., Beers, T. C., Allende Prieto, C., et al. 2011, AJ,
 818 141, 90, doi: [10.1088/0004-6256/141/3/90](https://doi.org/10.1088/0004-6256/141/3/90)
- 819 Lee, Y. S., Beers, T. C., Masseron, T., et al. 2013, AJ, 146,
 820 132, doi: [10.1088/0004-6256/146/5/132](https://doi.org/10.1088/0004-6256/146/5/132)
- 821 Leggett, S. K., Birmingham, B., Saumon, D., et al. 2010,
 822 ApJ, 710, 1627, doi: [10.1088/0004-637X/710/2/1627](https://doi.org/10.1088/0004-637X/710/2/1627)
- 823 Limberg, G., Rossi, S., Beers, T. C., et al. 2021a, ApJ, 907,
 824 10, doi: [10.3847/1538-4357/abcb87](https://doi.org/10.3847/1538-4357/abcb87)
- 825 Limberg, G., Santucci, R. M., Rossi, S., et al. 2021b, ApJ,
 826 913, 11, doi: [10.3847/1538-4357/abeefe](https://doi.org/10.3847/1538-4357/abeefe)
- 827 Lucatello, S., Beers, T. C., Christlieb, N., et al. 2006,
 828 ApJL, 652, L37, doi: [10.1086/509780](https://doi.org/10.1086/509780)
- 829 Majewski, S. R., Ostheimer, J. C., Kunkel, W. E., &
 830 Patterson, R. J. 2000, AJ, 120, 2550, doi: [10.1086/316836](https://doi.org/10.1086/316836)
- 831 Martini, P., Elias, J., Points, S., et al. 2014, in Proc. SPIE,
 832 Vol. 9147, Ground-based and Airborne Instrumentation
 833 for Astronomy V, 91470Z, doi: [10.1117/12.2056834](https://doi.org/10.1117/12.2056834)
- 834 Masseron, T., Johnson, J. A., Plez, B., et al. 2010, A&A,
 835 509, A93+, doi: [10.1051/0004-6361/200911744](https://doi.org/10.1051/0004-6361/200911744)
- 836 McKinney, W. 2010, in Proceedings of the 9th Python in
 837 Science Conference, ed. S. van der Walt & J. Millman, 51
 838 – 56
- 839 Mcmahon, L. E. 1979, in UNIX Programmer’s Manual - 7th
 840 Edition, volume 2, Bell Telephone Laboratories (Murray
 841 Hill)
- 842 Mendes de Oliveira, C., Ribeiro, T., Schoenell, W., et al.
 843 2019, MNRAS, 489, 241, doi: [10.1093/mnras/stz1985](https://doi.org/10.1093/mnras/stz1985)
- 844 Meynet, G., Ekström, S., & Maeder, A. 2006, A&A, 447,
 845 623, doi: [10.1051/0004-6361:20053070](https://doi.org/10.1051/0004-6361:20053070)
- 846 Molino, A., Costa-Duarte, M. V., Sampedro, L., et al. 2019,
 847 arXiv e-prints, arXiv:1907.06315.
 848 <https://arxiv.org/abs/1907.06315>
- 849 Norris, J. E., Bessell, M. S., Yong, D., et al. 2013, ApJ, 762,
 850 25, doi: [10.1088/0004-637X/762/1/25](https://doi.org/10.1088/0004-637X/762/1/25)
- 851 Oliphant, T. E. 2006, A guide to NumPy, Vol. 1 (Trelgol
 852 Publishing USA)
- 853 Placco, V. M., Frebel, A., Beers, T. C., & Stancliffe, R. J.
 854 2014, ApJ, 797, 21, doi: [10.1088/0004-637X/797/1/21](https://doi.org/10.1088/0004-637X/797/1/21)
- 855 Placco, V. M., Beers, T. C., Santucci, R. M., et al. 2018,
 856 AJ, 155, 256, doi: [10.3847/1538-3881/aac20c](https://doi.org/10.3847/1538-3881/aac20c)
- 857 Placco, V. M., Santucci, R. M., Beers, T. C., et al. 2019,
 858 ApJ, 870, 122, doi: [10.3847/1538-4357/aaf3b9](https://doi.org/10.3847/1538-4357/aaf3b9)
- 859 Placco, V. M., Roederer, I. U., Lee, Y. S., et al. 2021,
 860 ApJL, 912, L32, doi: [10.3847/2041-8213/abf93d](https://doi.org/10.3847/2041-8213/abf93d)
- 861 Rockosi, C. M., Lee, Y. S., Morrison, H. L., et al. 2022,
 862 ApJS, 259, 60, doi: [10.3847/1538-4365/ac5323](https://doi.org/10.3847/1538-4365/ac5323)
- 863 Schlegel, D. J., Finkbeiner, D. P., & Davis, M. 1998, ApJ,
 864 500, 525, doi: [10.1086/305772](https://doi.org/10.1086/305772)
- 865 Schuster, W. J., & Nissen, P. E. 1989, A&A, 221, 65
- 866 Shank, D., Beers, T. C., Placco, V. M., et al. 2022, ApJ,
 867 926, 26, doi: [10.3847/1538-4357/ac409a](https://doi.org/10.3847/1538-4357/ac409a)
- 868 Spite, M., Caffau, E., Bonifacio, P., et al. 2013, A&A, 552,
 869 A107, doi: [10.1051/0004-6361/201220989](https://doi.org/10.1051/0004-6361/201220989)
- 870 Starkenburg, E., Martin, N., Youakim, K., et al. 2017,
 871 MNRAS, 471, 2587, doi: [10.1093/mnras/stx1068](https://doi.org/10.1093/mnras/stx1068)
- 872 Taylor, M. B. 2006, in Astronomical Society of the Pacific
 873 Conference Series, Vol. 351, Astronomical Data Analysis
 874 Software and Systems XV, ed. C. Gabriel, C. Arviset,
 875 D. Ponz, & S. Enrique, 666
- 876 Tody, D. 1986, in Proc. SPIE, Vol. 627, Instrumentation in
 877 astronomy VI, ed. D. L. Crawford, 733,
 878 doi: [10.1117/12.968154](https://doi.org/10.1117/12.968154)
- 879 Tody, D. 1993, in Astronomical Society of the Pacific
 880 Conference Series, Vol. 52, Astronomical Data Analysis
 881 Software and Systems II, ed. R. J. Hanisch, R. J. V.
 882 Brissenden, & J. Barnes, 173
- 883 Venn, K. A., Irwin, M., Shetrone, M. D., et al. 2004, AJ,
 884 128, 1177, doi: [10.1086/422734](https://doi.org/10.1086/422734)
- 885 Wallerstein, G. 1964, PASP, 76, 175, doi: [10.1086/128079](https://doi.org/10.1086/128079)
- 886 Whitten, D. D., Placco, V. M., Beers, T. C., et al. 2019,
 887 A&A, 622, A182, doi: [10.1051/0004-6361/201833368](https://doi.org/10.1051/0004-6361/201833368)
- 888 —. 2021, ApJ, 912, 147, doi: [10.3847/1538-4357/abee7e](https://doi.org/10.3847/1538-4357/abee7e)
- 889 Williams, T., & Kelley, C. 2015, Gnuplot 5.0: an interactive
 890 plotting program, <http://www.gnuplot.info/>
- 891 Wilson, E. B. 1927, Journal of the American Statistical
 892 Association, 22, 209,
 893 doi: [10.1080/01621459.1927.10502953](https://doi.org/10.1080/01621459.1927.10502953)
- 894 Wolf, C., Onken, C. A., Luval, L. C., et al. 2018, PASA,
 895 35, e010, doi: [10.1017/pasa.2018.5](https://doi.org/10.1017/pasa.2018.5)
- 896 Woosley, S. E., & Weaver, T. A. 1995, ApJS, 101, 181,
 897 doi: [10.1086/192237](https://doi.org/10.1086/192237)
- 898 Yanny, B., Rockosi, C., Newberg, H. J., et al. 2009, AJ,
 899 137, 4377, doi: [10.1088/0004-6256/137/5/4377](https://doi.org/10.1088/0004-6256/137/5/4377)
- 900 Yoon, J., Whitten, D. D., Beers, T. C., et al. 2020, ApJ,
 901 894, 7, doi: [10.3847/1538-4357/ab7daf](https://doi.org/10.3847/1538-4357/ab7daf)
- 902 Yoon, J., Beers, T. C., Placco, V. M., et al. 2016, ApJ, 833,
 903 20, doi: [10.3847/0004-637X/833/1/20](https://doi.org/10.3847/0004-637X/833/1/20)
- 904 Yoon, J., Beers, T. C., Dietz, S., et al. 2018, ApJ, 861, 146,
 905 doi: [10.3847/1538-4357/aaccea](https://doi.org/10.3847/1538-4357/aaccea)
- 906 York, D. G., Adelman, J., Anderson, Jr., J. E., et al. 2000,
 907 AJ, 120, 1579, doi: [10.1086/301513](https://doi.org/10.1086/301513)
- 908 Youakim, K., Starkenburg, E., Aguado, D. S., et al. 2017,
 909 MNRAS, 472, 2963, doi: [10.1093/mnras/stx2005](https://doi.org/10.1093/mnras/stx2005)
- 910 Yuan, Z., Myeong, G. C., Beers, T. C., et al. 2020, ApJ,
 911 891, 39, doi: [10.3847/1538-4357/ab6ef7](https://doi.org/10.3847/1538-4357/ab6ef7)

Table 1. Observing Details

Star Name (2MASS)	α (J2000)	δ (J2000)	l (deg)	b (deg)	Date (UTC)	Telescope	Instrument	Proposal ID	Exp. (s)
J00044550+0101170	00:04:45.60	+01:01:15.6	99.307	-59.692	2020-12-26	Blanco	COSMOS	2020A-0032	360
J00173643+0009215	00:17:36.48	+00:09:21.6	104.962	-61.530	2020-12-27	Blanco	COSMOS	2020A-0032	360
J00255442-3050320	00:25:54.48	-30:50:31.2	357.784	-83.297	2020-12-27	Blanco	COSMOS	2020A-0032	360
J00271209-3133515	00:27:12.00	-31:33:50.4	351.455	-83.105	2020-12-25	Blanco	COSMOS	2020A-0032	360
J00271240+0100377	00:27:12.48	+01:00:36.0	110.255	-61.264	2020-12-26	Blanco	COSMOS	2020A-0032	360
J00355591-4204306	00:35:55.92	-42:04:30.0	313.910	-74.721	2021-01-11	Blanco	COSMOS	2020A-0032	180
J00503713-3154131	00:50:37.20	-31:54:14.4	305.016	-85.221	2020-12-28	Blanco	COSMOS	2020A-0032	540
J00503717-3408167	00:50:37.20	-34:08:16.8	304.318	-82.988	2021-01-11	Blanco	COSMOS	2020A-0032	90
J00520900-0046092	00:52:08.88	-00:46:08.4	123.332	-63.640	2019-10-17	Blanco	COSMOS	2019B-0069	600
J00542886-3001012	00:54:28.80	-30:01:01.2	290.094	-87.035	2020-12-25	Blanco	COSMOS	2020A-0032	480
J00552124-3031172	00:55:21.36	-30:31:15.6	288.971	-86.500	2020-12-26	Blanco	COSMOS	2020A-0032	600
J01044308-3941159	01:04:43.20	-39:41:16.8	291.379	-77.141	2020-12-24	Blanco	COSMOS	2020A-0032	1500
J01062973-3030595	01:06:29.76	-30:31:01.2	259.602	-85.272	2020-12-27	Blanco	COSMOS	2020A-0032	1200
J01072229-3257031	01:07:22.32	-32:57:03.6	273.274	-83.234	2021-01-10	Blanco	COSMOS	2020A-0032	240
J01115530-3439512	01:11:55.20	-34:39:50.4	273.970	-81.280	2020-12-27	Blanco	COSMOS	2020A-0032	540
J01115596-2924247	01:11:55.92	-29:24:25.2	240.922	-84.946	2021-01-08	Blanco	COSMOS	2020A-0032	600
J01132882-3505175	01:13:28.80	-35:05:16.8	273.663	-80.751	2020-12-22	Blanco	COSMOS	2020A-0032	900
J01142762-3229200	01:14:27.60	-32:29:20.4	261.359	-82.676	2020-12-28	Blanco	COSMOS	2020A-0032	780
J01153574-3148352	01:15:35.76	-31:48:36.0	256.067	-82.962	2021-01-10	Blanco	COSMOS	2020A-0032	360
J01153906-3234184	01:15:39.12	-32:34:19.2	260.440	-82.440	2021-01-11	Blanco	COSMOS	2020A-0032	150
J01174900-3149004	01:17:48.96	-31:49:01.2	253.756	-82.591	2021-01-10	Blanco	COSMOS	2020A-0032	780
J01205304-3435456	01:20:53.04	-34:35:45.6	264.529	-80.224	2020-12-28	Blanco	COSMOS	2020A-0032	660
J01232034-3218276	01:23:20.40	-32:18:28.8	251.649	-81.356	2020-12-26	Blanco	COSMOS	2020A-0032	1020
J01252234-3158080	01:25:22.32	-31:58:08.4	248.234	-81.179	2021-01-07	Blanco	COSMOS	2020A-0032	240
J01301783-2929538	01:30:17.76	-29:29:52.8	230.691	-81.129	2021-01-11	Blanco	COSMOS	2020A-0032	210
J01304113-2900179	01:30:41.04	-29:00:18.0	227.446	-81.144	2020-12-25	Blanco	COSMOS	2020A-0032	600
J01335531-2912330	01:33:55.20	-29:12:32.4	227.939	-80.413	2021-01-11	Blanco	COSMOS	2020A-0032	90
J01374941-3407505	01:37:49.44	-34:07:51.6	250.851	-77.824	2021-01-09	Blanco	COSMOS	2020A-0032	540
J01383820-2740120	01:38:38.16	-27:40:12.0	218.604	-79.514	2020-12-22	Blanco	COSMOS	2020A-0032	900
J01384849-3123136	01:38:48.48	-31:23:13.2	238.161	-78.833	2020-12-26	Blanco	COSMOS	2020A-0032	360
J01464720-0102503	01:46:47.28	-01:02:49.2	152.215	-60.732	2021-01-10	Blanco	COSMOS	2020A-0032	480
J01484480-2941171	01:48:44.88	-29:41:16.8	227.777	-77.150	2021-01-11	Blanco	COSMOS	2020A-0032	360
J01530531-2748141	01:53:05.28	-27:48:14.4	219.315	-76.317	2020-12-24	Blanco	COSMOS	2020A-0032	480
J01554444+0104512	01:55:44.40	+01:04:51.6	154.259	-57.826	2020-12-22	Blanco	COSMOS	2020A-0032	900
J02180715-3049591	02:18:07.20	-30:49:58.8	229.160	-70.717	2020-12-25	Blanco	COSMOS	2020A-0032	480
J02284062-3025508	02:28:40.56	-30:25:51.6	227.534	-68.481	2020-12-27	Blanco	COSMOS	2020A-0032	900
J02320469-3115085	02:32:04.80	-31:15:07.2	229.611	-67.702	2021-01-08	Blanco	COSMOS	2020A-0032	420
J02325680+0019492	02:32:56.88	+00:19:48.0	168.709	-53.270	2021-01-07	Blanco	COSMOS	2020A-0032	420
J02371447-4000452	02:37:14.40	-40:00:46.8	250.196	-64.617	2020-12-26	Blanco	COSMOS	2020A-0032	180
J02441085-5009042	02:44:10.80	-50:09:03.6	267.524	-58.510	2020-12-24	Blanco	COSMOS	2020A-0032	900
J02480029+0042038	02:48:00.24	+00:42:03.6	172.895	-50.506	2020-12-24	Blanco	COSMOS	2020A-0032	600
J02480538-3316558	02:48:05.28	-33:16:55.2	233.827	-64.149	2020-12-27	Blanco	COSMOS	2020A-0032	480
J03060042-3336317	03:06:00.48	-33:36:32.4	233.863	-60.396	2020-12-28	Blanco	COSMOS	2020A-0032	1500
J03060937-3308292	03:06:09.36	-33:08:27.6	232.913	-60.391	2020-12-26	Blanco	COSMOS	2020A-0032	1500
J03063076+0017480	03:06:30.72	+00:17:49.2	178.317	-47.516	2020-12-24	Blanco	COSMOS	2020A-0032	240
J03093503-3300063	03:09:35.04	-33:00:07.2	232.578	-59.679	2020-12-22	Blanco	COSMOS	2020A-0032	600
J03110634+0058038	03:11:06.24	+00:58:04.8	178.736	-46.217	2021-01-09	Blanco	COSMOS	2020A-0032	420
J03120419-3054279	03:12:04.32	-30:54:28.8	228.462	-59.150	2020-12-25	Blanco	COSMOS	2020A-0032	360
J03144847+0110166	03:14:48.48	+01:10:15.6	179.415	-45.396	2020-12-24	Blanco	COSMOS	2020A-0032	420
J03145801-3236489	03:14:58.08	-32:36:50.4	231.775	-58.556	2020-12-28	Blanco	COSMOS	2020A-0032	180
J03160457+0004038	03:16:04.56	+00:04:04.8	180.896	-45.891	2020-12-24	Blanco	COSMOS	2020A-0032	420
J03170771-3243481	03:17:07.68	-32:43:48.0	231.990	-58.101	2020-12-26	Blanco	COSMOS	2020A-0032	360
J03193648+0049320	03:19:36.48	+00:49:30.0	180.908	-44.728	2021-01-10	Blanco	COSMOS	2020A-0032	180
J03203189-5525405	03:20:31.92	-55:25:40.8	269.820	-51.017	2020-12-26	Blanco	COSMOS	2020A-0032	540
J03250464-0039506	03:25:04.56	-00:39:50.4	183.748	-44.638	2021-01-09	Blanco	COSMOS	2020A-0032	960
J03255861+0107414	03:25:58.56	+01:07:40.8	182.029	-43.322	2020-12-28	Blanco	COSMOS	2020A-0032	900
J03272930-0100042	03:27:29.28	-01:00:03.6	184.646	-44.378	2020-12-27	Blanco	COSMOS	2020A-0032	420
J0332804-0016148	03:33:28.08	-00:16:15.6	185.131	-42.752	2021-01-09	Blanco	COSMOS	2020A-0032	480
J03370237-3458142	03:37:02.40	-34:58:15.6	235.914	-53.940	2020-12-22	Blanco	COSMOS	2020A-0032	1200
J03384463-0047295	03:38:44.64	-00:47:31.2	186.778	-42.023	2021-01-09	Blanco	COSMOS	2020A-0032	420
J03384871-0058248	03:38:48.72	-00:58:26.4	186.988	-42.119	2020-12-25	Blanco	COSMOS	2020A-0032	420
J03391097-0046039	03:39:11.04	-00:46:04.8	186.841	-41.921	2021-01-08	Blanco	COSMOS	2020A-0032	600
J03394540+0111082	03:39:45.36	+01:11:09.6	184.896	-40.616	2020-12-28	Blanco	COSMOS	2020A-0032	1500

Table 1 *continued*

Table 1 (*continued*)

Star Name (2MASS)	α (J2000)	δ (J2000)	l (deg)	b (deg)	Date (UTC)	Telescope	Instrument	Proposal ID	Exp. (s)
J03412634+0053306	03:41:26.40	+00:53:31.2	185.542	-40.465	2020-12-27	Blanco	COSMOS	2020A-0032	360
J03441353+0033004	03:44:13.44	+00:33:00.0	186.453	-40.121	2021-01-09	Blanco	COSMOS	2020A-0032	90
J03443568+0045022	03:44:35.76	+00:45:03.6	186.318	-39.925	2020-12-27	Blanco	COSMOS	2020A-0032	120
J03445171+0054107	03:44:51.60	+00:54:10.8	186.212	-39.781	2021-01-08	Blanco	COSMOS	2020A-0032	300
J03465824-0009150	03:46:58.32	-00:09:14.4	187.727	-39.992	2020-12-25	Blanco	COSMOS	2020A-0032	1200
J03471548+0049366	03:47:15.60	+00:49:37.2	186.761	-39.348	2020-12-24	Blanco	COSMOS	2020A-0032	240
J03473639+0049039	03:47:36.48	+00:49:01.2	186.839	-39.285	2021-01-09	Blanco	COSMOS	2020A-0032	720
J03474822+0122390	03:47:48.24	+01:22:40.8	186.301	-38.908	2020-12-24	Blanco	COSMOS	2020A-0032	240
J03482415+0111192	03:48:24.24	+01:01:19.2	186.782	-39.003	2020-12-27	Blanco	COSMOS	2020A-0032	150
J03483507+0003027	03:48:35.04	+00:03:03.6	187.823	-39.546	2020-12-27	Blanco	COSMOS	2020A-0032	120
J03530888-0002590	03:53:08.88	-00:03:00.0	188.793	-38.682	2021-01-07	Blanco	COSMOS	2020A-0032	720
J03532457-0009297	03:53:24.48	-00:09:32.4	188.955	-38.693	2021-01-08	Blanco	COSMOS	2020A-0032	720
J03540382+0026534	03:54:03.84	+00:26:52.8	188.448	-38.205	2021-01-07	Blanco	COSMOS	2020A-0032	360
J03540459+0114066	03:54:04.80	+01:14:06.0	187.645	-37.738	2020-12-22	Blanco	COSMOS	2020A-0032	900
J03540956+0033304	03:54:09.60	+00:33:32.4	188.352	-38.121	2021-01-08	Blanco	COSMOS	2020A-0032	240
J03541889+0111247	03:54:18.96	+01:11:24.0	187.735	-37.717	2020-12-25	Blanco	COSMOS	2020A-0032	360
J03543044+0052026	03:54:30.48	+00:52:01.2	188.101	-37.869	2021-01-08	Blanco	COSMOS	2020A-0032	900
J03543348+0038140	03:54:33.60	+00:38:13.2	188.346	-37.994	2021-01-07	Blanco	COSMOS	2020A-0032	300
J03543771+0046406	03:54:37.68	+00:46:40.8	188.214	-37.897	2021-01-08	Blanco	COSMOS	2020A-0032	360
J03544342-0017209	03:54:43.44	-00:17:20.4	189.335	-38.500	2021-01-11	Blanco	COSMOS	2020A-0032	360
J03544466+0031400	03:54:44.64	+00:31:40.8	188.493	-38.021	2021-01-09	Blanco	COSMOS	2020A-0032	420
J03544663+0040139	03:54:46.56	+00:40:15.6	188.352	-37.930	2021-01-07	Blanco	COSMOS	2020A-0032	540
J03545635-0025496	03:54:56.40	-00:25:51.6	189.523	-38.538	2021-01-10	Blanco	COSMOS	2020A-0032	90
J03550876+0014345	03:55:08.88	+00:14:34.8	188.861	-38.105	2021-01-10	Blanco	COSMOS	2020A-0032	660
J03552342+0016535	03:55:23.52	+00:16:55.2	188.866	-38.033	2021-01-11	Blanco	COSMOS	2020A-0032	900
J03552487+0024132	03:55:24.96	+00:24:14.4	188.745	-37.957	2021-01-08	Blanco	COSMOS	2020A-0032	240
J03552546+0030381	03:55:25.44	+00:30:39.6	188.636	-37.893	2021-01-08	Blanco	COSMOS	2020A-0032	780
J03554412+0025099	03:55:44.16	+00:25:08.4	188.789	-37.883	2021-01-10	Blanco	COSMOS	2020A-0032	600
J03554671+0028063	03:55:46.80	+00:28:04.8	188.746	-37.846	2021-01-08	Blanco	COSMOS	2020A-0032	240
J03555316+0033071	03:55:53.04	+00:33:07.2	188.679	-37.775	2021-01-11	Blanco	COSMOS	2020A-0032	420
J03560990+0037133	03:56:09.84	+00:37:12.0	188.661	-37.679	2020-12-25	Blanco	COSMOS	2020A-0032	600
J03563384+0025258	03:56:33.84	+00:25:26.4	188.936	-37.712	2020-12-25	Blanco	COSMOS	2020A-0032	300
J03563495+0017457	03:56:35.04	+00:17:45.6	189.071	-37.782	2021-01-10	Blanco	COSMOS	2020A-0032	360
J03565939-0056148	03:56:59.52	-00:56:16.8	190.429	-38.409	2021-01-07	Blanco	COSMOS	2020A-0032	180
J03565954+0008420	03:56:59.52	+00:08:42.0	189.302	-37.787	2021-01-11	Blanco	COSMOS	2020A-0032	90
J03574129+0122357	03:57:41.28	+01:22:33.6	188.172	-36.927	2020-12-28	Blanco	COSMOS	2020A-0032	150
J03574260+0115213	03:57:42.72	+01:15:21.6	188.298	-36.993	2021-01-07	Blanco	COSMOS	2020A-0032	150
J03582339-3438018	03:58:23.28	-34:38:02.4	235.472	-49.554	2021-01-08	Blanco	COSMOS	2020A-0032	240
J03582979-3841492	03:58:29.76	-38:41:49.2	241.736	-49.542	2021-01-10	Blanco	COSMOS	2020A-0032	360
J03583937-3739179	03:58:39.36	-37:39:18.0	240.130	-49.540	2020-12-26	Blanco	COSMOS	2020A-0032	660
J03585338+0007050	03:58:53.28	+00:07:04.8	189.675	-37.415	2020-12-22	Blanco	COSMOS	2020A-0032	360
J03590482+0046515	03:59:04.80	+00:46:51.6	189.031	-36.993	2021-01-07	Blanco	COSMOS	2020A-0032	480
J03592020+0034443	03:59:20.16	+00:34:44.4	189.284	-37.058	2021-01-07	Blanco	COSMOS	2020A-0032	300
J03592418-3651140	03:59:24.24	-36:51:14.4	238.895	-49.398	2020-12-26	Blanco	COSMOS	2020A-0032	1020
J03592423+0043021	03:59:24.24	+00:43:01.2	189.155	-36.964	2020-12-24	Blanco	COSMOS	2020A-0032	180
J03592681+0022272	03:59:26.88	+00:22:26.4	189.514	-37.154	2020-12-22	Blanco	COSMOS	2020A-0032	300
J03592803+0036543	03:59:28.08	+00:36:54.0	189.271	-37.010	2021-01-11	Blanco	COSMOS	2020A-0032	90
J03593987+0106448	03:59:39.84	+01:06:43.2	188.801	-36.681	2020-12-28	Blanco	COSMOS	2020A-0032	180
J03594115+0043429	03:59:41.04	+00:43:44.4	189.194	-36.900	2021-01-10	Blanco	COSMOS	2020A-0032	90
J04003943-3513394	04:00:39.36	-35:13:40.8	236.412	-49.113	2020-12-27	Blanco	COSMOS	2020A-0032	900
J04085456-3948262	04:08:54.48	-39:48:25.2	243.304	-47.489	2021-01-07	Blanco	COSMOS	2020A-0032	780
J04095416-4007327	04:09:54.24	-40:07:33.6	243.766	-47.288	2020-12-28	Blanco	COSMOS	2020A-0032	240
J04105455-3321498	04:10:54.48	-33:21:50.4	233.843	-46.876	2021-01-09	Blanco	COSMOS	2020A-0032	360
J04115568-3341064	04:11:55.68	-33:41:06.0	234.339	-46.695	2020-12-25	Blanco	COSMOS	2020A-0032	360
J04140591-3727559	04:14:06.00	-37:27:57.6	239.870	-46.479	2020-12-24	Blanco	COSMOS	2020A-0032	420
J04145894-3255389	04:14:59.04	-32:55:40.8	233.342	-45.982	2020-12-22	Blanco	COSMOS	2020A-0032	1200
J04162964-4110418	04:16:29.76	-41:10:40.8	245.236	-46.003	2021-01-09	Blanco	COSMOS	2020A-0032	300
J04165229-3817335	04:16:52.32	-38:17:34.8	241.084	-45.951	2021-01-11	Blanco	COSMOS	2020A-0032	240
J04180140-3841420	04:18:01.44	-38:41:42.0	241.666	-45.733	2020-12-22	Blanco	COSMOS	2020A-0032	360
J04203417-3430458	04:20:34.08	-34:30:46.8	235.762	-44.991	2020-12-26	Blanco	COSMOS	2020A-0032	240
J04213793-3343353	04:21:37.92	-33:43:37.2	234.692	-44.691	2020-12-25	Blanco	COSMOS	2020A-0032	600
J04220661-4111088	04:22:06.72	-41:11:09.6	245.209	-44.946	2021-01-08	Blanco	COSMOS	2020A-0032	360
J04253919-3814243	04:25:39.12	-38:14:24.0	241.085	-44.227	2021-01-11	Blanco	COSMOS	2020A-0032	780
J04254177-3640132	04:25:41.76	-36:40:12.0	238.900	-44.130	2021-01-11	Blanco	COSMOS	2020A-0032	360
J04271588-4113523	04:27:15.84	-41:13:51.6	245.258	-43.977	2021-01-11	Blanco	COSMOS	2020A-0032	360
J04315718-4354175	04:31:57.12	-43:54:18.0	248.924	-43.065	2020-12-26	Blanco	COSMOS	2020A-0032	240

Table 1 *continued*

Table 1 (*continued*)

Star Name (2MASS)	α (J2000)	δ (J2000)	l (deg)	b (deg)	Date (UTC)	Telescope	Instrument	Proposal ID	Exp. (s)
J04322488-4639409	04:32:24.96	-46:39:39.6	252.677	-42.832	2021-01-10	Blanco	COSMOS	2020A-0032	360
J04322908-3947519	04:32:29.04	-39:47:52.8	243.306	-42.962	2020-12-25	Blanco	COSMOS	2020A-0032	1500
J04323909-4634270	04:32:38.88	-46:34:26.4	252.555	-42.799	2021-01-09	Blanco	COSMOS	2020A-0032	180
J04324431-3445588	04:32:44.40	-34:45:57.6	236.477	-42.528	2021-01-11	Blanco	COSMOS	2020A-0032	360
J04351543-4250160	04:35:15.36	-42:50:16.8	247.454	-42.485	2021-01-10	Blanco	COSMOS	2020A-0032	360
J04352215-4704488	04:35:22.08	-47:04:48.0	253.193	-42.297	2020-12-28	Blanco	COSMOS	2020A-0032	900
J04354512-4350225	04:35:45.12	-43:50:24.0	248.810	-42.382	2021-01-09	Blanco	COSMOS	2020A-0032	120
J04355217-4203517	04:35:52.08	-42:03:50.4	246.406	-42.371	2021-01-08	Blanco	COSMOS	2020A-0032	300
J04371974-4254147	04:37:19.68	-42:54:14.4	247.542	-42.105	2021-01-09	Blanco	COSMOS	2020A-0032	420
J04375734-3337240	04:37:57.36	-33:37:22.8	235.143	-41.310	2020-12-28	Blanco	COSMOS	2020A-0032	960
J04380295-4736337	04:38:02.88	-47:36:32.4	253.859	-41.806	2020-12-25	Blanco	COSMOS	2020A-0032	1020
J04382497-4215130	04:38:24.96	-42:15:14.4	246.669	-41.901	2021-01-08	Blanco	COSMOS	2020A-0032	240
J04402161-3549473	04:40:21.60	-35:49:48.0	238.138	-41.108	2020-12-26	Blanco	COSMOS	2020A-0032	540
J04404847-4214219	04:40:48.48	-42:14:24.0	246.659	-41.458	2021-01-07	Blanco	COSMOS	2020A-0032	120
J04424308-3630571	04:42:43.20	-36:30:57.6	239.111	-40.713	2020-12-24	Blanco	COSMOS	2020A-0032	780
J04425689-4627403	04:42:56.88	-46:27:39.6	252.269	-41.036	2020-12-27	Blanco	COSMOS	2020A-0032	540
J04441395-3356317	04:44:13.92	-33:56:31.2	235.815	-40.067	2021-01-10	Blanco	COSMOS	2020A-0032	90
J04484727-3945309	04:48:47.28	-39:45:32.4	243.491	-39.832	2020-12-28	Blanco	COSMOS	2020A-0032	780
J04485242-3709099	04:48:52.32	-37:09:10.8	240.122	-39.562	2020-12-26	Blanco	COSMOS	2020A-0032	480
J04495212-3210361	04:49:52.08	-32:10:37.2	233.825	-38.604	2020-12-26	Blanco	COSMOS	2020A-0032	960
J04504685-3946382	04:50:46.80	-39:46:37.2	243.555	-39.452	2021-01-10	Blanco	COSMOS	2020A-0032	360
J04512454-3139582	04:51:24.48	-31:39:57.6	233.265	-38.185	2020-12-24	Blanco	COSMOS	2020A-0032	300
J04543666-4754298	04:54:36.72	-47:54:28.8	254.080	-39.012	2021-01-07	Blanco	COSMOS	2020A-0032	540
J04545976-4212485	04:54:59.76	-42:12:50.4	246.762	-38.833	2020-12-22	Blanco	COSMOS	2020A-0032	480
J04551021-3249438	04:55:10.32	-32:49:44.4	234.905	-37.628	2020-12-24	Blanco	COSMOS	2020A-0032	780
J04590976-4632284	04:59:09.84	-46:32:27.6	252.326	-38.245	2021-01-10	Blanco	COSMOS	2020A-0032	360
J04592454-4518477	04:59:24.48	-45:18:46.8	250.764	-38.176	2021-01-08	Blanco	COSMOS	2020A-0032	420
J09580012-1803531	09:58:00.24	-18:03:54.0	255.099	28.281	2021-01-10	Blanco	COSMOS	2020A-0032	240
J09595158-0822008	09:59:51.60	-08:22:01.2	247.269	35.361	2021-01-07	Blanco	COSMOS	2020A-0032	300
J10003629-1725512	10:00:36.30	-17:25:51.3	255.108	29.167	2022-04-13	Blanco	COSMOS	2022A-210002	1500
J10005938-1800599	10:00:59.52	-18:01:01.2	255.646	28.806	2022-05-03	Gemini-South	GMOS-S	GS-2022A-Q-406	1200
J10011607-1747125	10:01:16.08	-17:47:13.2	255.520	29.018	2021-01-09	Blanco	COSMOS	2020A-0032	360
J10021099-0030092	10:02:11.04	-00:30:10.8	240.067	40.851	2020-12-26	Blanco	COSMOS	2020A-0032	360
J10024495-1716153	10:02:44.88	-17:16:15.6	255.407	29.635	2021-01-11	Blanco	COSMOS	2020A-0032	300
J10040075+0134108	10:04:00.72	+01:34:12.0	238.219	42.464	2021-06-16	Gemini-South	GMOS-S	GS-2021A-Q-419	1800
J10040252-0917128	10:04:02.64	-09:17:13.2	248.959	35.499	2020-12-26	Blanco	COSMOS	2020A-0032	420
J10040553+0235484	10:04:05.52	+02:35:49.2	237.103	43.084	2021-01-09	Blanco	COSMOS	2020A-0032	240
J10040693-1138417	10:04:06.72	-11:38:42.0	251.044	33.880	2021-01-08	Blanco	COSMOS	2020A-0032	180
J10043854-0939488	10:04:38.64	-09:39:50.4	249.420	35.348	2021-01-09	Blanco	COSMOS	2020A-0032	420
J10050873+0025517	10:05:08.64	+00:25:51.6	239.679	42.007	2021-01-09	Blanco	COSMOS	2020A-0032	300
J10052824-0911423	10:05:28.32	-09:11:42.0	249.174	35.818	2021-01-08	Blanco	COSMOS	2020A-0032	540
J10052863-1433198	10:05:28.64	-14:33:20.0	253.772	32.051	2022-04-13	Blanco	COSMOS	2022A-210002	600
J10053549-0924326	10:05:35.52	-09:24:32.4	249.390	35.693	2021-01-08	Blanco	COSMOS	2020A-0032	540
J10054690-1226387	10:05:46.90	-12:26:38.8	252.072	33.608	2022-04-13	Blanco	COSMOS	2022A-210002	360
J10062477-1950366	10:06:24.72	-19:50:38.4	258.129	28.330	2021-07-04	Gemini-South	GMOS-S	GS-2021A-Q-419	1200
J10072392-1317186	10:07:24.00	-13:17:20.4	253.120	33.284	2020-12-22	Blanco	COSMOS	2020A-0032	600
J10081117-1918306	10:08:11.28	-19:18:32.4	258.079	29.007	2021-01-11	Blanco	COSMOS	2020A-0032	300
J10092998-2057477	10:09:30.00	-20:57:46.8	259.583	27.967	2020-12-27	Blanco	COSMOS	2020A-0032	540
J10093999-1641194	10:09:40.08	-16:41:20.4	256.352	31.188	2020-12-26	Blanco	COSMOS	2020A-0032	360
J10105387-1754549	10:10:53.76	-17:54:54.0	257.562	30.475	2021-01-09	Blanco	COSMOS	2020A-0032	300
J10113371-1342160	10:11:33.84	-13:42:14.4	254.340	33.686	2021-01-09	Blanco	COSMOS	2020A-0032	180
J10154250-1611132	10:15:42.48	-16:11:13.2	257.223	32.531	2020-12-22	Blanco	COSMOS	2020A-0032	1200
J10165359-1937168	10:16:53.60	-19:37:17.2	260.098	30.113	2022-04-13	Blanco	COSMOS	2022A-210002	420
J10174646-2106150	10:17:46.56	-21:06:14.4	261.369	29.103	2021-01-08	Blanco	COSMOS	2020A-0032	360
J10184004-2031276	10:18:40.08	-20:31:26.4	261.133	29.684	2020-12-28	Blanco	COSMOS	2020A-0032	960
J10184162-1729364	10:18:41.52	-17:29:38.4	258.875	32.013	2020-12-27	Blanco	COSMOS	2020A-0032	1500
J10192807-2020499	10:19:28.08	-20:20:49.2	261.171	29.939	2020-12-26	Blanco	COSMOS	2020A-0032	960
J10193237-1638584	10:19:32.40	-16:39:00.0	258.407	32.786	2020-12-28	Blanco	COSMOS	2020A-0032	480
J10254045-1622201	10:25:40.56	-16:22:19.2	259.540	33.946	2020-12-26	Blanco	COSMOS	2020A-0032	1380
J10255315-1635461	10:25:53.04	-16:35:45.6	259.758	33.805	2020-12-25	Blanco	COSMOS	2020A-0032	360
J10261897-1459502	10:26:18.96	-14:59:49.2	258.614	35.101	2022-05-13	Gemini-South	GMOS-S	GS-2022A-Q-406	1500
J10264356-1425080	10:26:43.44	-14:25:08.4	258.250	35.606	2021-07-04	Gemini-South	GMOS-S	GS-2021A-Q-419	1200
J10285881-1527074	10:28:58.80	-15:27:07.2	259.574	35.161	2021-01-11	Blanco	COSMOS	2020A-0032	360
J10292435-1859548	10:29:24.24	-18:59:56.4	262.330	32.450	2020-12-25	Blanco	COSMOS	2020A-0032	480
J10315059-1914338	10:31:50.64	-19:14:34.8	263.049	32.607	2022-05-20	Gemini-South	GMOS-S	GS-2022A-Q-406	1800
J10320298-1650547	10:32:03.12	-16:50:56.4	261.340	34.533	2020-12-22	Blanco	COSMOS	2020A-0032	600

Table 1 *continued*

Table 1 (*continued*)

Star Name (2MASS)	α (J2000)	δ (J2000)	l (deg)	b (deg)	Date (UTC)	Telescope	Instrument	Proposal ID	Exp. (s)
J10323970-2044339	10:32:39.60	-20:44:34.8	264.291	31.521	2020-12-26	Blanco	COSMOS	2020A-0032	1080
J10341301-1753472	10:34:12.96	-17:53:49.2	262.610	34.019	2021-01-10	Blanco	COSMOS	2020A-0032	240
J10362492-1900221	10:36:24.96	-19:00:21.6	263.911	33.443	2021-01-10	Blanco	COSMOS	2020A-0032	360
J10371207-1855498	10:37:12.00	-18:55:51.6	264.037	33.614	2021-01-10	Blanco	COSMOS	2020A-0032	120
J10394834-1719284	10:39:48.24	-17:19:30.0	263.490	35.274	2021-01-08	Blanco	COSMOS	2020A-0032	420
J10414658-1827443	10:41:46.56	-18:27:43.2	264.767	34.628	2022-05-20	Gemini-South	GMOS-S	GS-2022A-Q-406	1650
J10414788-1715518	10:41:48.00	-17:15:50.4	263.918	35.605	2021-01-08	Blanco	COSMOS	2020A-0032	360
J10434103-1712132	10:43:41.04	-17:12:14.4	264.325	35.916	2021-01-08	Blanco	COSMOS	2020A-0032	300
J10482732-1707224	10:48:27.36	-17:07:22.8	265.425	36.637	2021-01-10	Blanco	COSMOS	2020A-0032	420
J10485833-2143574	10:48:58.32	-21:43:58.8	268.653	32.863	2021-01-09	Blanco	COSMOS	2020A-0032	180
J10511281-2136425	10:51:12.72	-21:36:43.2	269.100	33.244	2020-12-27	Blanco	COSMOS	2020A-0032	660
J10512357-2121108	10:51:23.52	-21:21:10.8	268.977	33.486	2021-01-09	Blanco	COSMOS	2020A-0032	480
J10570497-2215021	10:57:05.04	-22:15:03.6	270.889	33.410	2021-01-08	Blanco	COSMOS	2020A-0032	240
J10572425-2110418	10:57:24.24	-21:10:40.8	270.304	34.369	2021-01-11	Blanco	COSMOS	2020A-0032	660
J10573193-2223341	10:57:31.92	-22:23:34.8	271.082	33.340	2021-01-11	Blanco	COSMOS	2020A-0032	600
J10580923-2144147	10:58:09.36	-21:44:13.2	270.831	33.979	2021-01-11	Blanco	COSMOS	2020A-0032	240
J11001243-2111286	11:00:12.48	-21:11:27.6	270.994	34.691	2021-01-08	Blanco	COSMOS	2020A-0032	420
J11002053-1833151	11:00:20.64	-18:33:14.4	269.363	36.973	2020-12-27	Blanco	COSMOS	2020A-0032	780
J11022646-2342494	11:02:26.40	-23:42:50.4	273.034	32.754	2020-12-24	Blanco	COSMOS	2020A-0032	420
J11030563-2231467	11:03:05.52	-22:31:48.0	272.502	33.861	2021-01-09	Blanco	COSMOS	2020A-0032	150
J11081009-1944043	11:08:10.08	-19:44:06.0	272.104	36.879	2022-05-13	Gemini-South	GMOS-S	GS-2022A-Q-406	1815
J11083127-2235143	11:08:31.20	-22:35:13.2	273.864	34.410	2020-12-24	Blanco	COSMOS	2020A-0032	420
J11120172-2212075	11:12:01.68	-22:12:07.2	274.522	35.127	2020-12-25	Blanco	COSMOS	2020A-0032	480
J11124929-2357161	11:12:49.20	-23:57:18.0	275.679	33.645	2020-12-24	Blanco	COSMOS	2020A-0032	1200
J11135686-2041051	11:13:56.88	-20:41:06.0	274.156	36.680	2021-01-10	Blanco	COSMOS	2020A-0032	180
J11135726-2222091	11:13:57.12	-22:22:08.4	275.100	35.180	2021-01-09	Blanco	COSMOS	2020A-0032	90
J11144560-2212214	11:14:45.60	-22:12:21.6	275.215	35.409	2020-12-28	Blanco	COSMOS	2020A-0032	540
J11162403-1843000	11:16:24.00	-18:43:01.2	273.663	38.694	2020-12-25	Blanco	COSMOS	2020A-0032	540
J11171192-1911211	11:17:12.00	-19:11:24.0	274.154	38.359	2021-01-09	Blanco	COSMOS	2020A-0032	150
J11190308-1846350	11:19:03.12	-18:46:33.6	274.415	38.926	2021-01-10	Blanco	COSMOS	2020A-0032	180
J11194427-2308401	11:19:44.16	-23:08:42.0	276.981	35.064	2022-04-25	Gemini-South	GMOS-S	GS-2022A-Q-406	1320
J11194933-2317327	11:19:49.44	-23:17:31.2	277.079	34.939	2021-01-11	Blanco	COSMOS	2020A-0032	240
J11201142-1933447	11:20:11.52	-19:33:43.2	275.171	38.342	2020-12-24	Blanco	COSMOS	2020A-0032	420
J11203812-2356163	11:20:38.16	-23:56:16.8	277.614	34.431	2021-01-10	Blanco	COSMOS	2020A-0032	180
J11220137-2330358	11:22:01.44	-23:30:36.0	277.750	34.952	2020-12-27	Blanco	COSMOS	2020A-0032	420
J11222244-1818163	11:22:22.56	-18:18:18.0	275.058	39.698	2022-05-20	Gemini-South	GMOS-S	GS-2022A-Q-406	1080
J11225058-2243447	11:22:50.64	-22:43:44.4	277.565	35.741	2021-01-07	Blanco	COSMOS	2020A-0032	420
J11225672-1902327	11:22:56.64	-19:02:34.8	275.630	39.092	2020-12-25	Blanco	COSMOS	2020A-0032	420
J11230328-2126276	11:23:03.36	-21:26:27.6	276.955	36.933	2020-12-25	Blanco	COSMOS	2020A-0032	480
J11241118-2115149	11:24:11.28	-21:15:14.4	277.158	37.213	2021-01-10	Blanco	COSMOS	2020A-0032	780
J11254036-2034269	11:25:40.37	-20:34:27.4	277.201	37.975	2022-04-13	Blanco	COSMOS	2022A-210002	1800
J11254158-2449096	11:25:41.52	-24:49:08.4	279.319	34.091	2021-01-10	Blanco	COSMOS	2020A-0032	240
J11300605-2138213	11:30:06.00	-21:38:20.4	278.936	37.414	2020-12-25	Blanco	COSMOS	2020A-0032	1200
J11304517-2347312	11:30:45.36	-23:47:31.2	280.135	35.483	2021-01-11	Blanco	COSMOS	2020A-0032	180
J11312025-1957045	11:31:20.16	-19:57:03.6	278.434	39.080	2022-04-28	Gemini-South	GMOS-S	GS-2022A-Q-406	1200
J11312204-2148119	11:31:22.08	-21:48:10.8	279.357	37.376	2021-01-10	Blanco	COSMOS	2020A-0032	360
J11325195-1228109	11:32:52.08	-12:28:12.0	274.707	46.052	2021-01-10	Blanco	COSMOS	2020A-0032	240
J11345006-2056390	11:34:50.16	-20:56:38.4	279.893	38.477	2020-12-24	Blanco	COSMOS	2020A-0032	300
J11363130-1945100	11:36:31.20	-19:45:10.8	279.794	39.729	2021-01-10	Blanco	COSMOS	2020A-0032	300
J11373260-2257565	11:37:32.64	-22:57:57.6	281.558	36.820	2021-01-11	Blanco	COSMOS	2020A-0032	360
J11383060-1825588	11:38:30.72	-18:25:58.8	279.725	41.129	2021-01-10	Blanco	COSMOS	2020A-0032	240
J11403793-2013014	11:40:37.92	-20:13:01.2	281.182	39.646	2021-01-11	Blanco	COSMOS	2020A-0032	90
J11404863-0231525	11:40:48.48	-02:31:51.6	270.307	55.801	2022-04-25	Gemini-South	GMOS-S	GS-2022A-Q-406	1500
J11420747-2236055	11:42:07.44	-22:36:07.2	282.646	37.524	2021-01-10	Blanco	COSMOS	2020A-0032	180
J11434535-1852575	11:43:45.36	-18:52:58.8	281.479	41.152	2021-01-08	Blanco	COSMOS	2020A-0032	360
J11440387-1658068	11:44:03.84	-16:58:08.4	280.674	42.972	2021-01-08	Blanco	COSMOS	2020A-0032	360
J11443172-2122152	11:44:31.74	-21:22:15.4	282.796	38.870	2022-04-11	Blanco	COSMOS	2022A-210002	1800
J11445275-2030317	11:44:52.75	-20:30:31.8	282.528	39.711	2022-04-13	Blanco	COSMOS	2022A-210002	480
J11445318-1958567	11:44:53.28	-19:58:55.2	282.302	40.209	2021-01-09	Blanco	COSMOS	2020A-0032	180
J11464483-1936295	11:46:44.81	-19:36:29.6	282.682	40.706	2022-04-13	Blanco	COSMOS	2022A-210002	360
J11464646-2216104	11:46:46.56	-22:16:12.0	283.797	38.187	2021-01-07	Blanco	COSMOS	2020A-0032	660
J11464903-2105098	11:46:48.96	-21:05:09.6	283.326	39.313	2021-01-07	Blanco	COSMOS	2020A-0032	240
J11482911-2109456	11:48:29.04	-21:09:46.8	283.835	39.363	2020-12-27	Blanco	COSMOS	2020A-0032	480
J11493550-2101315	11:49:35.52	-21:01:30.0	284.097	39.574	2021-01-11	Blanco	COSMOS	2020A-0032	300
J11500693-1943013	11:50:06.96	-19:43:01.2	283.720	40.856	2020-12-24	Blanco	COSMOS	2020A-0032	480
J11503041-2209074	11:50:30.48	-22:09:07.2	284.799	38.565	2021-07-05	Gemini-South	GMOS-S	GS-2021A-Q-419	1200

Table 1 *continued*

Table 1 (*continued*)

Star Name	α	δ	l	b	Date	Telescope	Instrument	Proposal ID	Exp.
(2MASS)	(J2000)	(J2000)	(deg)	(deg)	(UTC)				(s)
J111511408–2159328	11:51:14.16	–21:59:34.8	284.945	38.767	2021-01-11	Blanco	COSMOS	2020A-0032	90
J111514550–1834578	11:51:45.60	–18:34:58.8	283.744	42.054	2021-01-07	Blanco	COSMOS	2020A-0032	300
J111525640–2035404	11:52:56.39	–20:35:41.0	284.901	40.220	2022-04-13	Blanco	COSMOS	2022A-210002	300
J111562039–1936572	11:56:20.40	–19:36:57.6	285.538	41.387	2021-01-07	Blanco	COSMOS	2020A-0032	600
J12023299–1931447	12:02:32.98	–19:31:44.9	287.392	41.863	2022-04-13	Blanco	COSMOS	2022A-210002	420
J12023816–1957058	12:02:38.16	–19:57:07.2	287.561	41.459	2020-12-27	Blanco	COSMOS	2020A-0032	540
J12040768–0234051	12:04:07.68	–02:34:04.8	280.074	58.189	2022-05-10	Gemini-South	GMOS-S	GS-2022A-Q-406	1650
J12064282+0004032	12:06:42.72	+00:04:04.8	279.446	60.884	2021-01-07	Blanco	COSMOS	2020A-0032	240
J12090903–1508048	12:09:09.12	–15:08:06.0	288.021	46.509	2020-12-28	Blanco	COSMOS	2020A-0032	660
J12112971–0212276	12:11:29.70	–02:12:27.7	283.198	59.125	2022-04-12	Blanco	COSMOS	2022A-210002	360
J12141957–0036482	12:14:19.44	–00:36:50.4	283.599	60.857	2020-12-27	Blanco	COSMOS	2020A-0032	240
J12184512+0051359	12:18:45.12	+00:51:35.9	284.953	62.585	2022-04-12	Blanco	COSMOS	2022A-210002	540
J12203518–0057582	12:20:35.15	–00:57:58.7	286.894	60.941	2022-04-13	Blanco	COSMOS	2022A-210002	300
J12233624–1522120	12:23:36.25	–15:22:12.7	293.075	46.968	2022-04-13	Blanco	COSMOS	2022A-210002	300
J12234076–0131031	12:23:40.76	–01:31:03.4	288.696	60.585	2022-04-11	Blanco	COSMOS	2022A-210002	1200
J12253942–1452401	12:25:39.36	–14:52:40.8	293.685	47.530	2021-01-10	Blanco	COSMOS	2020A-0032	150
J12290963–0059118	12:29:09.64	–00:59:11.9	291.245	61.379	2022-04-13	Blanco	COSMOS	2022A-210002	1080
J12292867+0115087	12:29:28.63	+01:15:08.5	290.512	63.593	2022-04-13	Blanco	COSMOS	2022A-210002	420
J12381720–1503087	12:38:17.21	–15:03:08.6	298.212	47.699	2022-04-13	Blanco	COSMOS	2022A-210002	900
J12413337–1318137	12:41:33.36	–13:18:14.4	299.229	49.497	2020-12-28	Blanco	COSMOS	2020A-0032	480
J12543883–1440173	12:54:38.88	–14:40:19.2	304.097	48.192	2022-04-28	Gemini-South	GMOS-S	GS-2022A-Q-406	1500
J12551524–1533478	12:55:15.36	–15:33:46.8	304.288	47.299	2021-01-08	Blanco	COSMOS	2020A-0032	540
J12581969–1423114	12:58:19.68	–14:23:13.2	305.448	48.451	2021-01-11	Blanco	COSMOS	2020A-0032	720
J13011453–1455403	13:01:14.64	–14:55:40.8	306.465	47.876	2020-12-28	Blanco	COSMOS	2020A-0032	300
J13012016–1442042	13:01:20.16	–14:42:03.6	306.517	48.102	2021-01-10	Blanco	COSMOS	2020A-0032	300
J13070601–1452022	13:07:06.00	–14:52:01.2	308.574	47.833	2022-04-11	Gemini-South	GMOS-S	GS-2022A-Q-406	1620
J13073449–1327258	13:07:34.56	–13:27:25.2	308.946	49.226	2021-01-10	Blanco	COSMOS	2020A-0032	180
J13073627–1158131	13:07:36.24	–11:58:12.0	309.182	50.705	2022-04-11	Gemini-South	GMOS-S	GS-2022A-Q-406	1800
J13080410–1327591	13:08:04.08	–13:27:57.6	309.127	49.206	2021-01-07	Blanco	COSMOS	2020A-0032	540
J13083350–1313027	13:08:33.60	–13:13:01.2	309.348	49.441	2022-05-14	Gemini-South	GMOS-S	GS-2022A-Q-406	1800
J13091852–1528133	13:09:18.48	–15:28:12.0	309.273	47.182	2021-01-07	Blanco	COSMOS	2020A-0032	240
J13102690–1513172	13:09:26.91	–15:13:17.3	309.361	47.425	2022-04-13	Blanco	COSMOS	2022A-210002	960
J13103235–1257092	13:10:32.40	–12:57:10.8	310.131	49.652	2021-01-07	Blanco	COSMOS	2020A-0032	180
J13115341–1352295	13:11:53.52	–13:52:30.0	310.465	48.697	2021-01-11	Blanco	COSMOS	2020A-0032	360
J13131774–1148370	13:13:17.76	–11:48:36.0	311.395	50.702	2021-06-27	Gemini-South	GMOS-S	GS-2021A-Q-419	1200
J13162234–1439423	13:16:22.32	–14:39:43.2	311.924	47.774	2021-01-07	Blanco	COSMOS	2020A-0032	300
J13175379–0017126	13:17:53.78	–00:17:12.7	317.067	61.857	2022-04-13	Blanco	COSMOS	2022A-210002	1500
J13202007–0850032	13:20:20.05	–08:50:03.2	314.950	53.362	2022-04-13	Blanco	COSMOS	2022A-210002	300
J13202534–1405312	13:20:25.44	–14:05:31.2	313.505	48.184	2021-01-11	Blanco	COSMOS	2020A-0032	450
J13224728+0027099	13:22:47.27	+00:27:09.7	319.980	62.282	2022-04-13	Blanco	COSMOS	2022A-210002	150
J13230218–1401407	13:23:02.19	–14:01:40.6	314.457	48.135	2022-04-13	Blanco	COSMOS	2022A-210002	1200
J13234665–1456070	13:23:46.65	–14:56:06.9	314.471	47.211	2022-04-11	Blanco	COSMOS	2022A-210002	600
J13255973–1331509	13:25:59.76	–13:31:51.2	315.661	48.485	2022-04-13	Blanco	COSMOS	2022A-210002	840
J13260147–1420519	13:26:01.49	–14:20:52.5	315.427	47.683	2022-04-13	Blanco	COSMOS	2022A-210002	360
J13263400–0751220	13:26:33.99	–07:51:22.1	317.841	53.996	2022-04-13	Blanco	COSMOS	2022A-210002	720
J13263837–1351343	13:26:38.40	–13:51:36.0	315.791	48.131	2021-01-09	Blanco	COSMOS	2020A-0032	180
J13273793–0736314	13:27:37.94	–07:36:31.3	318.378	54.174	2022-04-13	Blanco	COSMOS	2022A-210002	900
J13285008–0753313	13:28:50.09	–07:53:31.5	318.753	53.827	2022-04-13	Blanco	COSMOS	2022A-210002	1200
J13285225–1453128	13:28:52.27	–14:53:12.9	316.258	47.014	2022-04-13	Blanco	COSMOS	2022A-210002	300
J13285822–1428027	13:28:58.32	–14:28:01.2	316.425	47.419	2021-06-05	Gemini-South	GMOS-S	GS-2021A-Q-419	498
J13302081–1053210	13:30:20.80	–10:53:21.1	318.161	50.828	2022-04-13	Blanco	COSMOS	2022A-210002	420
J13303025–1445223	13:30:30.24	–14:45:21.6	316.865	47.056	2022-05-09	Gemini-South	GMOS-S	GS-2022A-Q-406	1380
J13304241–1258149	13:30:42.48	–12:58:15.6	317.538	48.784	2021-01-09	Blanco	COSMOS	2020A-0032	300
J13305370–0812151	13:30:53.70	–08:12:15.2	319.453	53.397	2022-04-13	Blanco	COSMOS	2022A-210002	960
J13305807–1524301	13:30:58.07	–15:24:30.3	316.813	46.395	2022-04-13	Blanco	COSMOS	2022A-210002	1320
J1330549–1143314	13:33:05.48	–11:43:31.4	318.864	49.853	2022-04-13	Blanco	COSMOS	2022A-210002	420
J13331559–1032347	13:33:15.60	–10:32:34.8	319.396	50.987	2022-04-13	Blanco	COSMOS	2022A-210002	960
J13334281–0635309	13:33:42.83	–06:35:30.9	321.341	54.762	2022-04-11	Blanco	COSMOS	2022A-210002	1800
J13354161–1231003	13:35:41.52	–12:31:01.2	319.498	48.926	2021-01-08	Blanco	COSMOS	2020A-0032	180
J13354927–1013160	13:35:49.26	–10:13:16.0	320.498	51.131	2022-04-13	Blanco	COSMOS	2022A-210002	480
J13363905–1148292	13:36:39.06	–11:48:29.2	320.131	49.548	2022-04-12	Blanco	COSMOS	2022A-210002	960
J13374402–1217279	13:37:44.04	–12:17:28.0	320.322	49.011	2022-04-13	Blanco	COSMOS	2022A-210002	420
J13382471–0958520	13:38:24.73	–09:58:52.2	321.581	51.182	2022-04-13	Blanco	COSMOS	2022A-210002	420
J13390885–1305334	13:39:08.88	–13:05:34.8	320.491	48.145	2021-01-08	Blanco	COSMOS	2020A-0032	600
J13392436–0847090	13:39:24.48	–08:47:09.6	322.530	52.251	2021-01-09	Blanco	COSMOS	2020A-0032	300
J13394057–0636508	13:39:40.56	–06:36:50.6	323.763	54.295	2022-04-13	Blanco	COSMOS	2022A-210002	360

Table 1 *continued*

Table 1 (*continued*)

Star Name	α	δ	l	b	Date	Telescope	Instrument	Proposal ID	Exp.
(2MASS)	(J2000)	(J2000)	(deg)	(deg)	(UTC)				(s)
J13404551-0633557	13:40:45.60	-06:33:57.6	324.226	54.254	2021-01-09	Blanco	COSMOS	2020A-0032	300
J13410860-1232133	13:41:08.60	-12:32:13.2	321.429	48.541	2022-04-13	Blanco	COSMOS	2022A-210002	840
J13420799-1157040	13:42:07.92	-11:57:03.6	322.041	49.031	2021-06-27	Gemini-South	GMOS-S	GS-2021A-Q-419	300
J13430545-0807438	13:43:05.46	-08:07:43.7	324.287	52.588	2022-04-13	Blanco	COSMOS	2022A-210002	660
J13431375-0948485	13:43:13.75	-09:48:48.5	323.462	50.982	2022-04-13	Blanco	COSMOS	2022A-210002	660
J13432075-1113168	13:43:20.88	-11:13:15.6	322.816	49.636	2022-05-07	Gemini-South	GMOS-S	GS-2022A-Q-406	1800
J13432477-0922116	13:43:24.76	-09:22:11.7	323.756	51.388	2022-04-13	Blanco	COSMOS	2022A-210002	540
J13440121-0910128	13:44:01.20	-09:10:13.4	324.087	51.529	2022-04-13	Blanco	COSMOS	2022A-210002	420
J13442905-0831492	13:44:29.04	-08:31:49.5	324.602	52.095	2022-04-13	Blanco	COSMOS	2022A-210002	360
J13444602-1445281	13:44:46.03	-14:45:28.1	321.712	46.160	2022-04-11	Blanco	COSMOS	2022A-210002	900
J13450057-0640371	13:45:00.57	-06:40:37.1	325.853	53.794	2022-04-12	Blanco	COSMOS	2022A-210002	420
J13452554-0746249	13:45:25.54	-07:46:24.8	325.381	52.729	2022-04-13	Blanco	COSMOS	2022A-210002	360
J13460151-0819059	13:46:01.51	-08:19:06.1	325.303	52.166	2022-04-12	Blanco	COSMOS	2022A-210002	720
J13462090-1507098	13:46:20.90	-15:07:09.7	322.081	45.701	2022-04-13	Blanco	COSMOS	2022A-210002	900
J13481357-0615460	13:48:13.59	-06:15:46.0	327.370	53.893	2022-04-13	Blanco	COSMOS	2022A-210002	660
J13482307-0731330	13:48:23.09	-07:31:33.3	326.658	52.703	2022-04-13	Blanco	COSMOS	2022A-210002	240
J13490050-1404170	13:49:00.46	-14:04:17.2	323.434	46.496	2022-04-13	Blanco	COSMOS	2022A-210002	300
J13501035-1423065	13:50:10.32	-14:23:06.0	323.673	46.108	2021-01-10	Blanco	COSMOS	2020A-0032	360
J13504014-1044541	13:50:40.14	-10:44:54.1	325.672	49.490	2022-04-13	Blanco	COSMOS	2022A-210002	420
J13505366-0750034	13:50:53.76	-07:50:02.4	327.422	52.188	2021-07-10	Gemini-South	GMOS-S	GS-2021A-Q-419	660
J13510296-1324579	13:51:02.98	-13:24:58.1	324.431	46.952	2022-04-12	Blanco	COSMOS	2022A-210002	480
J13511758-0214080	13:51:17.60	-02:14:08.0	331.447	57.285	2022-04-13	Blanco	COSMOS	2022A-210002	720
J13521214-1256228	13:52:12.24	-12:56:24.0	325.057	47.304	2022-05-20	Gemini-South	GMOS-S	GS-2022A-Q-406	1800
J13533510-0617040	13:53:35.09	-06:17:04.2	329.428	53.360	2022-04-13	Blanco	COSMOS	2022A-210002	1500
J13542102-0748421	13:54:21.03	-07:48:42.1	328.721	51.882	2022-04-11	Blanco	COSMOS	2022A-210002	360
J13544697-0056033	13:54:46.98	-00:56:03.5	333.986	58.066	2022-04-13	Blanco	COSMOS	2022A-210002	480
J13550907-01101322	13:55:09.12	-01:01:33.6	334.061	57.942	2021-06-22	Gemini-South	GMOS-S	GS-2021A-Q-419	480
J13552684-1533012	13:55:26.84	-15:33:01.1	324.826	44.583	2022-04-13	Blanco	COSMOS	2022A-210002	1020
J13552725-0226158	13:55:27.36	-02:26:16.8	333.002	56.649	2021-01-11	Blanco	COSMOS	2020A-0032	360
J13554812-1421502	13:55:48.24	-14:21:50.4	325.527	45.665	2021-01-11	Blanco	COSMOS	2020A-0032	330
J13554903-1024575	13:55:48.96	-10:24:57.6	327.669	49.339	2021-01-11	Blanco	COSMOS	2020A-0032	420
J13555260-1202077	13:55:52.61	-12:02:08.0	326.776	47.831	2022-04-13	Blanco	COSMOS	2022A-210002	480
J13562879-0651334	13:56:28.81	-06:51:33.4	330.133	52.543	2022-04-12	Blanco	COSMOS	2022A-210002	1500
J13563597-1406119	13:56:36.00	-14:06:10.8	325.918	45.840	2022-05-20	Gemini-South	GMOS-S	GS-2022A-Q-406	1500
J13563913-1031441	13:56:39.13	-10:31:44.4	327.894	49.156	2022-04-13	Blanco	COSMOS	2022A-210002	780
J13565864-0452027	13:56:58.65	-04:52:02.6	331.725	54.299	2022-04-13	Blanco	COSMOS	2022A-210002	300
J13570105-1533133	13:57:00.96	-15:33:32.4	325.318	44.443	2022-05-13	Gemini-South	GMOS-S	GS-2022A-Q-406	1800
J13573148-1529155	13:57:31.44	-15:29:16.8	325.514	44.467	2021-06-24	Gemini-South	GMOS-S	GS-2021A-Q-419	360
J13575322-0635347	13:57:53.21	-06:35:34.8	330.838	52.641	2022-04-13	Blanco	COSMOS	2022A-210002	720
J13575436+0138509	13:57:54.24	+01:38:49.2	337.738	59.949	2021-06-27	Gemini-South	GMOS-S	GS-2021A-Q-419	660
J13580211-1147193	13:58:02.16	-11:47:20.4	327.643	47.862	2022-05-09	Gemini-South	GMOS-S	GS-2022A-Q-406	1800
J13590545-1331507	13:59:05.44	-13:31:50.5	327.030	46.152	2022-04-13	Blanco	COSMOS	2022A-210002	600
J14000698-0724400	14:00:06.98	-07:24:40.0	331.094	51.666	2022-04-13	Blanco	COSMOS	2022A-210002	300
J14004719-1323003	14:00:47.26	-13:23:02.0	327.661	46.131	2022-04-13	Blanco	COSMOS	2022A-210002	600
J14005144-1052395	14:00:51.45	-10:52:39.9	329.130	48.431	2022-04-13	Blanco	COSMOS	2022A-210002	600
J14013381-0702242	14:01:33.81	-07:02:24.4	331.875	51.847	2022-04-13	Blanco	COSMOS	2022A-210002	480
J14014158-0653325	14:01:41.58	-06:53:32.7	332.026	51.966	2022-04-12	Blanco	COSMOS	2022A-210002	480
J14021343-0620160	14:02:13.40	-06:20:15.9	332.616	52.406	2022-04-13	Blanco	COSMOS	2022A-210002	360
J14135326-2528368	14:13:53.28	-25:28:37.2	325.409	33.771	2021-06-27	Gemini-South	GMOS-S	GS-2021A-Q-419	1200
J14151573-2527453	14:15:15.74	-25:27:45.3	325.761	33.666	2022-04-13	Blanco	COSMOS	2022A-210002	540
J14184988-2520449	14:18:49.88	-25:20:45.4	326.706	33.459	2022-04-12	Blanco	COSMOS	2022A-210002	720
J14233651-2537324	14:23:36.48	-25:37:33.6	327.747	32.766	2021-07-14	Gemini-South	GMOS-S	GS-2021A-Q-419	480
J14244532-2542471	14:24:45.36	-25:42:46.8	327.983	32.579	2021-06-18	Gemini-South	GMOS-S	GS-2021A-Q-419	420
J14271500+0600227	14:27:15.01	+06:00:22.6	354.420	58.936	2022-04-13	Blanco	COSMOS	2022A-210002	600
J14502910-2526048	14:50:29.04	-25:26:06.0	334.149	30.124	2021-06-05	Gemini-South	GMOS-S	GS-2021A-Q-419	900
J14511827-2055451	14:51:18.24	-20:55:44.4	337.117	33.867	2022-04-28	Gemini-South	GMOS-S	GS-2022A-Q-406	1650
J14513033-2512253	14:51:30.34	-25:12:25.5	334.513	30.201	2022-04-12	Blanco	COSMOS	2022A-210002	480
J14521073-2106049	14:52:10.80	-21:06:03.6	337.213	33.612	2022-04-28	Gemini-South	GMOS-S	GS-2022A-Q-406	1500
J14523635-2139456	14:52:36.24	-21:39:46.8	336.952	33.085	2021-06-20	Gemini-South	GMOS-S	GS-2021A-Q-419	780
J14523952+0505565	14:52:39.51	+05:05:56.7	1.018	53.693	2022-04-11	Blanco	COSMOS	2022A-210002	480
J14532817-2239567	14:53:28.17	-22:39:57.1	336.517	32.130	2022-04-13	Blanco	COSMOS	2022A-210002	900
J14533245-2110176	14:53:32.40	-21:10:19.2	337.488	33.381	2022-05-13	Gemini-South	GMOS-S	GS-2022A-Q-406	1800
J14533615+0526514	14:53:36.16	+05:26:51.2	1.724	53.740	2022-04-11	Blanco	COSMOS	2022A-210002	420
J14541347-2336512	14:54:13.49	-23:36:51.0	336.096	31.235	2022-04-13	Blanco	COSMOS	2022A-210002	1500
J14550579-2505475	14:55:05.79	-25:05:47.4	335.381	29.872	2022-04-11	Blanco	COSMOS	2022A-210002	780
J14551208-2232367	14:55:12.00	-22:32:38.4	336.992	32.018	2021-06-21	Gemini-South	GMOS-S	GS-2021A-Q-419	1200

Table 1 *continued*

Table 1 (*continued*)

Star Name (2MASS)	α (J2000)	δ (J2000)	l (deg)	b (deg)	Date (UTC)	Telescope	Instrument	Proposal ID	Exp. (s)
J14561699–2059219	14:56:17.04	–20:59:20.4	338.249	33.185	2022-05-09	Gemini-South	GMOS-S	GS-2022A-Q-406	1500
J14561723–2202397	14:56:17.24	–22:02:39.7	337.561	32.302	2022-04-11	Blanco	COSMOS	2022A-210002	1800
J14563893+0459229	14:56:38.93	+04:59:23.0	1.954	52.865	2022-04-12	Blanco	COSMOS	2022A-210002	1500
J14564274–2310276	14:56:42.72	–23:10:26.4	336.936	31.300	2021-06-18	Gemini-South	GMOS-S	GS-2021A-Q-419	1500
J19584551+0054253	19:58:45.54	+00:54:25.3	41.611	–14.503	2022-04-13	Blanco	COSMOS	2022A-210002	660
J19585614+0047295	19:58:56.15	+00:47:29.5	41.528	–14.597	2022-04-13	Blanco	COSMOS	2022A-210002	1200
J19590382+0119513	19:59:03.84	+01:19:51.6	42.034	–14.368	2021-06-14	Gemini-South	GMOS-S	GS-2021A-Q-419	1500
J19590543–0105589	19:59:05.52	–01:06:00.0	39.820	–15.523	2019-05-08	Gemini-South	GMOS-S	GS-2019A-Q-408	1800
J19593741+0050858	19:59:37.42	+00:50:06.0	41.773	–14.664	2022-04-13	Blanco	COSMOS	2022A-210002	900
J19595905+0113391	19:59:59.06	+01:13:39.1	42.053	–14.620	2022-04-13	Blanco	COSMOS	2022A-210002	1500
J20002309+0035205	20:00:23.04	+00:35:20.4	41.521	–15.012	2021-06-10	Gemini-South	GMOS-S	GS-2021A-Q-419	900
J20002987+0114169	20:00:29.86	+01:14:17.0	42.126	–14.728	2022-04-13	Blanco	COSMOS	2022A-210002	300
J20003435–0021415	20:00:34.32	–00:21:43.2	40.676	–15.503	2021-07-12	Gemini-South	GMOS-S	GS-2021A-Q-419	300
J20004079+0058381	20:00:40.80	+00:58:37.2	41.911	–14.892	2021-06-21	Gemini-South	GMOS-S	GS-2021A-Q-419	1200
J20005889+0041324	20:00:58.80	+00:41:31.2	41.689	–15.094	2021-06-27	Gemini-South	GMOS-S	GS-2021A-Q-419	900
J20010859+0056428	20:01:08.58	+00:56:41.6	41.939	–15.009	2022-04-13	Blanco	COSMOS	2022A-210002	420
J20011680–0116257	20:01:16.80	–01:16:25.8	39.926	–16.088	2022-04-13	Blanco	COSMOS	2022A-210002	600
J20012799–0023095	20:01:28.08	–00:23:09.6	40.764	–15.712	2021-06-21	Gemini-South	GMOS-S	GS-2021A-Q-419	900
J20013415–0058565	20:01:34.08	–00:58:55.2	40.229	–16.015	2021-06-10	Gemini-South	GMOS-S	GS-2021A-Q-419	1500
J20014181–0019202	20:01:41.82	–00:19:20.8	40.850	–15.732	2022-04-13	Blanco	COSMOS	2022A-210002	540
J20015964–0015327	20:01:59.65	–00:15:32.7	40.945	–15.768	2022-04-13	Blanco	COSMOS	2022A-210002	720
J20021702–0005218	20:02:17.01	–00:05:22.0	41.135	–15.752	2022-04-11	Blanco	COSMOS	2022A-210002	720
J20023118+0104018	20:02:31.17	+01:04:01.7	42.220	–15.253	2022-04-13	Blanco	COSMOS	2022A-210002	720
J20023405+0021449	20:02:34.00	+00:21:43.1	41.583	–15.600	2022-04-13	Blanco	COSMOS	2022A-210002	240
J20035721–0116184	20:03:57.12	–01:16:19.2	40.254	–16.677	2021-06-25	Gemini-South	GMOS-S	GS-2021A-Q-419	900
J20051837+0001271	20:05:18.24	+00:01:26.4	41.612	–16.362	2021-06-30	Gemini-South	GMOS-S	GS-2021A-Q-419	1200
J20052052–0120319	20:05:20.64	–01:20:31.2	40.360	–17.017	2019-04-26	Gemini-South	GMOS-S	GS-2019A-Q-408	1500
J20053795+0017075	20:05:37.92	+00:17:06.0	41.892	–16.310	2021-06-25	Gemini-South	GMOS-S	GS-2021A-Q-419	1200
J20054459–0055530	20:05:44.64	–00:55:55.2	40.788	–16.912	2021-06-20	Gemini-South	GMOS-S	GS-2021A-Q-419	1200
J20061788–0013289	20:06:17.76	–00:13:30.0	41.506	–16.699	2021-06-15	Gemini-South	GMOS-S	GS-2021A-Q-419	300
J20073634+0057150	20:07:36.35	+00:57:15.0	42.750	–16.423	2022-04-13	Blanco	COSMOS	2022A-210002	1800
J20075027–0020098	20:07:50.40	–00:20:09.6	41.596	–17.091	2021-07-12	Gemini-South	GMOS-S	GS-2021A-Q-419	720
J20085488+0057297	20:08:54.96	+00:57:28.8	42.918	–16.709	2019-05-18	Gemini-South	GMOS-S	GS-2019A-Q-408	1800
J20090004+0105370	20:09:00.00	+01:05:38.4	43.053	–16.662	2021-07-12	Gemini-South	GMOS-S	GS-2021A-Q-419	300
J20090076–0036452	20:09:00.72	–00:36:46.8	41.486	–17.481	2021-06-27	Gemini-South	GMOS-S	GS-2021A-Q-419	1500
J20091617–0048192	20:09:16.08	–00:48:18.0	41.341	–17.628	2019-05-08	Gemini-South	GMOS-S	GS-2019A-Q-408	1500
J20092146+0051002	20:09:21.36	+00:51:00.0	42.875	–16.857	2021-06-25	Gemini-South	GMOS-S	GS-2021A-Q-419	420
J20095425–0007011	20:09:54.24	–00:07:01.1	42.055	–17.441	2022-04-12	Blanco	COSMOS	2022A-210002	720
J20101610–0014480	20:10:16.08	–00:14:49.2	41.981	–17.583	2019-05-18	Gemini-South	GMOS-S	GS-2019A-Q-408	1200
J20114178+0122331	20:11:41.76	+01:22:33.6	43.651	–17.115	2019-04-26	Gemini-South	GMOS-S	GS-2019A-Q-408	1800
J20121125–0005105	20:12:11.28	–00:05:09.6	42.370	–17.928	2021-07-13	Gemini-South	GMOS-S	GS-2021A-Q-419	1080
J20122497+0113575	20:12:24.96	+01:13:58.8	43.612	–17.342	2021-06-27	Gemini-South	GMOS-S	GS-2021A-Q-419	1200
J20123247+0101043	20:12:32.40	+01:01:04.8	43.430	–17.473	2019-06-07	Gemini-South	GMOS-S	GS-2019A-Q-408	1800
J20133793+0116431	20:13:37.93	+01:16:43.0	43.808	–17.586	2022-04-12	Blanco	COSMOS	2022A-210002	420
J20141258+0056212	20:14:12.72	+00:56:20.4	43.570	–17.877	2021-07-14	Gemini-South	GMOS-S	GS-2021A-Q-419	900
J20143504–0052087	20:14:35.04	–00:52:08.4	41.947	–18.828	2021-07-14	Gemini-South	GMOS-S	GS-2021A-Q-419	720
J20145209+0101365	20:14:52.08	+01:01:37.2	43.735	–17.978	2021-07-04	Gemini-South	GMOS-S	GS-2021A-Q-419	900
J20154337+0030123	20:15:43.44	+00:30:10.8	43.361	–18.419	2019-06-07	Gemini-South	GMOS-S	GS-2019A-Q-408	1800
J20160412–0056393	20:16:04.08	–00:56:42.0	42.063	–19.190	2021-07-14	Gemini-South	GMOS-S	GS-2021A-Q-419	900
J20185694+0118567	20:18:56.88	+01:18:57.6	44.524	–18.728	2019-05-24	Gemini-South	GMOS-S	GS-2019A-Q-408	1800
J20200678–0021468	20:20:06.79	–00:21:46.8	43.120	–19.798	2022-04-12	Blanco	COSMOS	2022A-210002	900
J20231520+0120002	20:23:15.12	+01:19:58.8	45.099	–19.656	2019-05-15	Gemini-South	GMOS-S	GS-2019A-Q-408	1800
J20232142–0000254	20:23:21.36	–00:00:25.2	43.869	–20.335	2019-05-23	Gemini-South	GMOS-S	GS-2019A-Q-408	1200
J20244141+0020139	20:24:41.52	+00:20:13.2	44.363	–20.459	2019-05-15	Gemini-South	GMOS-S	GS-2019A-Q-408	1200
J20251633–0113560	20:25:16.32	–01:13:55.2	42.970	–21.347	2021-06-30	Gemini-South	GMOS-S	GS-2021A-Q-419	1200
J20261334+0058212	20:26:13.20	+00:58:22.8	45.155	–20.479	2019-05-23	Gemini-South	GMOS-S	GS-2019A-Q-408	1200
J20265350+0041583	20:26:53.52	+00:42:00.0	44.989	–20.760	2021-06-13	Gemini-South	GMOS-S	GS-2021A-Q-419	477
J20275057+0045295	20:27:50.64	+00:45:28.8	45.169	–20.939	2021-07-14	Gemini-South	GMOS-S	GS-2021A-Q-419	900
J20311940+0045509	20:31:19.44	+00:45:50.4	45.637	–21.692	2021-06-04	Gemini-South	GMOS-S	GS-2021A-Q-419	1800
J20321142+0102056	20:32:11.41	+01:02:05.2	46.005	–21.745	2022-04-13	Blanco	COSMOS	2022A-210002	240
J20334782–0107490	20:33:47.76	–01:07:51.6	44.181	–23.162	2019-04-26	Gemini-South	GMOS-S	GS-2019A-Q-408	1800
J20343070+0027091	20:34:30.72	+00:27:10.8	45.772	–22.538	2021-06-04	Gemini-South	GMOS-S	GS-2021A-Q-419	750
J20381130+0038211	20:38:11.28	+00:38:20.4	46.445	–23.241	2019-05-23	Gemini-South	GMOS-S	GS-2019A-Q-408	1800
J20422273+0048380	20:42:22.74	+00:48:37.9	47.183	–24.060	2022-04-11	Blanco	COSMOS	2022A-210002	360
J20500458–0048444	20:50:04.58	–00:48:44.5	46.706	–26.540	2022-04-13	Blanco	COSMOS	2022A-210002	1920
J20514291+0104552	20:51:42.96	+01:04:55.2	48.756	–25.928	2021-07-12	Gemini-South	GMOS-S	GS-2021A-Q-419	1200

Table 1 *continued*

Table 1 (*continued*)

Star Name	α	δ	l	b	Date	Telescope	Instrument	Proposal ID	Exp.
(2MASS)	(J2000)	(J2000)	(deg)	(deg)	(UTC)				(s)
J20514829+0000230	20:51:48.29	+00:00:23.0	47.739	-26.499	2022-04-11	Blanco	COSMOS	2022A-210002	900
J20531505-0016063	20:53:15.12	-00:16:08.4	47.680	-26.950	2021-06-15	Gemini-South	GMOS-S	GS-2021A-Q-419	1500
J20540726-0113274	20:54:07.20	-01:13:26.4	46.877	-27.621	2019-05-18	Gemini-South	GMOS-S	GS-2019A-Q-408	1417
J20563226+0102264	20:56:32.16	+01:02:27.6	49.415	-26.979	2021-07-13	Gemini-South	GMOS-S	GS-2021A-Q-419	600
J20574846-4356271	20:57:48.44	-43:56:27.3	356.935	-40.703	2022-04-13	Blanco	COSMOS	2022A-210002	600
J21025360-3721177	21:02:53.52	-37:21:18.0	5.720	-41.342	2021-07-16	Gemini-South	GMOS-S	GS-2021A-Q-419	360
J21025985-5014054	21:02:59.76	-50:14:06.0	348.546	-41.272	2021-06-28	Gemini-South	GMOS-S	GS-2021A-Q-419	1200
J21030015-4641514	21:03:00.24	-46:41:52.8	353.248	-41.553	2021-06-09	Gemini-South	GMOS-S	GS-2021A-Q-419	900
J21040930-4708338	21:04:09.36	-47:08:34.8	352.638	-41.724	2021-06-23	Gemini-South	GMOS-S	GS-2021A-Q-419	1200
J21041356-3019010	21:04:13.68	-30:19:01.2	15.002	-40.604	2021-06-22	Gemini-South	GMOS-S	GS-2021A-Q-419	1500
J21041365-3146396	21:04:13.68	-31:46:40.8	13.107	-40.873	2021-06-10	Gemini-South	GMOS-S	GS-2021A-Q-419	1500
J21041794-4105082	21:04:18.00	-41:05:09.6	0.763	-41.846	2021-06-28	Gemini-South	GMOS-S	GS-2021A-Q-419	1200
J21042799-0049341	21:04:28.08	-00:49:33.6	48.770	-29.643	2019-05-17	Gemini-South	GMOS-S	GS-2019A-Q-408	1200
J21045538-5054052	21:04:55.44	-50:54:03.6	347.617	-41.499	2021-06-18	Gemini-South	GMOS-S	GS-2021A-Q-419	900
J21054026-2527599	21:05:40.32	-25:28:01.2	21.282	-39.810	2021-07-16	Gemini-South	GMOS-S	GS-2021A-Q-419	360
J21055882-4118416	21:05:58.80	-41:18:43.2	0.470	-42.168	2021-06-25	Gemini-South	GMOS-S	GS-2021A-Q-419	600
J21074117+0100513	21:07:41.04	+01:00:50.4	51.055	-29.362	2019-05-18	Gemini-South	GMOS-S	GS-2019A-Q-408	1800
J21113775-2658131	21:11:37.68	-26:58:12.0	19.797	-41.475	2021-07-16	Gemini-South	GMOS-S	GS-2021A-Q-419	600
J21115655-3708366	21:11:56.64	-37:08:38.4	6.207	-43.120	2021-06-25	Gemini-South	GMOS-S	GS-2021A-Q-419	210
J21142351-2947278	21:14:23.52	-29:47:27.6	16.254	-42.663	2021-06-27	Gemini-South	GMOS-S	GS-2021A-Q-419	1200
J21152435-2635448	21:15:24.24	-26:35:45.6	20.550	-42.207	2021-07-14	Gemini-South	GMOS-S	GS-2021A-Q-419	900
J21162790-3504557	21:16:27.84	-35:04:55.2	9.147	-43.852	2021-06-08	Gemini-South	GMOS-S	GS-2021A-Q-419	1500
J21213312+0002451	21:21:33.12	+00:02:45.6	52.281	-32.805	2021-07-04	Gemini-South	GMOS-S	GS-2021A-Q-419	1200
J21254198-0120151	21:25:42.00	-01:20:13.2	51.555	-34.424	2019-05-18	Gemini-South	GMOS-S	GS-2019A-Q-408	1500
J21263701+0119228	21:26:36.96	+01:19:22.8	54.383	-33.156	2021-06-27	Gemini-South	GMOS-S	GS-2021A-Q-419	1500
J21304688+0046211	21:30:46.80	+00:46:19.2	54.536	-34.327	2021-06-09	Gemini-South	GMOS-S	GS-2021A-Q-419	1500
J21341378-2932056	21:34:13.68	-29:32:06.0	17.667	-46.861	2021-06-18	Gemini-South	GMOS-S	GS-2021A-Q-419	480
J21344068-0045499	21:34:40.80	-00:45:50.4	53.642	-35.993	2021-07-12	Gemini-South	GMOS-S	GS-2021A-Q-419	900
J21430119+0058067	21:43:01.20	+00:58:04.8	56.882	-36.726	2021-06-14	Gemini-South	GMOS-S	GS-2021A-Q-419	900
J21435071-2056106	21:43:50.64	-20:56:09.6	30.663	-46.963	2021-06-18	Gemini-South	GMOS-S	GS-2021A-Q-419	750
J21510918+0004279	21:51:09.12	+00:04:26.4	57.467	-38.898	2019-10-16	Blanco	COSMOS	2019B-0069	900
J21551357-0114578	21:55:13.68	-01:15:00.0	56.844	-40.499	2019-06-07	Gemini-South	GMOS-S	GS-2019A-Q-408	1500
J21562470-0233483	21:56:24.72	-02:33:50.4	55.646	-41.497	2021-06-14	Gemini-South	GMOS-S	GS-2021A-Q-419	900
J21570410-0025558	21:57:04.08	-00:25:55.2	58.069	-40.391	2021-07-14	Gemini-South	GMOS-S	GS-2021A-Q-419	840
J21590612+0029207	21:59:06.24	+00:29:20.4	59.436	-40.248	2019-05-21	Gemini-South	GMOS-S	GS-2019A-Q-408	1500
J21595072+0027368	21:59:50.64	+00:27:36.0	59.553	-40.413	2019-10-16	Blanco	COSMOS	2019B-0069	1500
J22024068-0112054	22:02:40.56	-01:12:07.2	58.351	-41.977	2019-05-22	Gemini-South	GMOS-S	GS-2019A-Q-408	1800
J22093470+0047105	22:09:34.80	+00:47:09.6	61.891	-42.128	2019-10-17	Blanco	COSMOS	2019B-0069	1800
J22165605+0013206	22:16:55.92	+00:13:22.8	62.883	-43.908	2019-06-07	Gemini-South	GMOS-S	GS-2019A-Q-408	1800
J22174445-0107091	22:17:44.40	-01:07:08.4	61.603	-44.911	2021-06-27	Gemini-South	GMOS-S	GS-2021A-Q-419	360
J22223335-2934216	22:22:33.36	-29:34:22.8	19.728	-57.291	2021-07-14	Gemini-South	GMOS-S	GS-2021A-Q-419	900
J22245762-0059071	22:24:57.60	-00:59:06.0	63.383	-46.224	2021-07-12	Gemini-South	GMOS-S	GS-2021A-Q-419	840
J22302534-0055095	22:30:25.44	-00:55:08.4	64.747	-47.222	2019-06-21	Gemini-South	GMOS-S	GS-2019A-Q-408	1800
J22390604-0102356	22:39:06.00	-01:02:34.8	66.762	-48.927	2021-06-09	Gemini-South	GMOS-S	GS-2021A-Q-419	1500
J22430733+0103384	22:43:07.44	+01:03:39.6	70.114	-48.205	2021-06-09	Gemini-South	GMOS-S	GS-2021A-Q-419	1200
J22460189+0052078	22:46:01.92	+00:52:08.4	70.686	-48.854	2021-06-27	Gemini-South	GMOS-S	GS-2021A-Q-419	900
J22481036+0006493	22:48:10.32	+00:06:46.8	70.451	-49.768	2021-06-09	Gemini-South	GMOS-S	GS-2021A-Q-419	900
J23073186-0115408	23:07:31.92	-01:15:39.6	74.638	-54.088	2019-06-06	Gemini-South	GMOS-S	GS-2019A-Q-408	1200
J23131269-0036247	23:13:12.72	-00:36:25.2	77.215	-54.516	2019-06-07	Gemini-South	GMOS-S	GS-2019A-Q-408	1200
J23174221-0124338	23:17:42.24	-01:24:32.4	77.845	-55.848	2021-06-27	Gemini-South	GMOS-S	GS-2021A-Q-419	1500
J23233976-0048009	23:23:39.84	-00:48:00.0	80.621	-56.284	2020-12-28	Blanco	COSMOS	2020A-0032	150
J23243811-0115388	23:24:38.16	-01:15:39.6	80.472	-56.798	2020-12-27	Blanco	COSMOS	2020A-0032	240
J23271618+0008407	23:27:16.08	+00:08:42.0	82.926	-56.046	2020-12-28	Blanco	COSMOS	2020A-0032	240
J23274511+0014400	23:27:45.12	+00:14:38.4	83.205	-56.033	2019-05-18	Gemini-South	GMOS-S	GS-2019A-Q-408	1200
J23400902-4205187	23:40:09.12	-42:05:20.4	342.547	-69.133	2020-12-28	Blanco	COSMOS	2020A-0032	480
J23414363-0122023	23:41:43.68	-01:22:01.2	87.037	-59.291	2020-12-27	Blanco	COSMOS	2020A-0032	240
J23433448+0042013	23:43:34.56	+00:42:00.0	89.797	-57.739	2021-06-27	Gemini-South	GMOS-S	GS-2021A-Q-419	1500

Table 2. S-PLUS Photometry

Star Name	uJAVA	σ	J0378	σ	J0395	σ	J0410	σ	J0430	σ	gSDSS	σ	J0515	σ	rSDSS	σ	J0660	σ	iSDSS	σ	J0861	σ	zSDSS	σ
J00044550+0101170	15.150	0.004	14.629	0.004	14.530	0.006	14.283	0.004	14.195	0.004	13.862	0.001	13.659	0.003	13.313	0.001	13.275	0.001	13.093	0.001	13.014	0.002	12.978	0.001
J00173643+0009215	15.996	0.006	15.434	0.006	15.321	0.008	14.994	0.006	14.889	0.005	14.523	0.002	14.284	0.004	13.908	0.001	13.841	0.002	13.529	0.002	13.498	0.001		
J00255442-3053220	15.891	0.008	15.341	0.008	15.168	0.011	14.946	0.009	14.803	0.008	14.350	0.003	14.043	0.005	13.609	0.003	13.349	0.001	13.299	0.001	13.123	0.002	13.039	0.001
J00271249-3133515	15.082	0.005	14.655	0.005	14.498	0.006	14.090	0.006	13.845	0.002	13.609	0.003	13.349	0.001	13.299	0.001	13.123	0.002	13.042	0.002	13.039	0.001		
J00271240+0108377	15.296	0.005	14.837	0.005	14.711	0.007	14.485	0.005	14.385	0.005	14.144	0.002	13.934	0.003	13.658	0.001	13.622	0.001	13.394	0.002	13.370	0.001		
J003555591-4204306	15.575	0.005	15.142	0.006	14.967	0.008	14.758	0.006	14.668	0.006	14.480	0.002	14.280	0.004	14.033	0.002	14.046	0.002	13.883	0.003	13.835	0.003	13.808	0.002
J00503713-3154131	16.459	0.009	15.981	0.010	15.805	0.013	15.606	0.010	15.500	0.010	15.251	0.004	15.059	0.007	14.790	0.002	14.743	0.003	14.535	0.004	14.501	0.003		
J00503717-3408167	15.724	0.006	15.058	0.005	14.892	0.008	14.436	0.005	14.190	0.005	14.190	0.002	13.487	0.003	12.997	0.001	12.926	0.001	12.658	0.001	12.550	0.001		
J00520900-3046092	15.402	0.004	14.967	0.005	14.787	0.006	14.626	0.005	14.528	0.004	14.316	0.002	14.129	0.003	13.881	0.001	13.853	0.002	13.723	0.001	13.660	0.002		
J00528286-3001012	15.796	0.004	15.352	0.007	15.218	0.011	15.002	0.007	14.886	0.006	14.640	0.003	14.496	0.004	14.184	0.002	14.152	0.002	13.950	0.002	13.922	0.003		
J0052124-3431172	16.433	0.008	15.941	0.009	15.754	0.011	15.562	0.009	15.407	0.008	15.101	0.003	14.899	0.005	14.588	0.002	14.540	0.002	14.358	0.002	14.282	0.003		
J01044308-3941159	16.458	0.009	15.921	0.010	15.778	0.012	15.596	0.010	15.444	0.010	15.170	0.003	14.979	0.006	14.663	0.002	14.621	0.002	14.426	0.002	14.338	0.003		
J01062973-3030595	17.833	0.015	17.243	0.016	17.049	0.023	16.725	0.017	16.563	0.015	16.215	0.005	15.972	0.009	15.589	0.003	15.505	0.004	15.236	0.003	15.176	0.005		
J01072229-3257031	15.493	0.005	15.076	0.006	14.904	0.008	14.720	0.006	14.624	0.005	14.378	0.002	14.201	0.004	13.926	0.001	13.733	0.001	13.675	0.002	13.659	0.002		
J01115530-3439312	16.798	0.010	16.247	0.010	16.123	0.015	15.814	0.011	15.702	0.010	15.291	0.004	15.071	0.006	14.688	0.002	14.614	0.003	14.405	0.002	14.287	0.003		
J01115536-2922427	17.148	0.012	16.581	0.014	16.406	0.015	16.124	0.015	16.016	0.014	15.646	0.005	15.413	0.008	15.079	0.003	15.058	0.003	14.809	0.002	14.708	0.004		
J0112882-3505175	14.646	0.003	14.093	0.004	13.937	0.005	13.664	0.004	13.545	0.004	13.189	0.001	12.987	0.002	12.623	0.001	12.542	0.002	12.354	0.001	12.254	0.001		
J01142762-3229200	16.890	0.010	16.417	0.011	16.287	0.014	16.075	0.011	15.956	0.010	15.706	0.004	15.512	0.007	15.222	0.003	15.164	0.003	15.011	0.003	14.934	0.004		
J01153574-31448352	16.285	0.007	15.672	0.008	15.454	0.009	15.302	0.007	15.168	0.007	14.936	0.003	14.822	0.005	14.580	0.002	14.455	0.002	14.405	0.002	14.347	0.003		
J01153906-3234184	15.753	0.006	15.186	0.006	15.088	0.008	14.733	0.006	14.592	0.005	14.291	0.002	14.103	0.003	13.615	0.001	13.539	0.002	13.207	0.002	13.207	0.001		
J01174900-3149904	17.409	0.013	16.961	0.015	16.724	0.017	16.531	0.014	16.320	0.013	16.291	0.005	16.126	0.009	15.833	0.004	15.668	0.004	15.536	0.006	15.572	0.005		
J01205304-3435456	16.865	0.010	16.359	0.011	16.208	0.015	15.974	0.012	15.848	0.011	15.548	0.004	15.364	0.007	15.049	0.003	15.000	0.003	14.820	0.002	14.739	0.004		
J01232034-3218276	17.027	0.011	16.448	0.012	16.194	0.015	16.094	0.012	15.906	0.011	15.695	0.004	15.526	0.007	15.218	0.003	15.157	0.003	15.015	0.003	14.942	0.005		
J01232234-3158080	16.007	0.007	15.318	0.007	15.063	0.009	14.770	0.006	14.554	0.005	14.075	0.002	13.817	0.003	13.316	0.001	13.237	0.001	12.964	0.001	12.795	0.001		
J01301753-2929538	15.794	0.006	15.376	0.007	15.170	0.009	14.992	0.007	14.847	0.007	14.566	0.003	14.462	0.005	14.207	0.002	14.146	0.002	14.011	0.002	13.935	0.003		
J013041113-2901179	16.488	0.008	15.897	0.009	15.766	0.012	15.435	0.009	15.280	0.009	14.936	0.003	14.696	0.005	14.352	0.002	14.266	0.002	14.207	0.002	14.177	0.002		
J01335531-2912330	14.944	0.004	14.462	0.004	14.353	0.006	14.039	0.004	13.958	0.005	13.638	0.002	13.474	0.003	13.130	0.001	13.089	0.001	12.862	0.002	12.820	0.001		
J01374941-3407505	17.598	0.013	17.008	0.014	16.791	0.018	16.486	0.014	16.288	0.012	15.901	0.005	15.665	0.008	15.237	0.003	15.160	0.003	14.936	0.004	14.796	0.003		
J01383820-2740120	15.784	0.006	15.213	0.006	15.030	0.008	14.826	0.006	14.683	0.006	14.351	0.002	14.139	0.004	13.771	0.001	13.717	0.002	13.508	0.001	13.397	0.002		
J01384849-3123136	15.983	0.006	15.463	0.007	15.311	0.009	14.975	0.007	14.848	0.007	14.513	0.002	14.303	0.004	13.952	0.002	13.882	0.002	13.697	0.001	13.582	0.002		
J01464720-0102503	17.034	0.007	16.680	0.008	16.150	0.008	16.174	0.007	16.121	0.007	15.841	0.003	15.673	0.005	15.433	0.002	15.415	0.002	15.297	0.002	15.239	0.002		
J01484480-2911171	16.771	0.009	16.249	0.011	16.076	0.016	15.640	0.010	15.640	0.009	15.324	0.003	14.948	0.003	14.779	0.001	14.531	0.002	14.455	0.004	14.411	0.002		
J01530531-2748141	15.005	0.004	14.533	0.005	14.361	0.006	14.118	0.005	13.995	0.005	13.761	0.002	13.580	0.003	13.285	0.001	13.260	0.001	13.002	0.002	12.989	0.001		
J01554444+010512	16.432	0.007	15.875	0.007	15.746	0.009	15.470	0.007	15.363	0.006	15.025	0.002	14.791	0.004	14.445	0.005	14.405	0.002	14.204	0.004	14.078	0.002		
J02180715-3049391	15.698	0.006	15.236	0.007	15.081	0.009	14.918	0.007	14.805	0.007	14.564	0.003	14.391	0.004	14.114	0.002	14.055	0.002	13.912	0.002	13.842	0.002		
J02284062-3025508	17.085	0.010	16.635	0.012	16.448	0.016	16.219	0.012	16.122	0.011	15.856	0.004	15.645	0.007	15.382	0.003	15.340	0.003	15.164	0.003	15.079	0.003		
J02320469-3115085	17.228	0.011	16.549	0.011	16.276	0.014	15.951	0.010	15.719	0.009	15.245	0.003	14.993	0.005	14.459	0.009	14.376	0.002	14.126	0.002	14.298	0.003		
J03060042-3336317	17.760	0.015	17.265	0.018	17.075	0.024	16.907	0.019	16.750	0.017	16.494	0.006	16.306	0.011	15.991	0.004	15.532	0.005	15.767	0.004	15.636	0.006		
J03060937-3308492	17.428	0.013	16.853	0.014	16.705	0.019	16.507	0.015	16.367	0.014	16.072	0.005	15.880	0.009	15.543	0.003	15.494	0.004	15.299	0.003	15.224	0.005		
J030603076-3307480	13.844	0.001	13.264	0.001	13.130	0.002	12.841	0.001	12.702	0.001	12.456	0.000	12.262	0.001	11.938	0.000	11.910	0.000	11.733	0.001	11.645	0.001		
J03093503-3300063	15.506	0.005	14.910	0.005	14.745	0.007	14.428	0.005	14.235	0.005	13.873	0.002	13.664	0.004	13.240	0.001	13.189	0.001	12.932	0.002	12.843	0.002		
J03110634+0058038	16.825	0.012	16.396	0																				

Table 2 (continued)

Star Name	uJAVA	σ	J0378	σ	J0395	σ	J0410	σ	J0430	σ	gSDSS	σ	J0515	σ	rSDSS	σ	J0660	σ	iSDSS	σ	J0861	σ	zSDSS	σ	σ
J03144847+0110166	15.087	0.005	14.701	0.006	14.523	0.007	14.363	0.005	14.241	0.005	14.013	0.002	13.805	0.003	13.504	0.001	13.487	0.001	13.284	0.001	13.183	0.002	13.171	0.001	
J03145891−3236489	14.677	0.003	14.196	0.004	14.093	0.005	13.724	0.004	13.624	0.003	13.302	0.001	13.096	0.002	12.784	0.001	12.734	0.001	12.535	0.001	12.463	0.001	12.435	0.001	
J03160457+0040388	15.682	0.005	15.110	0.005	14.958	0.007	14.660	0.005	14.325	0.005	14.324	0.002	14.088	0.003	13.775	0.001	13.748	0.002	13.588	0.001	13.447	0.002	13.425	0.001	
J03170771−3243481	16.084	0.006	15.447	0.007	15.296	0.009	14.898	0.006	14.896	0.006	14.257	0.002	14.038	0.003	13.600	0.001	13.522	0.001	13.291	0.001	13.189	0.002	13.134	0.001	
J03136418+0049320	15.317	0.004	14.876	0.005	14.666	0.006	14.525	0.005	14.417	0.005	14.229	0.009	14.059	0.003	13.810	0.001	13.804	0.002	13.659	0.001	13.606	0.002	13.575	0.001	
J032031189−5523405	16.470	0.008	16.199	0.009	15.852	0.012	15.666	0.009	15.295	0.003	15.125	0.006	14.815	0.004	14.769	0.002	14.660	0.002	14.518	0.003	14.502	0.002			
J03250464−0039306	17.610	0.015	17.183	0.016	17.038	0.020	16.840	0.016	16.704	0.014	16.435	0.006	16.258	0.010	15.940	0.004	15.886	0.004	15.726	0.004	15.643	0.006	15.622	0.004	
J03255861+0107414	17.042	0.005	16.683	0.006	16.574	0.008	16.335	0.005	16.210	0.005	15.932	0.002	15.723	0.003	15.407	0.007	15.384	0.002	15.178	0.001	15.099	0.002	15.069	0.002	
J03272930−0100042	16.201	0.006	15.779	0.007	15.711	0.010	15.368	0.007	15.238	0.007	14.945	0.002	14.712	0.004	14.372	0.002	14.311	0.002	14.117	0.002	14.040	0.003	13.982	0.002	
J03332804−0016148	17.104	0.008	16.630	0.009	16.538	0.012	16.229	0.009	16.110	0.008	15.772	0.003	15.532	0.005	15.172	0.002	15.133	0.003	14.917	0.002	14.816	0.004	14.774	0.002	
J03370237−3458142	16.538	0.008	15.894	0.008	15.727	0.011	15.479	0.008	15.273	0.007	14.885	0.003	14.634	0.004	14.216	0.002	14.115	0.002	13.916	0.002	13.793	0.002	13.771	0.002	
J03384463−0047295	16.782	0.009	16.426	0.011	16.236	0.014	16.032	0.012	15.894	0.010	15.669	0.003	15.430	0.007	15.166	0.002	15.112	0.003	14.933	0.002	14.857	0.004	14.845	0.003	
J03384871−0058248	15.748	0.005	15.326	0.006	15.189	0.008	14.918	0.007	14.796	0.006	14.501	0.002	14.268	0.004	13.932	0.001	13.874	0.002	13.680	0.001	13.589	0.002	13.555	0.001	
J03391097−0046039	17.461	0.013	16.858	0.014	16.735	0.018	16.404	0.014	16.287	0.012	15.934	0.004	15.701	0.008	15.293	0.003	15.221	0.003	14.858	0.004	14.841	0.003			
J03394540+0110182	17.859	0.018	17.530	0.023	16.969	0.022	16.853	0.018	16.723	0.016	16.349	0.005	16.132	0.010	15.744	0.004	15.708	0.004	15.524	0.003	15.450	0.006	15.417	0.004	
J03412634+0053306	15.862	0.006	15.282	0.007	15.152	0.009	14.876	0.007	14.747	0.006	14.467	0.002	14.269	0.004	13.943	0.002	13.901	0.002	13.720	0.001	13.649	0.002	13.605	0.002	
J034143358+0033004	13.661	0.002	13.339	0.002	13.215	0.003	12.806	0.002	12.713	0.002	12.415	0.001	12.226	0.001	11.968	0.001	11.844	0.001	11.753	0.001	11.677	0.001			
J03443568+0045022	13.683	0.002	13.326	0.002	13.246	0.003	12.776	0.002	12.697	0.002	12.390	0.001	12.160	0.001	11.940	0.001	12.207	0.001	11.773	0.001	11.597	0.001			
J03445171+0054107	16.451	0.007	15.913	0.008	15.856	0.011	15.424	0.007	15.296	0.007	14.805	0.002	14.587	0.004	14.146	0.002	14.054	0.002	13.813	0.001	13.639	0.002	13.629	0.001	
J03465824−0009150	16.616	0.008	16.229	0.009	16.091	0.011	15.876	0.009	15.790	0.008	15.527	0.003	15.345	0.006	15.051	0.001	15.082	0.002	14.838	0.002	14.800	0.004	14.736	0.003	
J03471548+0049366	14.546	0.003	14.040	0.003	13.928	0.004	13.505	0.003	13.382	0.003	13.004	0.001	12.776	0.002	12.395	0.001	12.551	0.001	12.139	0.001	12.102	0.001	12.03	0.001	
J03473639+0049039	17.329	0.011	16.897	0.013	16.737	0.017	16.522	0.013	16.411	0.012	16.156	0.004	15.950	0.008	15.642	0.003	15.396	0.004	15.418	0.003	15.317	0.005	15.293	0.004	
J03474822+0125290	14.755	0.003	14.120	0.003	13.910	0.004	13.537	0.003	13.303	0.003	13.030	0.001	12.826	0.002	12.538	0.001	12.356	0.001	12.187	0.001	12.039	0.001			
J03492415+0101192	14.347	0.003	13.918	0.003	13.786	0.004	13.410	0.003	13.302	0.003	13.030	0.001	12.804	0.002	12.565	0.001	12.364	0.001	12.302	0.001	12.280	0.001			
J03495507+0003027	13.819	0.002	13.549	0.002	13.437	0.003	12.936	0.002	12.848	0.002	12.466	0.001	12.282	0.001	11.945	0.001	12.237	0.001	11.760	0.001	11.731	0.001			
J035350888−0002590	17.114	0.011	16.627	0.011	16.514	0.014	16.215	0.011	16.055	0.012	15.723	0.004	15.445	0.006	15.016	0.003	14.943	0.003	14.683	0.002	14.355	0.003			
J035352457−0009297	17.543	0.015	17.364	0.017	17.190	0.023	16.857	0.017	16.557	0.013	16.471	0.014	16.063	0.005	15.792	0.007	15.384	0.003	15.330	0.003	15.084	0.004			
J03540352+0026534	16.335	0.007	15.850	0.008	15.635	0.010	15.357	0.008	15.158	0.007	14.766	0.002	14.519	0.004	14.082	0.002	14.014	0.002	13.750	0.002	13.612	0.002			
J03540459+0140466	15.496	0.005	15.125	0.006	15.000	0.008	14.750	0.006	14.615	0.005	14.038	0.002	14.078	0.003	13.698	0.001	13.669	0.001	13.415	0.001	13.267	0.001			
J03540956+0033304	16.354	0.007	15.886	0.008	15.760	0.011	15.205	0.007	15.042	0.006	14.435	0.002	14.144	0.003	13.537	0.001	13.425	0.001	13.085	0.001	12.898	0.002			
J03541889+0112447	15.421	0.005	14.975	0.005	14.816	0.007	14.461	0.005	14.329	0.004	14.023	0.002	13.808	0.003	13.446	0.001	13.437	0.001	13.201	0.001	13.106	0.002			
J03543044+0052026	17.812	0.015	17.364	0.017	17.190	0.023	16.791	0.016	16.635	0.014	16.192	0.005	15.950	0.008	15.446	0.006	15.376	0.003	15.086	0.003	14.925	0.004			
J03543348+0038140	16.632	0.008	16.149	0.009	15.993	0.012	15.517	0.008	15.335	0.007	14.827	0.002	14.542	0.004	13.978	0.001	13.883	0.002	13.544	0.001	13.302	0.002			
J03543771+0046406	16.570	0.008	16.067	0.009	15.875	0.012	15.347	0.008	15.344	0.007	14.986	0.003	14.723	0.004	14.295	0.002	14.239	0.002	13.975	0.002	13.834	0.002			
J03544342−0017209	17.268	0.012	16.844	0.012	16.722	0.016	16.263	0.011	16.112	0.012	16.078	0.004	15.413	0.006	14.543	0.004	14.254	0.003	14.507	0.002	14.353	0.002			
J03544466+0031400	17.455	0.008	15.723	0.009	15.594	0.014	15.123	0.008	14.966	0.007	14.539	0.002	14.253	0.004	13.762	0.002	14.677	0.002	14.333	0.002	14.170	0.003			
J035454633+0040139	17.091	0.010	16.550	0.011	16.370	0.015	15.964	0.010	15.803	0.009	15.307	0.003	15.021	0.005	14.496	0.002	14.420	0.002	14.057	0.007	13.923	0.003			
J035456355−0025496	14.955	0.004	14.506	0.004	14.357	0.005	13.806	0.003	13.659	0.004	13.181	0.001	12.899	0.002	12.388	0.001	12.551	0.001	12.051	0.001	11.842	0.001			
J03554471+0028063	17.750	0.020	17.320	0.020	17.130	0.020	16.830	0.020	16.660	0.020	16.290	0.020	15.990	0.020	15.570	0.020	15.510	0.020	15.310	0.020	15.200	0.020			
J03552342+0016535	18.031	0.022	17.466	0.023	17.359	0.036	17.031	0.019	16.774	0.017	16.361	0.005	16.078	0.009	15.609	0.003	15.543	0.004							

Table 2 (*continued*)

Star Name	uJAVA	σ	J0378	σ	J0395	σ	J0410	σ	J0430	σ	gSDSS	σ	J0515	σ	rSDSS	σ	J0660	σ	iSDSS	σ	J0861	σ	zSDSS	σ	σ
J03574260+0115214	15.211	0.005	14.752	0.006	14.598	0.009	14.343	0.005	14.213	0.005	13.945	0.002	13.724	0.003	13.407	0.001	13.378	0.001	13.167	0.001	13.044	0.002	13.030	0.001	
J03582339-3438018	15.844	0.006	15.327	0.007	15.152	0.009	14.969	0.007	14.830	0.007	14.538	0.003	14.346	0.005	14.039	0.002	13.976	0.002	13.795	0.002	13.707	0.003	13.690	0.002	
J03582979-3841492	16.700	0.009	16.186	0.010	16.046	0.013	15.806	0.010	15.701	0.010	15.426	0.004	15.207	0.006	14.925	0.002	14.871	0.003	14.702	0.002	14.629	0.004	14.602	0.003	
J03583397-3739179	16.823	0.010	16.287	0.013	16.132	0.015	15.922	0.012	15.810	0.011	15.470	0.004	15.275	0.007	14.926	0.003	14.857	0.003	14.683	0.002	14.614	0.004	14.570	0.003	
J03585338+0007050	14.689	0.004	14.202	0.004	14.077	0.007	13.614	0.004	13.472	0.003	13.082	0.002	12.829	0.002	12.439	0.001	12.526	0.001	12.033	0.001	11.983	0.001			
J03590482+0046515	16.488	0.009	16.098	0.011	15.905	0.017	15.662	0.010	15.486	0.009	15.118	0.003	14.899	0.005	14.480	0.002	14.423	0.002	14.141	0.002	14.040	0.003	13.965	0.002	
J03592020+0034443	16.692	0.010	16.230	0.012	16.058	0.018	15.517	0.008	15.328	0.008	14.669	0.002	14.407	0.004	13.748	0.001	13.613	0.002	13.244	0.001	13.047	0.002	12.978	0.001	
J03592418-3651140	17.594	0.015	17.053	0.020	16.892	0.022	16.643	0.017	16.497	0.015	16.169	0.005	15.961	0.009	15.598	0.004	15.549	0.004	15.341	0.003	15.240	0.005	15.210	0.004	
J03592423+0430214	14.202	0.003	13.772	0.004	13.622	0.006	13.178	0.003	13.031	0.003	12.663	0.001	12.454	0.002	12.073	0.001	12.174	0.001	11.783	0.001	11.743	0.001	11.638	0.001	
J03592681+0022272	14.027	0.003	13.547	0.003	13.414	0.005	12.912	0.003	12.772	0.002	12.354	0.001	12.114	0.001	11.674	0.001	11.806	0.001	11.376	0.001	11.419	0.001	11.192	0.001	
J03592803+0036543	15.246	0.005	14.815	0.006	14.702	0.009	14.223	0.005	14.077	0.004	13.601	0.001	13.359	0.003	12.875	0.005	12.799	0.001	12.513	0.001	12.388	0.001	12.335	0.001	
J03593987+0106448	14.893	0.004	14.472	0.005	14.341	0.008	13.904	0.004	13.748	0.004	13.377	0.001	13.177	0.002	12.780	0.001	12.751	0.001	12.505	0.001	12.381	0.001	12.355	0.001	
J03594115+0043429	14.263	0.003	13.845	0.004	13.678	0.006	13.281	0.003	13.141	0.003	12.839	0.001	12.649	0.002	12.354	0.004	12.477	0.001	12.134	0.004	12.071	0.001	12.021	0.001	
J04003943-3513394	17.400	0.012	16.825	0.013	16.642	0.017	16.365	0.014	16.207	0.012	15.891	0.004	15.668	0.008	15.321	0.003	15.253	0.003	15.063	0.003	14.954	0.004	14.942	0.003	
J04048546-3948262	17.665	0.014	16.772	0.018	16.487	0.014	16.258	0.012	15.849	0.004	15.618	0.007	15.151	0.003	15.079	0.003	14.829	0.002	14.702	0.004	14.674	0.003			
J04049546-4007327	15.826	0.006	15.260	0.007	15.120	0.009	14.760	0.006	14.606	0.006	14.234	0.002	14.008	0.004	13.638	0.001	13.359	0.002	13.248	0.002	13.223	0.001			
J04105455-3321498	16.970	0.010	16.373	0.011	16.204	0.014	15.876	0.011	15.695	0.009	15.296	0.003	15.090	0.006	14.673	0.002	14.584	0.004	14.299	0.002	14.252	0.003	14.209	0.002	
J04115568-3341064	15.714	0.006	15.142	0.006	15.011	0.008	14.677	0.006	14.532	0.002	13.940	0.003	13.530	0.001	13.449	0.001	13.258	0.001	13.151	0.002	13.101	0.001			
J04140591-3727559	15.606	0.005	15.091	0.006	14.894	0.007	14.706	0.006	14.573	0.006	14.296	0.002	14.085	0.004	13.772	0.002	13.714	0.002	13.540	0.001	13.445	0.002	13.416	0.001	
J04145894-3255389	16.565	0.008	16.009	0.009	15.816	0.011	15.552	0.009	15.404	0.008	15.083	0.003	14.881	0.005	14.509	0.009	14.459	0.002	14.224	0.002	14.135	0.003	14.105	0.002	
J04162904-4110418	16.081	0.009	15.597	0.010	15.437	0.013	15.220	0.010	15.127	0.009	14.910	0.004	14.724	0.006	14.480	0.003	14.437	0.003	14.279	0.002	14.228	0.004	14.187	0.003	
J04165229-3817335	16.298	0.008	15.744	0.009	15.554	0.012	15.338	0.009	15.214	0.008	15.020	0.003	14.873	0.006	14.611	0.002	14.613	0.003	14.441	0.002	14.396	0.004	14.367	0.003	
J04180140-3841420	14.433	0.003	13.952	0.004	13.772	0.005	13.580	0.004	13.460	0.004	13.232	0.001	13.036	0.002	12.752	0.001	12.693	0.001	12.523	0.001	12.456	0.001	12.433	0.001	
J04203417-3430458	15.699	0.006	15.146	0.006	15.022	0.010	14.654	0.006	14.518	0.005	14.116	0.002	13.879	0.003	13.511	0.001	13.434	0.001	13.233	0.001	13.125	0.002	13.090	0.001	
J04213733-3344353	16.266	0.007	15.768	0.008	15.582	0.010	15.275	0.008	15.137	0.007	14.848	0.003	14.613	0.005	14.288	0.002	14.198	0.002	14.037	0.002	13.905	0.003	13.892	0.002	
J04220661-411088	16.516	0.009	15.961	0.010	15.806	0.013	15.544	0.010	15.380	0.009	15.085	0.003	14.870	0.006	14.538	0.002	14.473	0.003	14.269	0.002	14.174	0.003	14.146	0.002	
J04233919-3814243	17.685	0.019	17.220	0.023	16.940	0.028	16.779	0.021	16.614	0.019	16.342	0.006	16.104	0.011	15.831	0.004	15.774	0.004	15.588	0.004	15.491	0.006	15.479	0.004	
J042454177-3640132	16.710	0.008	16.222	0.010	16.059	0.013	15.795	0.011	15.681	0.010	15.425	0.004	15.248	0.006	14.939	0.002	14.895	0.003	14.702	0.002	14.612	0.004	14.595	0.003	
J04271588-4113323	17.027	0.012	16.459	0.013	16.343	0.018	16.044	0.013	15.937	0.012	15.603	0.004	15.390	0.007	15.066	0.003	14.811	0.003	14.741	0.004	14.686	0.003			
J04315718-4354175	15.606	0.006	15.043	0.006	14.909	0.010	14.695	0.007	14.441	0.006	14.175	0.004	13.969	0.004	13.622	0.001	13.574	0.002	13.422	0.001	13.350	0.002	13.338	0.002	
J04322488-4639409	17.026	0.012	16.458	0.013	16.368	0.017	16.059	0.013	15.947	0.012	15.635	0.004	15.447	0.007	15.112	0.002	15.041	0.003	14.869	0.002	14.797	0.004	14.752	0.003	
J04322908-3947519	17.275	0.013	16.762	0.015	16.530	0.018	16.367	0.019	16.237	0.013	15.953	0.005	15.755	0.008	15.437	0.003	15.365	0.004	15.173	0.003	15.089	0.005	15.052	0.004	
J04323909-4634270	15.348	0.005	14.959	0.006	14.836	0.008	14.619	0.006	14.507	0.006	14.306	0.002	14.151	0.004	13.889	0.002	13.862	0.002	13.714	0.001	13.671	0.002	13.648	0.002	
J043445588-3445588	17.318	0.012	16.663	0.013	16.515	0.018	16.110	0.013	15.917	0.011	15.525	0.004	15.260	0.007	14.855	0.003	14.752	0.003	14.556	0.002	14.431	0.003	14.388	0.002	
J04351543-425160	16.848	0.013	16.625	0.015	16.453	0.018	15.747	0.014	15.562	0.011	15.282	0.004	15.033	0.007	14.657	0.003	14.598	0.003	14.305	0.002	14.304	0.004	14.263	0.003	
J04352215-4704488	17.096	0.012	16.584	0.013	16.423	0.017	16.233	0.014	16.093	0.013	15.852	0.008	15.644	0.008	15.346	0.003	15.295	0.004	15.128	0.003	15.005	0.005	15.014	0.003	
J04354512-4350225	15.268	0.005	14.818	0.006	14.714	0.009	14.459	0.007	14.364	0.006	14.132	0.002	13.939	0.004	13.694	0.002	13.654	0.002	13.490	0.002	13.377	0.002			
J04355217-4203517	16.438	0.010	15.825	0.011	15.671	0.014	15.384	0.011	15.272	0.010	14.944	0.004	14.726	0.006	14.401	0.002	14.364	0.003	14.152	0.002	14.064	0.003	14.021	0.002	
J04371974-4254147	17.126	0.015	16.633	0.017	16.467	0.022	16.252	0.017	16.146	0.015	15.839	0.005	15.663	0.01											

Table 2 (continued)

Star Name	uJAVA	σ	J0378	σ	J0395	σ	J0410	σ	J0430	σ	gSDSS	σ	J0515	σ	rSDSS	σ	J0660	σ	iSDSS	σ	J0861	σ	zSDSS	σ	σ
J04512454–3139582	15.043	0.003	14.485	0.004	14.370	0.005	14.064	0.004	13.939	0.003	13.611	0.001	13.394	0.002	13.055	0.001	12.994	0.001	12.739	0.001	12.690	0.002	12.646	0.001	
J04543666–4754298	16.618	0.009	16.072	0.010	15.878	0.014	15.696	0.011	15.547	0.010	15.247	0.004	15.054	0.006	14.714	0.002	14.450	0.003	14.482	0.002	14.371	0.003	14.337	0.002	
J04545976–4212485	14.930	0.004	14.444	0.004	14.250	0.006	14.061	0.004	13.948	0.004	13.712	0.002	13.521	0.003	13.233	0.001	13.216	0.001	13.040	0.001	12.949	0.002	12.930	0.001	
J04551021–3249438	16.671	0.007	16.051	0.008	15.848	0.010	15.437	0.007	15.271	0.007	14.862	0.002	14.607	0.004	14.179	0.002	14.117	0.002	13.872	0.001	13.770	0.003	13.755	0.002	
J04580976–4632284	16.765	0.010	16.215	0.011	16.104	0.015	15.776	0.011	15.640	0.010	15.296	0.004	15.094	0.006	14.733	0.002	14.671	0.003	14.389	0.003	14.346	0.002			
J04582454–4518477	16.585	0.010	16.051	0.010	15.872	0.013	15.678	0.010	15.552	0.009	15.251	0.003	15.060	0.006	14.736	0.002	14.672	0.002	14.492	0.002	14.395	0.003	14.370	0.002	
J09580012–1803531	16.219	0.007	15.682	0.008	15.434	0.010	15.135	0.008	15.016	0.007	14.820	0.003	14.625	0.004	14.367	0.002	14.184	0.002	14.124	0.003	14.099	0.002			
J09585158–0829008	16.103	0.007	15.498	0.007	15.339	0.009	14.978	0.007	14.775	0.006	14.389	0.002	14.139	0.004	13.690	0.001	13.606	0.002	13.371	0.001	13.236	0.002	13.200	0.001	
J1.0003629–1725512	17.499	0.016	16.977	0.016	16.821	0.022	16.589	0.017	16.464	0.015	16.166	0.005	15.969	0.009	15.656	0.004	15.587	0.004	15.408	0.003	15.344	0.005	15.301	0.004	
J1.00040252–180599	18.034	0.021	17.415	0.020	17.235	0.027	16.972	0.021	16.790	0.018	16.516	0.006	16.323	0.011	15.953	0.004	15.887	0.005	15.636	0.004	15.592	0.006	15.553	0.005	
J1.0011607–1747125	16.830	0.010	16.340	0.011	16.181	0.015	15.957	0.012	15.805	0.010	15.550	0.004	15.371	0.007	15.063	0.003	15.007	0.003	14.847	0.002	14.770	0.004	14.735	0.003	
J1.0021099–0330092	15.952	0.006	15.409	0.007	15.682	0.008	15.434	0.010	15.135	0.008	14.811	0.006	14.461	0.002	14.255	0.004	13.863	0.001	13.797	0.002	13.589	0.001	13.487	0.002	
J1.0024475–1716153	16.757	0.010	16.127	0.010	16.010	0.016	15.672	0.010	15.503	0.009	15.211	0.003	15.006	0.006	14.651	0.010	14.592	0.002	14.402	0.002	14.308	0.003	14.279	0.002	
J1.0040075+0134108	17.626	0.015	17.155	0.017	17.063	0.023	16.719	0.016	16.674	0.015	16.400	0.005	16.228	0.010	15.976	0.004	15.910	0.004	15.645	0.003	15.499	0.006	15.434	0.004	
J1.0040252–0911728	15.991	0.007	15.539	0.008	15.444	0.011	15.166	0.008	15.042	0.007	14.756	0.003	14.572	0.005	14.254	0.002	14.194	0.002	14.015	0.002	13.929	0.003	13.905	0.002	
J1.0040553+0235484	16.019	0.006	15.408	0.007	15.217	0.009	15.026	0.008	14.890	0.007	14.658	0.002	14.468	0.004	14.176	0.002	14.122	0.002	13.969	0.002	13.898	0.003	13.873	0.002	
J1.0040693–1138417	14.681	0.004	14.326	0.006	14.200	0.010	14.086	0.005	13.893	0.004	13.666	0.002	13.493	0.003	13.237	0.001	13.214	0.001	13.053	0.001	12.988	0.002	12.985	0.001	
J1.0043854–0939488	16.831	0.011	16.395	0.012	16.261	0.016	16.001	0.012	15.866	0.011	15.579	0.004	15.397	0.007	15.065	0.003	14.939	0.004	14.822	0.003	14.752	0.004	14.719	0.003	
J1.0050873+0025147	16.236	0.007	15.615	0.007	15.370	0.009	15.218	0.007	15.098	0.006	14.936	0.003	14.784	0.005	14.551	0.010	14.557	0.002	14.406	0.002	14.335	0.003	14.338	0.002	
J1.0052824–0911423	17.488	0.015	16.794	0.015	16.712	0.020	16.341	0.014	16.137	0.013	15.723	0.004	15.524	0.008	15.050	0.003	14.951	0.001	14.715	0.002	14.589	0.004	14.557	0.003	
J1.0052863–1433198	16.755	0.012	16.208	0.012	16.101	0.017	15.816	0.015	15.730	0.011	15.330	0.004	15.129	0.007	14.776	0.003	14.711	0.003	14.517	0.002	14.423	0.003	14.390	0.002	
J1.0053549–0924326	16.701	0.010	16.257	0.012	16.065	0.015	15.903	0.012	15.786	0.011	15.557	0.004	15.400	0.007	15.127	0.003	15.075	0.003	14.928	0.003	14.835	0.004	14.841	0.003	
J1.0054630–1226387	15.907	0.007	15.372	0.009	15.201	0.009	14.885	0.007	14.737	0.006	14.341	0.002	14.106	0.004	13.737	0.001	13.691	0.002	13.463	0.001	13.303	0.002	13.266	0.001	
J1.0062477–195366	17.288	0.011	16.851	0.014	16.670	0.018	16.322	0.014	16.378	0.013	16.177	0.005	16.196	0.009	15.757	0.004	15.747	0.004	15.748	0.004	15.532	0.006	15.505	0.002	
J1.0072392–1317186	15.502	0.006	14.909	0.006	14.762	0.008	14.459	0.006	14.225	0.006	13.905	0.002	13.717	0.004	13.293	0.003	13.207	0.001	12.939	0.001	12.878	0.002	12.841	0.001	
J1.0081117–1918306	16.385	0.007	15.959	0.009	15.761	0.011	15.527	0.009	15.429	0.008	15.229	0.003	15.036	0.006	14.791	0.001	14.755	0.003	14.606	0.002	14.541	0.003	14.518	0.003	
J1.0092998–2057477	16.354	0.008	15.892	0.009	15.706	0.012	15.507	0.009	15.412	0.009	15.199	0.003	15.019	0.006	14.779	0.002	14.748	0.003	14.577	0.002	14.511	0.003	14.489	0.003	
J1.0093999–1641194	15.786	0.006	15.344	0.007	15.174	0.009	14.927	0.007	14.809	0.006	14.563	0.002	14.382	0.004	14.082	0.002	14.025	0.002	13.870	0.001	13.791	0.002	13.768	0.002	
J1.0105387–1753449	17.081	0.011	16.356	0.016	16.178	0.014	15.713	0.010	15.469	0.009	15.193	0.003	14.675	0.004	14.094	0.002	13.712	0.001	13.393	0.002	13.517	0.002	13.510	0.002	
J1.0113371–1342160	16.420	0.008	16.022	0.022	16.252	0.028	16.078	0.022	16.859	0.019	16.501	0.005	16.320	0.011	16.896	0.005	16.505	0.004	16.501	0.004	15.471	0.004	15.444	0.004	
J1.01192807–202499	17.479	0.013	16.931	0.015	16.673	0.018	16.533	0.015	16.366	0.013	16.093	0.005	15.885	0.008	15.567	0.003	15.492	0.004	15.317	0.003	15.198	0.004	15.188	0.004	
J1.01193237–1638584	16.646	0.010	16.027	0.010	16.258	0.013	15.648	0.009	15.376	0.008	15.029	0.003	14.804	0.005	14.385	0.002	14.305	0.002	14.055	0.002	13.977	0.003	13.940	0.002	
J1.01254045–1622201	17.516	0.015	17.140	0.018	16.995	0.025	16.712	0.018	16.629	0.017	16.420	0.006	16.271	0.011	15.968	0.004	15.891	0.006	15.638	0.004	15.527	0.006	15.484	0.004	
J1.01255315–1635461	15.437	0.005	14.967	0.006	14.561	0.006	14.420	0.006	14.131	0.002	13.918	0.004	13.588	0.001	13.522	0.002	13.335	0.001	13.245	0.002	13.226	0.001			
J1.01261807–1459502	18.213	0.028	17.755	0.031	17.597	0.048	17.345	0.031	17.146	0.032	16.854	0.009	16.667	0.015	16.262	0.005	16.195	0.007	15.971	0.004	15.839	0.007	15.812	0.005	
J1.01264336–1425080	17.564	0.018	17.080	0.020	16.791	0.029	16.730	0.020	16.632	0.023	16.440	0.007	16.275	0.012	16.113	0.005	16.120	0.002	15.978	0.005	15.921	0.006	15.924	0.006	
J1.01264358–1522074	17.044	0.012	16.446	0.013	16.256	0.020	15.942	0.013	15.816	0.014	15.607	0.004	15.381	0.007	15.109	0.003	15.062	0.004	14.886	0.003	14.812	0.004	14.795	0.003	
J1.01292435–1859348	16.306	0.007	15.686	0.008	15.553	0.011	15.267	0.008	15.135	0.008	14.726	0.003	14.507	0.005	14.105	0.002	14.022	0.002	13.813	0.002	13.706	0.002	13.660	0.002	
J1.01315039–1914338	18.203	0.019	17.746	0.022	17.545																				

Table 2 (*continued*)

Star Name	uJAVA	σ	J0378	σ	J0395	σ	J0410	σ	J0430	σ	gSDSS	σ	J0515	σ	rSDSS	σ	J0660	σ	iSDSS	σ	J0861	σ	zSDSS	σ
J10434788-1715518	17.524	0.021	16.736	0.017	16.475	0.022	16.030	0.015	15.715	0.013	15.087	0.004	14.827	0.007	14.188	0.002	14.077	0.002	13.767	0.002	13.619	0.002	13.559	0.002
J10434103-1712132	16.150	0.007	15.714	0.010	15.518	0.011	15.315	0.009	15.182	0.008	14.950	0.003	14.761	0.005	14.501	0.002	14.453	0.002	14.300	0.002	14.230	0.003	14.216	0.002
J10432732-1707224	17.285	0.013	16.703	0.017	16.367	0.019	16.308	0.014	16.182	0.013	15.809	0.004	15.615	0.008	15.243	0.003	15.181	0.003	14.983	0.004	14.889	0.004	14.859	0.003
J10455833-2143374	15.217	0.004	14.890	0.005	14.729	0.007	14.582	0.005	14.474	0.005	14.292	0.002	14.129	0.003	13.907	0.001	13.887	0.002	13.757	0.001	13.714	0.002	13.695	0.002
J1051284-2136425	16.814	0.009	16.301	0.010	16.168	0.014	16.145	0.010	16.117	0.009	15.482	0.002	15.289	0.006	14.938	0.002	14.866	0.003	14.612	0.004	14.577	0.003		
J11001243-2112108	17.131	0.011	16.628	0.012	16.492	0.016	16.319	0.013	16.173	0.011	15.886	0.004	15.699	0.007	15.370	0.003	15.314	0.003	15.141	0.003	15.034	0.005	15.027	0.003
J10570437-2215021	15.764	0.006	15.317	0.007	15.181	0.009	14.939	0.007	14.812	0.006	14.552	0.002	14.363	0.004	14.073	0.002	14.046	0.006	13.854	0.003	13.780	0.003	13.748	0.002
J10572425-2110418	17.384	0.012	16.842	0.013	16.705	0.018	16.410	0.013	16.291	0.012	15.966	0.004	15.763	0.008	15.379	0.003	15.335	0.003	15.113	0.003	15.011	0.004	14.980	0.003
J10573193-2223341	17.353	0.014	16.781	0.014	16.568	0.018	16.337	0.013	16.270	0.012	15.981	0.005	15.796	0.008	15.496	0.003	15.477	0.004	15.277	0.003	15.212	0.005	15.180	0.004
J10580923-2141447	16.416	0.007	15.895	0.008	15.798	0.011	15.413	0.008	15.296	0.007	14.936	0.003	14.706	0.005	14.335	0.002	14.263	0.002	14.063	0.002	13.964	0.003	13.934	0.002
J11001243-2112286	17.459	0.013	16.723	0.013	16.524	0.018	16.153	0.013	16.153	0.011	15.924	0.004	15.789	0.006	15.415	0.004	15.115	0.006	14.612	0.002	14.240	0.002	14.071	0.003
J11002053-1833151	17.280	0.011	16.659	0.012	16.462	0.015	16.195	0.012	16.026	0.010	15.709	0.004	15.484	0.006	15.132	0.002	15.055	0.003	14.859	0.002	14.741	0.004	14.708	0.003
J11022646-2342494	15.504	0.006	15.050	0.008	14.937	0.009	14.640	0.007	14.337	0.007	14.237	0.002	14.036	0.004	13.706	0.002	13.666	0.002	13.458	0.001	13.382	0.002	13.356	0.002
J11030563-2231467	15.777	0.007	15.144	0.007	15.012	0.009	14.694	0.007	14.526	0.006	14.236	0.002	14.033	0.004	13.674	0.002	13.598	0.002	13.353	0.001	13.290	0.002	13.261	0.001
J11081009-1940403	18.275	0.020	17.737	0.021	17.552	0.030	17.420	0.023	17.199	0.020	16.945	0.007	16.762	0.013	16.414	0.005	16.368	0.006	16.188	0.005	16.097	0.008	16.082	0.007
J11083127-2235143	15.697	0.007	15.187	0.007	15.075	0.009	14.843	0.007	14.722	0.006	14.417	0.002	14.241	0.004	13.904	0.002	13.846	0.002	13.668	0.001	13.584	0.002	13.539	0.002
J11120172-2212075	16.018	0.007	15.609	0.008	15.434	0.010	15.210	0.008	15.132	0.007	14.908	0.003	14.640	0.005	14.330	0.002	14.294	0.002	14.110	0.002	14.034	0.003	14.004	0.002
J11124929-2357161	16.990	0.011	16.421	0.012	16.228	0.015	15.971	0.011	15.805	0.010	15.374	0.004	15.142	0.006	14.707	0.002	14.619	0.002	14.380	0.003	14.258	0.003	14.216	0.002
J11135656-2041051	15.942	0.006	15.366	0.006	15.229	0.008	14.852	0.006	14.710	0.005	14.287	0.002	14.062	0.003	13.628	0.001	13.455	0.001	13.357	0.001	13.229	0.002	13.188	0.001
J11135726-2222091	14.576	0.004	14.123	0.004	13.978	0.005	13.783	0.004	13.677	0.004	13.413	0.001	13.238	0.002	12.958	0.001	12.747	0.001	12.664	0.001	12.654	0.001		
J11144560-2212214	16.446	0.009	16.048	0.009	15.864	0.012	15.613	0.009	15.493	0.008	15.250	0.003	15.026	0.006	14.755	0.005	14.712	0.003	14.523	0.002	14.458	0.004	14.431	0.002
J111622403-1843000	16.455	0.008	15.852	0.008	15.655	0.010	15.391	0.008	15.216	0.007	14.908	0.003	14.699	0.004	14.340	0.002	14.281	0.001	14.061	0.002	13.975	0.003	13.937	0.002
J11171192-1911211	15.083	0.004	14.762	0.005	14.612	0.006	14.404	0.005	14.278	0.005	14.031	0.002	13.842	0.003	13.574	0.001	13.520	0.001	13.381	0.001	13.346	0.002	13.304	0.001
J11190308-1946350	16.212	0.007	15.588	0.007	15.480	0.008	15.098	0.008	14.872	0.006	14.484	0.002	14.246	0.004	13.811	0.001	13.729	0.002	13.491	0.001	13.379	0.002	13.334	0.001
J11194427-2308401	17.852	0.015	17.352	0.017	17.201	0.022	16.994	0.017	16.867	0.015	16.551	0.006	16.407	0.010	16.047	0.004	15.989	0.005	15.805	0.005	15.730	0.006	15.677	0.005
J11194933-2317327	16.423	0.007	15.947	0.008	15.848	0.011	15.615	0.008	15.410	0.007	15.059	0.003	14.861	0.005	14.492	0.002	14.427	0.002	14.225	0.002	14.140	0.003	14.098	0.002
J11201142-1933447	15.374	0.004	14.886	0.005	14.723	0.007	14.426	0.005	14.322	0.005	14.025	0.002	13.811	0.003	13.491	0.001	13.427	0.001	13.241	0.001	13.138	0.002	13.122	0.001
J112033812-2356163	16.013	0.009	15.427	0.008	15.247	0.011	14.820	0.008	14.692	0.007	14.159	0.003	13.873	0.004	13.446	0.001	13.333	0.001	13.058	0.001	12.962	0.002	12.930	0.001
J11220137-2330558	16.530	0.009	16.003	0.009	15.872	0.012	15.446	0.009	15.261	0.010	15.018	0.009	14.859	0.003	14.123	0.002	13.792	0.002	13.755	0.002				
J11222244-17322	0.011	16.869	0.014	16.676	0.018	16.470	0.015	16.373	0.010	16.136	0.005	15.965	0.009	15.668	0.004	15.468	0.003	15.389	0.006	15.375	0.004			
J11225058-2243447	16.726	0.010	16.049	0.010	15.895	0.012	15.531	0.009	15.523	0.008	14.946	0.003	14.703	0.005	14.271	0.002	14.167	0.007	14.002	0.002	13.930	0.002	13.764	0.002
J11225672-1902327	15.722	0.005	15.240	0.006	15.072	0.008	14.781	0.006	14.714	0.006	14.398	0.002	14.176	0.004	13.857	0.007	13.804	0.002	13.625	0.001	13.527	0.002	13.475	0.001
J11230328-2126276	16.040	0.007	15.496	0.008	15.261	0.010	15.089	0.008	15.032	0.007	14.739	0.003	14.549	0.005	14.291	0.002	14.242	0.002	14.080	0.002	13.987	0.003	13.979	0.002
J11241118-2115149	17.616	0.016	17.162	0.018	16.934	0.023	16.805	0.019	16.696	0.017	16.442	0.006	16.327	0.011	16.046	0.005	15.966	0.004	15.748	0.004	15.735	0.005		
J11254036-2034269	17.488	0.013	17.147	0.016	17.054	0.020	16.823	0.016	16.688	0.014	16.439	0.005	16.237	0.010	15.941	0.006	15.715	0.004	15.466	0.006	15.630	0.004		
J112541158-2440906	15.978	0.008	15.706	0.011	15.594	0.013	15.300	0.010	15.173	0.009	14.914	0.004	14.673	0.006	14.374	0.002	14.320	0.002	14.149	0.002	14.050	0.003	14.050	0.002
J113006065-2138213	16.978	0.010	16.511	0.012	16.293	0.015	16.137	0.012	15.994	0.011	15.728	0.004	15.538	0.007	15.226	0.003	15.168	0.003	14.992	0.003	14.908	0.004	14.889	0.003
J113045117-2347312	15.642	0.006	15.286	0.008	15.089	0.009	14.986	0.007	14.880	0.007	14.716	0.003	14.572	0.005	14.373	0.002	14.366	0.002	14.242	0.002	14.210	0.003	14.193	0.002
J11312025-1957045	17.620	0.015	17.196	0.017	17.003	0.024	16.870	0.020	16.725	0.017	16.504	0.007	16.327	0.011	16.046	0.005	15.900	0.00						

Table 2 (continued)

Star Name	uJAVA	σ	J0378	σ	J0395	σ	J0410	σ	J0430	σ	gSDSS	σ	J0515	σ	rSDSS	σ	J0660	σ	iSDSS	σ	J0861	σ	zSDSS	σ
J11445275-203317	16.385	0.009	15.840	0.009	15.712	0.012	15.351	0.008	15.226	0.008	14.834	0.003	14.607	0.004	14.207	0.002	14.129	0.002	13.926	0.002	13.816	0.003	13.780	0.002
J11445318-1958567	15.065	0.004	14.488	0.005	14.235	0.006	14.097	0.005	13.975	0.004	13.802	0.002	13.643	0.003	13.411	0.001	13.378	0.001	13.240	0.001	13.178	0.002	13.172	0.001
J114464483-1936295	15.585	0.005	15.126	0.006	14.927	0.008	14.743	0.006	14.638	0.006	14.438	0.002	14.239	0.004	14.007	0.002	13.973	0.002	13.822	0.001	13.750	0.002	13.739	0.002
J11464646-2216104	17.540	0.011	16.798	0.010	16.610	0.013	16.276	0.010	16.042	0.008	15.607	0.003	15.358	0.005	14.879	0.002	14.804	0.002	14.545	0.002	14.494	0.002	14.365	0.002
J11464903-21050998	16.001	0.006	15.364	0.007	15.230	0.009	14.792	0.006	14.587	0.005	14.109	0.002	13.847	0.003	13.381	0.001	13.291	0.001	13.028	0.001	12.893	0.002	12.855	0.001
J11482911-21040456	16.363	0.008	15.879	0.009	15.734	0.011	15.595	0.011	15.408	0.008	15.380	0.008	15.110	0.003	14.929	0.005	14.611	0.002	14.559	0.002	14.372	0.002	14.287	0.003
J11493550-2101315	16.219	0.007	15.764	0.007	15.595	0.011	15.408	0.008	15.281	0.007	15.066	0.003	14.895	0.005	14.623	0.002	14.601	0.002	14.425	0.002	14.352	0.003	14.335	0.002
J11500663-1943013	15.852	0.006	15.313	0.007	15.125	0.008	14.916	0.007	14.766	0.006	14.506	0.002	14.313	0.004	13.998	0.002	13.959	0.002	13.756	0.001	13.680	0.002	13.659	0.002
J11503041-2209074	17.721	0.015	17.315	0.018	17.102	0.023	16.938	0.017	16.822	0.016	16.647	0.006	16.457	0.010	16.236	0.004	16.211	0.005	16.071	0.004	16.023	0.008	16.010	0.006
J11511408-2159328	15.066	0.003	14.668	0.003	14.457	0.004	14.200	0.003	14.094	0.003	13.904	0.001	13.735	0.002	13.513	0.001	13.486	0.001	13.347	0.001	13.295	0.001	13.282	0.001
J11514550-1834578	15.754	0.006	15.263	0.006	15.121	0.009	14.821	0.007	14.715	0.006	14.455	0.005	14.344	0.005	14.179	0.002	14.032	0.003	13.818	0.001	13.587	0.001	13.475	0.002
J11525640-2035404	15.221	0.004	14.817	0.005	14.616	0.006	14.455	0.005	14.344	0.005	14.179	0.002	14.032	0.003	13.813	0.002	13.641	0.002	13.618	0.001	13.618	0.001		
J11562039-1936572	16.756	0.009	16.289	0.010	16.106	0.013	15.902	0.005	15.803	0.009	15.543	0.003	15.366	0.006	15.057	0.007	15.030	0.003	14.845	0.005	14.759	0.004	14.747	0.003
J12023289-1931447	15.980	0.006	15.506	0.006	15.304	0.008	15.059	0.006	14.914	0.006	14.665	0.002	14.470	0.004	14.172	0.002	14.149	0.002	13.966	0.001	13.892	0.002	13.856	0.002
J12023816-1957058	16.505	0.007	16.039	0.008	15.855	0.011	15.611	0.008	15.479	0.007	15.206	0.003	14.999	0.005	14.680	0.002	14.630	0.002	14.437	0.002	14.345	0.003	14.319	0.002
J12040768-0234051	18.043	0.018	17.534	0.019	17.350	0.025	17.230	0.020	17.072	0.018	16.824	0.007	16.673	0.012	16.354	0.005	16.302	0.005	16.140	0.004	16.041	0.007	16.048	0.006
J12064288+0004032	16.054	0.007	15.358	0.007	15.129	0.009	14.801	0.006	14.590	0.006	14.112	0.005	13.856	0.003	13.362	0.001	13.269	0.001	12.884	0.002	12.850	0.001		
J12090903-1508048	16.973	0.010	16.435	0.011	16.308	0.015	16.018	0.015	15.882	0.010	15.500	0.004	15.298	0.006	14.904	0.002	14.811	0.003	14.623	0.002	14.522	0.003	14.484	0.002
J121112971-0212276	15.496	0.005	14.976	0.006	14.799	0.007	14.584	0.005	14.471	0.005	14.198	0.002	13.987	0.003	13.680	0.001	13.618	0.001	13.441	0.001	13.356	0.002	13.323	0.001
J12141957-0036482	15.386	0.005	14.942	0.006	14.729	0.007	14.544	0.006	14.436	0.006	14.202	0.002	13.997	0.004	13.742	0.002	13.678	0.002	13.512	0.001	13.444	0.002	13.437	0.002
J12184512+0051359	16.481	0.008	15.925	0.009	15.737	0.012	15.492	0.010	15.327	0.008	15.015	0.003	14.817	0.005	14.444	0.002	14.366	0.002	14.192	0.002	14.072	0.003	14.065	0.002
J1220351518-00575782	15.118	0.004	14.657	0.005	14.473	0.006	14.303	0.005	14.190	0.005	13.984	0.002	13.806	0.003	13.576	0.001	13.549	0.001	13.350	0.001	13.351	0.002	13.317	0.001
J12233624-1522120	15.255	0.004	14.777	0.005	14.680	0.006	14.332	0.005	14.302	0.004	14.160	0.002	13.767	0.003	13.743	0.001	13.716	0.001	13.570	0.001	13.570	0.002	13.511	0.001
J12234076-0131031	17.231	0.011	16.718	0.013	16.520	0.017	16.320	0.014	16.207	0.012	15.955	0.005	15.768	0.008	15.449	0.003	15.393	0.004	15.228	0.003	15.159	0.005	15.111	0.004
J12253942-1452401	15.613	0.005	15.034	0.005	14.833	0.007	14.593	0.005	14.456	0.005	14.341	0.002	14.159	0.003	13.948	0.001	13.722	0.002	13.573	0.001	13.533	0.002	13.495	0.001
J12290963-0059118	17.529	0.015	16.943	0.015	16.757	0.020	16.513	0.015	16.434	0.014	16.066	0.005	15.844	0.008	15.517	0.007	15.461	0.004	15.277	0.003	15.187	0.005	15.158	0.004
J12292867+0115087	17.562	0.006	15.314	0.007	15.102	0.009	14.994	0.007	14.869	0.006	14.698	0.003	14.533	0.004	14.319	0.002	14.292	0.002	14.168	0.002	14.122	0.003	14.103	0.002
J12351720-1503087	17.247	0.015	16.703	0.016	16.545	0.026	16.313	0.016	16.212	0.015	15.871	0.005	15.357	0.007	14.557	0.004	14.357	0.003	14.028	0.005	14.965	0.004		
J12413337-1318137	16.006	0.007	15.381	0.007	15.217	0.009	14.980	0.006	14.860	0.006	14.346	0.002	14.232	0.004	13.749	0.001	13.474	0.002	13.350	0.002	13.398	0.001		
J12453883-1440173	18.117	0.015	17.606	0.016	17.417	0.022	17.232	0.016	17.135	0.014	16.782	0.005	16.600	0.009	16.253	0.003	16.192	0.004	16.033	0.003	15.919	0.005	15.886	0.004
J12551524-1533478	17.081	0.008	16.568	0.009	16.354	0.011	16.075	0.009	15.946	0.008	15.637	0.003	15.379	0.005	15.034	0.004	14.968	0.002	14.764	0.003	14.642	0.003	14.621	0.002
J125811969-1423114	17.458	0.009	16.944	0.009	16.730	0.012	16.562	0.009	16.414	0.009	16.142	0.004	15.949	0.006	15.620	0.002	15.563	0.003	15.367	0.002	15.276	0.004	15.247	0.003
J13011453-145403	15.314	0.003	14.871	0.003	14.672	0.004	14.465	0.003	14.339	0.003	14.075	0.001	13.879	0.002	13.576	0.001	13.527	0.001	13.364	0.001	13.296	0.001	13.259	0.001
J13012016-1442042	16.519	0.005	16.061	0.006	15.861	0.008	15.653	0.006	15.531	0.006	15.254	0.002	15.057	0.004	14.733	0.015	14.394	0.005	16.133	0.005	16.059	0.007		
J13070601-1452022	18.103	0.029	17.694	0.032	17.574	0.043	17.432	0.032	17.318	0.026	17.048	0.028	16.816	0.011	16.600	0.017	16.253	0.006	16.027	0.004	15.905	0.007		
J13073449-1327258	15.933	0.007	15.320	0.007	15.149	0.008	14.903	0.007	14.747	0.007	14.476	0.003	14.272	0.004	13.941	0.002	13.788	0.002	13.705	0.001	13.649	0.002	13.586	0.002
J13073627-1158131	18.192	0.016	16.830	0.017	16.531	0.023	16.568	0.013	16.361	0.026	17.233	0.014	16.968	0.008	16.801	0.014	16.417	0.006	16.251	0.005	16.159	0.009	16.135	0.006
J13080410-1327591	17.252	0.015	16.551	0.014	16.333	0.017	15.995	0.012	15.719	0.011	15.295	0.004	15.022	0.006	14.515	0.005	14.456	0.003	14.327	0.007	14.337	0.003	14.326	0.002
J13083330-1313027	18.412	0.014	17.176	0.016	16.924	0.023	16.521	0.017	16.493	0.008	16.058	0.006	16.375	0.011	16.172									

Table 2 (*continued*)

Star Name	uJAVA	σ	J0378	σ	J0395	σ	J0410	σ	J0430	σ	gSDSS	σ	J0515	σ	rSDSS	σ	J0660	σ	iSDSS	σ	J0861	σ	zSDSS	σ
J13255973-1331509	17.240	0.012	16.739	0.013	16.593	0.018	16.410	0.014	16.290	0.013	16.000	0.005	15.821	0.008	15.526	0.003	15.477	0.004	15.295	0.003	15.232	0.005	15.198	0.004
J13260147-1420519	15.767	0.005	15.362	0.006	15.183	0.008	14.976	0.006	14.847	0.006	14.642	0.002	14.460	0.004	14.224	0.002	14.205	0.002	14.040	0.002	13.984	0.003	13.956	0.002
J13263400-0751220	17.210	0.011	16.699	0.012	16.527	0.016	16.301	0.013	16.154	0.012	15.857	0.004	15.676	0.007	15.327	0.003	15.289	0.003	15.110	0.003	15.020	0.004	15.000	0.003
J13263837-1351343	15.510	0.005	14.837	0.005	14.512	0.006	14.247	0.005	14.121	0.004	13.896	0.002	13.715	0.003	13.420	0.001	13.367	0.001	13.181	0.001	13.090	0.002	13.053	0.001
J13273733-0736314	17.074	0.010	16.529	0.011	16.300	0.014	16.131	0.012	15.944	0.010	15.703	0.004	15.543	0.007	15.206	0.003	15.141	0.003	14.937	0.003	14.870	0.004	14.862	0.003
J13285008-0753313	17.453	0.014	16.933	0.015	16.723	0.021	16.498	0.016	16.353	0.014	16.106	0.005	15.917	0.009	15.600	0.004	15.361	0.003	15.367	0.003	15.278	0.005	15.241	0.004
J13285225-1453128	15.719	0.005	15.171	0.006	14.943	0.016	14.741	0.017	14.741	0.016	14.602	0.005	14.396	0.002	14.214	0.004	13.960	0.001	13.908	0.002	13.752	0.002	13.684	0.002
J13285822-1428027	17.335	0.012	16.936	0.013	16.706	0.017	16.561	0.014	16.455	0.013	16.199	0.005	16.039	0.009	15.764	0.004	15.736	0.003	15.557	0.003	15.488	0.006	15.461	0.004
J13302081-1053210	16.185	0.007	15.625	0.008	15.421	0.010	15.217	0.008	15.073	0.007	14.737	0.003	14.536	0.004	14.197	0.002	14.112	0.002	13.940	0.002	13.848	0.002	13.820	0.002
J13303025-1445123	17.925	0.016	17.449	0.018	17.283	0.025	17.067	0.019	16.978	0.019	16.634	0.006	16.420	0.011	16.116	0.004	16.059	0.005	15.871	0.004	15.760	0.007	15.740	0.005
J13304241-1258149	15.981	0.006	15.404	0.007	15.240	0.009	14.991	0.007	14.859	0.006	14.541	0.002	14.336	0.004	13.988	0.002	13.955	0.002	13.731	0.001	13.636	0.003	13.599	0.002
J13305370-0812151	17.317	0.013	16.794	0.015	16.627	0.020	16.421	0.015	16.273	0.014	15.981	0.005	15.793	0.009	15.454	0.004	15.390	0.004	15.209	0.003	15.122	0.005	15.096	0.004
J13350807-1524301	17.730	0.014	17.364	0.017	17.171	0.023	16.912	0.018	16.776	0.017	16.472	0.006	16.244	0.010	15.894	0.004	15.623	0.004	15.638	0.004	15.497	0.006	15.510	0.005
J13350549-1143314	15.850	0.006	15.374	0.007	15.230	0.009	14.986	0.007	14.865	0.007	14.568	0.002	14.369	0.004	14.063	0.002	13.836	0.002	13.767	0.003	13.736	0.002		
J13331559-1032347	17.516	0.013	16.985	0.015	16.790	0.020	16.573	0.015	16.442	0.013	16.155	0.005	15.962	0.008	15.658	0.003	15.591	0.004	15.448	0.003	15.345	0.005	15.305	0.004
J13334221-0633509	17.901	0.021	17.362	0.025	17.140	0.031	16.991	0.024	16.814	0.020	16.486	0.007	16.296	0.013	15.914	0.005	15.553	0.005	15.643	0.004	15.536	0.006	15.509	0.005
J13351616-1231003	15.799	0.006	15.253	0.006	15.053	0.009	14.760	0.007	14.615	0.006	14.251	0.002	14.024	0.004	13.642	0.002	13.540	0.002	13.211	0.002	13.197	0.001		
J13354927-1013160	16.091	0.006	15.586	0.007	15.447	0.009	15.170	0.007	15.044	0.007	14.756	0.002	14.547	0.004	14.252	0.002	14.209	0.002	14.013	0.002	13.937	0.003	13.906	0.002
J13363905-1148292	17.192	0.012	16.740	0.014	16.475	0.017	16.284	0.014	16.172	0.013	15.905	0.005	15.708	0.008	15.397	0.003	15.345	0.004	15.160	0.003	15.035	0.005	15.048	0.004
J13374402-1217279	16.247	0.007	15.710	0.008	15.362	0.025	15.140	0.031	16.991	0.024	16.814	0.020	16.486	0.007	16.296	0.013	15.914	0.005	15.553	0.005	15.536	0.006	15.509	0.005
J13382471-0958520	15.926	0.006	15.520	0.007	15.346	0.009	15.117	0.007	15.012	0.007	14.772	0.003	14.595	0.004	14.297	0.002	14.249	0.002	14.099	0.002	14.046	0.003	13.999	0.002
J13390855-1050534	17.380	0.011	16.856	0.012	16.630	0.016	16.421	0.012	16.270	0.011	16.934	0.004	15.720	0.007	15.341	0.003	15.284	0.003	15.045	0.003	14.930	0.004	14.905	0.003
J13392436-0847090	15.691	0.005	15.038	0.006	14.818	0.007	14.448	0.005	14.244	0.005	14.082	0.002	13.571	0.003	13.131	0.001	13.082	0.002	12.640	0.002	12.640	0.001		
J13394057-0636508	15.884	0.006	15.401	0.007	15.220	0.010	15.008	0.008	14.888	0.006	14.632	0.003	14.451	0.004	14.172	0.002	14.135	0.002	13.988	0.003	13.863	0.002		
J13404551-0633557	15.098	0.004	14.613	0.005	14.407	0.006	14.184	0.005	14.049	0.004	13.757	0.002	13.587	0.003	13.294	0.001	13.248	0.001	13.057	0.001	12.970	0.002	12.951	0.001
J13410860-1232133	17.309	0.013	16.851	0.014	16.693	0.019	16.444	0.015	16.303	0.013	16.032	0.005	15.820	0.009	15.478	0.003	15.394	0.004	15.226	0.003	15.124	0.005	15.097	0.004
J13420799-1157040	15.251	0.005	14.866	0.005	14.623	0.007	14.476	0.006	14.379	0.005	14.240	0.002	14.065	0.004	13.877	0.002	13.876	0.002	13.744	0.001	13.740	0.003	13.707	0.002
J13430545-0807438	16.887	0.009	16.305	0.011	16.128	0.014	15.877	0.010	15.720	0.009	15.391	0.003	15.196	0.006	14.820	0.002	14.749	0.009	14.546	0.006	14.448	0.003	14.408	0.002
J13431375-0948485	16.797	0.010	16.299	0.011	16.105	0.014	15.713	0.011	15.400	0.004	15.104	0.004	14.805	0.006	14.585	0.003	14.356	0.003	14.161	0.004	14.111	0.002	14.077	0.004
J13432075-06405371	16.342	0.007	16.732	0.007	16.493	0.010	16.257	0.007	16.036	0.007	15.705	0.004	15.406	0.007	14.704	0.002	14.410	0.002	14.030	0.002	13.810	0.001	13.725	0.002
J13432554-0746249	16.043	0.006	15.499	0.007	15.388	0.010	15.040	0.007	14.923	0.006	14.744	0.002	14.326	0.004	13.977	0.001	13.916	0.002	13.706	0.001	13.646	0.002		
J134360151-0819059	16.810	0.010	16.330	0.011	16.142	0.015	15.966	0.011	15.836	0.010	15.560	0.004	15.378	0.006	15.066	0.002	15.018	0.003	14.847	0.007	14.766	0.004		
J13442090-1507098	17.488	0.009	17.060	0.010	16.897	0.013	16.555	0.010	16.418	0.009	16.126	0.003	15.902	0.006	15.583	0.002	15.510	0.003	15.329	0.002	15.210	0.003	15.118	0.001
J13444602-1445281	17.094	0.013	16.551	0.013	16.372	0.016	16.179	0.013	16.022	0.011	15.755	0.004	15.524	0.007	15.117	0.006	14.698	0.002	14.618	0.003	14.365	0.003	14.243	0.003
J13450507-06405371	16.342	0.007	16.732	0.007	16.493	0.010	16.257	0.007	16.036	0.007	15.705	0.004	15.406	0.007	14.704	0.002	14.410	0.002	14.030	0.002	13.810	0.001		
J134522307-0731330	15.302	0.004	14.723	0.005	14.535	0.006	14.293	0.005	14.147	0.004	13.927	0.002	13.757	0.003	13.481	0.001	13.455	0.001	13.275	0.002	13.181	0.001		
J13452477-0922116	16.483	0.008	16.030	0.010	15.897	0.013	15.626	0.011	15.223	0.009	15.214	0.003	15.020	0.006	14.697	0.007	14.643	0.003	14.473	0.003	14.384	0.003		
J13440121-0910128	15.856	0.006	15.400	0.007	15.240	0.009	15.010	0.007	14.908	0.007	14.625	0.002	14.430	0.004	14.135	0.005	14.098	0.002	13.920	0.002	13.836	0.003		
J13442905-08331492	15.942	0.006	15.463	0.007	15.253	0.009	14.925	0.007	14.777	0.006	14.404	0.002	14.175	0.004	13.799	0.001	13.730	0.001	13.542	0.001	13.433	0.002		
J13451357-0615460	17.119	0.011	16.																					

Table 2 (*continued*)

Star Name	uJAVA	σ	J0378	σ	J0395	σ	J0410	σ	J0430	σ	gSDSS	σ	J0515	σ	rSDSS	σ	J0660	σ	iSDSS	σ	J0861	σ	zSDSS	σ	σ
J13552684-1533012	17.726	0.018	17.114	0.018	16.923	0.022	16.650	0.017	16.510	0.015	16.231	0.006	16.026	0.010	15.674	0.004	15.612	0.004	15.436	0.003	15.331	0.006	15.299	0.004	
J13552725-0226158	15.777	0.005	15.184	0.006	14.971	0.008	14.774	0.006	14.624	0.006	14.310	0.002	14.093	0.003	13.739	0.001	13.670	0.002	13.469	0.001	13.373	0.002	13.334	0.001	
J13554812-1421502	16.248	0.008	15.738	0.008	15.457	0.010	15.151	0.007	15.000	0.007	14.559	0.002	14.326	0.004	13.909	0.002	13.848	0.002	13.660	0.001	13.495	0.002	13.460	0.002	
J13554903-1024575	16.470	0.008	16.038	0.009	15.847	0.012	15.604	0.009	15.464	0.008	15.235	0.003	15.017	0.005	14.756	0.002	14.714	0.002	14.562	0.002	14.473	0.003	14.460	0.002	
J13555260-1202077	16.350	0.006	15.833	0.007	15.752	0.009	15.407	0.007	15.278	0.006	14.890	0.002	14.667	0.004	14.294	0.001	14.211	0.002	14.014	0.001	13.906	0.002	13.867	0.001	
J13552879-0651334	17.429	0.014	16.911	0.015	16.662	0.019	16.494	0.015	16.359	0.015	16.359	0.005	15.852	0.009	15.522	0.003	15.448	0.004	15.273	0.003	15.172	0.005	15.144	0.004	
J13553507-1406119	17.912	0.010	17.480	0.012	17.278	0.015	17.009	0.011	16.913	0.010	16.634	0.004	16.412	0.007	16.101	0.001	16.043	0.003	15.848	0.005	15.749	0.005	15.730	0.003	
J13563913-1031441	17.096	0.011	16.633	0.012	16.490	0.017	16.238	0.013	16.113	0.011	15.842	0.004	15.630	0.007	15.333	0.003	15.282	0.003	15.114	0.003	15.023	0.005	15.008	0.003	
J13565864-0452027	15.395	0.005	14.807	0.005	14.649	0.007	14.278	0.005	14.127	0.005	13.759	0.002	13.520	0.003	13.110	0.001	13.058	0.001	12.841	0.001	12.724	0.001	12.714	0.001	
J13570105-1533213	18.054	0.023	17.693	0.026	17.469	0.031	17.321	0.027	17.149	0.023	16.954	0.009	16.755	0.015	16.472	0.006	16.415	0.007	16.263	0.005	16.193	0.009	16.157	0.007	
J1357148-1529155	15.403	0.005	14.924	0.005	14.766	0.007	14.451	0.005	14.293	0.005	13.983	0.002	13.751	0.003	13.375	0.001	13.293	0.001	13.097	0.002	12.974	0.002	12.944	0.001	
J13575322-0635347	17.069	0.011	16.622	0.013	16.441	0.017	16.211	0.014	16.098	0.012	15.825	0.005	15.605	0.006	15.333	0.003	15.286	0.003	15.126	0.003	15.035	0.005	15.026	0.003	
J13575436+0135509	16.414	0.008	15.919	0.009	15.738	0.012	15.560	0.009	15.424	0.008	15.214	0.003	15.031	0.006	14.767	0.002	14.722	0.003	14.559	0.003	14.493	0.004	14.471	0.003	
J13580211-1147193	18.040	0.015	17.507	0.016	17.328	0.020	17.151	0.016	16.978	0.014	16.673	0.005	16.464	0.009	16.094	0.003	16.049	0.004	15.835	0.003	15.734	0.005	15.708	0.004	
J13590545-1331507	16.676	0.007	16.215	0.007	16.079	0.009	15.773	0.007	15.660	0.007	15.334	0.003	15.143	0.004	14.800	0.002	14.726	0.002	14.551	0.001	14.458	0.002	14.434	0.002	
J14000668-0724400	15.487	0.005	14.832	0.006	14.626	0.007	14.231	0.005	14.005	0.004	13.593	0.002	13.341	0.003	12.874	0.001	12.787	0.001	12.553	0.001	12.442	0.001	12.389	0.001	
J14004719-1323003	16.430	0.006	16.086	0.007	16.022	0.009	15.817	0.012	15.615	0.009	15.501	0.003	15.225	0.002	15.065	0.004	14.691	0.002	14.623	0.002	14.339	0.002	14.310	0.002	
J14005144-1052395	16.504	0.008	16.167	0.009	15.802	0.012	15.511	0.009	15.301	0.008	15.008	0.003	14.791	0.002	14.671	0.002	14.494	0.002	14.404	0.003	14.389	0.002			
J14013381-0702242	16.227	0.007	15.747	0.009	15.589	0.011	15.364	0.008	15.234	0.008	14.922	0.003	14.746	0.005	14.435	0.002	14.368	0.002	14.204	0.002	14.121	0.003	14.095	0.002	
J14014158-0653325	16.407	0.008	15.871	0.009	15.671	0.012	15.448	0.009	15.303	0.008	14.947	0.003	14.736	0.005	14.383	0.002	14.311	0.002	14.121	0.002	14.022	0.003	13.939	0.002	
J14021343-0620160	15.775	0.006	15.325	0.007	15.144	0.009	14.922	0.007	14.813	0.007	14.558	0.003	14.390	0.004	14.110	0.002	14.085	0.002	13.904	0.003	13.845	0.003	13.819	0.002	
J14135326-25228368	17.262	0.012	16.924	0.015	16.626	0.019	16.527	0.016	16.404	0.014	16.303	0.006	16.119	0.010	15.942	0.002	15.924	0.005	15.807	0.004	15.767	0.007	15.747	0.005	
J14151573-2522453	16.305	0.007	16.285	0.009	15.738	0.012	15.469	0.009	15.335	0.008	15.045	0.003	14.847	0.006	14.515	0.001	14.495	0.003	14.476	0.002	14.426	0.003	14.415	0.002	
J14184988-2520449	16.736	0.009	16.285	0.011	16.085	0.014	15.785	0.011	15.591	0.011	15.305	0.004	15.132	0.007	15.011	0.003	14.958	0.004	14.866	0.004	14.636	0.003	14.656	0.003	
J14233651-2537324	16.621	0.008	16.071	0.009	15.910	0.012	15.591	0.009	15.490	0.008	15.044	0.003	14.817	0.005	14.415	0.002	14.331	0.002	14.116	0.002	13.939	0.003	13.967	0.002	
J14244532-2542471	16.279	0.007	15.622	0.007	15.348	0.009	15.105	0.007	14.857	0.006	14.435	0.002	14.175	0.003	13.711	0.001	13.605	0.001	13.406	0.001	13.207	0.002	13.168	0.001	
J14271150+0602227	16.736	0.009	16.127	0.009	15.970	0.012	15.758	0.009	15.610	0.008	15.277	0.003	15.074	0.005	14.727	0.002	14.679	0.002	14.479	0.002	14.387	0.003	14.344	0.002	
J14502910-2526648	16.207	0.006	15.638	0.007	15.498	0.009	15.192	0.007	15.026	0.006	14.707	0.002	14.490	0.004	14.107	0.007	14.021	0.002	13.805	0.001	13.679	0.002	13.649	0.002	
J14511827-2054511	18.054	0.020	17.639	0.024	17.474	0.027	17.166	0.025	17.077	0.021	16.768	0.007	16.569	0.012	16.258	0.005	16.103	0.007	15.951	0.008	15.915	0.005	15.818	0.003	
J14513033-2512253	16.550	0.007	15.950	0.008	15.768	0.011	15.505	0.008	15.315	0.007	14.945	0.003	14.747	0.004	14.297	0.002	14.205	0.002	13.968	0.002	13.832	0.002			
J14521073-2106049	17.855	0.018	17.398	0.021	17.237	0.027	16.989	0.022	16.858	0.018	16.547	0.006	16.294	0.011	15.962	0.002	15.912	0.005	15.637	0.007	15.554	0.004			
J14523635-21349456	16.506	0.009	16.008	0.010	15.851	0.013	15.605	0.010	15.446	0.009	15.075	0.003	14.872	0.005	14.458	0.002	14.384	0.002	14.159	0.002	14.036	0.003			
J14523952+0505565	16.435	0.009	15.824	0.010	15.590	0.014	15.359	0.010	15.158	0.009	14.828	0.003	14.600	0.005	14.208	0.002	14.120	0.002	13.901	0.002	13.780	0.003			
J14528187-2239567	17.040	0.011	16.621	0.013	16.482	0.017	16.276	0.014	16.103	0.012	15.751	0.004	15.553	0.008	15.215	0.003	15.173	0.004	14.938	0.003	14.835	0.004			
J14532845-2110176	18.067	0.021	17.747	0.025	17.411	0.027	17.290	0.026	17.130	0.021	16.788	0.008	16.544	0.012	16.251	0.005	16.222	0.006	16.026	0.004	15.924	0.002			
J14533615+0526514	16.290	0.009	15.655	0.010	15.425	0.013	15.209	0.009	15.019	0.008	14.648	0.003	14.430	0.005	14.012	0.003	13.928	0.002	13.667	0.003	13.530	0.002			
J14541347-2336512	17.642	0.016	17.206	0.017	16.955	0.022	16.682	0.017	16.541	0.015	16.277	0.006	16.076	0.010	15.691	0.004	15.531	0.004	15.480	0.005	15.328	0.004			
J14550579-2505475	16.831	0.008	16.419	0.010	16.245	0.013	16.006	0.010	15.900	0.010	15.588	0.004	15.391	0.006	15.037	0.002	14.990	0.003	14.777	0.002	14.674	0.004			
J14551208-2233267	17.126	0.012	16.660	0.013	16.531	0.018	16.482	0.017	16.111	0.012	15.812	0.005	15.593	0.008	15.273	0.003	15.122	0.004	14.937	0.005	14.895	0.003			

Table 2 (continued)

Star Name	uJAVA	σ	J0378	σ	J0395	σ	J0410	σ	J0430	σ	gSDSS	σ	J0515	σ	rSDSS	σ	J0660	σ	iSDSS	σ	J0861	σ	zSDSS	σ
J20003435+0021415	16.205	0.005	15.685	0.008	15.506	0.009	15.301	0.006	15.184	0.005	14.840	0.002	14.598	0.003	14.221	0.001	14.002	0.002	13.896	0.001	13.767	0.002	13.731	0.001
J20004079+0058381	17.892	0.014	17.210	0.019	17.000	0.025	16.750	0.017	16.566	0.016	16.279	0.006	16.010	0.010	15.634	0.004	15.541	0.004	15.317	0.003	15.161	0.006	15.131	0.004
J20005889+0041324	17.330	0.010	16.829	0.015	16.635	0.020	16.371	0.014	16.273	0.013	15.963	0.005	15.750	0.009	15.400	0.004	15.331	0.004	15.152	0.003	15.031	0.005	15.05	0.003
J2010859+0056428	15.813	0.005	15.347	0.007	15.136	0.009	15.003	0.007	14.855	0.006	14.635	0.003	14.406	0.005	14.143	0.002	14.101	0.002	13.918	0.002	13.809	0.003	13.795	0.002
J2011680+0116257	16.620	0.007	16.080	0.010	15.731	0.010	15.444	0.006	15.290	0.006	15.007	0.002	14.710	0.003	14.324	0.001	14.293	0.001	13.924	0.002	13.870	0.001		
J20012799+0023095	16.886	0.008	16.225	0.011	16.129	0.013	15.777	0.008	15.631	0.007	15.287	0.002	15.061	0.004	14.665	0.002	14.603	0.002	14.339	0.001	14.248	0.002	14.207	0.002
J20013415+0058265	16.761	0.007	16.274	0.011	16.074	0.012	15.892	0.008	15.783	0.007	15.570	0.003	15.387	0.005	15.125	0.002	15.126	0.003	14.932	0.002	14.868	0.003	14.833	0.002
J20014181+0019202	15.993	0.005	15.519	0.008	15.236	0.008	15.157	0.005	15.043	0.005	14.832	0.002	14.653	0.003	14.396	0.001	14.405	0.002	14.181	0.001	14.104	0.002	14.084	0.002
J20015964+0015327	16.465	0.006	15.971	0.010	15.815	0.011	15.579	0.007	15.481	0.006	15.185	0.002	14.982	0.004	14.664	0.002	14.652	0.002	14.413	0.001	14.320	0.002	14.293	0.002
J20021702+0005218	16.927	0.008	16.265	0.012	16.086	0.012	15.844	0.008	15.703	0.007	15.387	0.002	15.167	0.004	14.801	0.002	14.770	0.002	14.504	0.002	14.383	0.003	14.358	0.002
J20023118+0104018	16.911	0.008	16.157	0.010	15.963	0.013	15.737	0.010	15.574	0.009	15.297	0.004	15.080	0.006	14.784	0.003	14.711	0.003	14.452	0.002	14.417	0.004	14.387	0.002
J20023405+0021449	15.123	0.003	14.625	0.005	14.406	0.006	14.200	0.004	14.072	0.004	13.874	0.002	13.666	0.003	13.399	0.001	13.341	0.001	13.168	0.001	13.088	0.002	13.059	0.001
J20035712+0116184	17.241	0.009	16.782	0.015	16.543	0.015	16.182	0.010	16.040	0.009	15.654	0.003	15.415	0.005	15.022	0.002	14.746	0.002	14.720	0.002	14.608	0.003	14.557	0.002
J20051837+0001271	18.050	0.020	17.690	0.020	17.490	0.020	17.250	0.020	17.040	0.020	16.760	0.020	16.160	0.020	16.100	0.020	15.910	0.020	15.890	0.020	15.830	0.020		
J20052052+0120319	17.824	0.016	17.496	0.022	17.312	0.032	17.011	0.020	16.901	0.022	16.589	0.006	16.421	0.013	15.999	0.004	16.054	0.005	15.750	0.004	15.700	0.007	15.613	0.005
J20053705+0017075	16.401	0.008	15.935	0.008	15.848	0.010	15.500	0.007	15.412	0.007	14.991	0.003	14.793	0.005	14.366	0.002	14.313	0.002	14.063	0.002	13.937	0.003	13.910	0.002
J20054459+0055530	17.714	0.014	17.294	0.016	17.212	0.030	16.910	0.018	16.771	0.020	16.434	0.011	16.256	0.011	16.843	0.004	16.845	0.005	16.579	0.004	16.431	0.004	16.381	0.004
J20061788+0013289	15.254	0.004	14.745	0.005	14.217	0.015	14.364	0.005	14.235	0.005	13.860	0.002	13.642	0.003	13.262	0.001	13.180	0.001	12.958	0.001	12.785	0.001		
J20073634+0057150	17.523	0.015	16.968	0.015	16.859	0.014	16.469	0.012	16.172	0.005	15.929	0.008	15.573	0.003	15.485	0.004	15.455	0.004	15.299	0.005	15.180	0.005	15.139	0.003
J20075027+0020098	16.708	0.009	16.156	0.010	16.023	0.015	15.795	0.010	15.674	0.011	15.331	0.003	15.082	0.006	14.716	0.002	14.609	0.003	14.407	0.002	14.262	0.003	14.239	0.002
J20085488+0057297	18.429	0.027	17.872	0.025	17.719	0.033	17.554	0.024	17.426	0.020	17.172	0.008	16.975	0.014	16.666	0.006	16.615	0.006	16.446	0.005	16.342	0.009	16.327	0.007
J20090004+0103370	15.822	0.006	15.307	0.006	15.226	0.008	14.896	0.005	14.772	0.005	14.409	0.002	14.186	0.003	13.802	0.002	13.733	0.002	13.514	0.001	13.395	0.002		
J20090076+0036452	17.583	0.014	17.092	0.017	16.893	0.025	16.768	0.017	16.644	0.019	16.496	0.006	16.277	0.012	16.098	0.005	16.046	0.006	15.819	0.008	15.735	0.008		
J20091617+0048192	18.280	0.021	17.725	0.025	17.485	0.036	17.298	0.024	17.144	0.025	16.842	0.007	16.572	0.014	16.194	0.005	16.105	0.006	15.809	0.004	15.715	0.005		
J20092146+0051002	15.132	0.004	14.460	0.004	14.240	0.005	14.079	0.004	13.965	0.003	13.759	0.001	13.564	0.003	13.312	0.001	13.258	0.001	13.113	0.001	13.021	0.002		
J20095425+0007011	16.932	0.010	16.422	0.012	16.241	0.016	16.045	0.011	15.889	0.012	15.553	0.004	15.329	0.007	14.960	0.003	14.914	0.003	14.682	0.002	14.538	0.004		
J20101610+0014480	17.188	0.012	16.729	0.013	16.545	0.015	16.281	0.011	16.160	0.010	15.837	0.004	15.562	0.007	15.171	0.003	15.117	0.003	14.864	0.002	14.777	0.004		
J20114178+0122331	18.481	0.038	18.051	0.056	17.904	0.061	17.638	0.038	17.319	0.011	17.122	0.019	16.815	0.010	16.761	0.010	16.596	0.010	16.478	0.012	16.460	0.018		
J20121125+0056105	17.322	0.018	16.832	0.024	16.794	0.027	16.451	0.017	16.331	0.011	16.101	0.010	15.533	0.003	15.283	0.006	14.739	0.002	14.582	0.002	14.302	0.003		
J20122497+0113575	17.422	0.018	16.860	0.024	16.794	0.027	16.451	0.017	16.342	0.014	16.051	0.005	15.744	0.008	15.409	0.004	15.330	0.005	15.124	0.004	15.015	0.005		
J20123247+0101043	18.258	0.033	17.822	0.048	17.602	0.050	17.426	0.033	17.316	0.025	17.042	0.009	16.804	0.015	16.488	0.008	16.432	0.008	16.229	0.008	16.117	0.009		
J20123379+0164311	16.071	0.008	15.466	0.010	15.373	0.012	15.092	0.008	14.957	0.006	14.566	0.003	14.307	0.007	13.889	0.002	13.806	0.002	13.554	0.002	13.416	0.002		
J20141258+0056212	16.352	0.010	15.858	0.013	15.743	0.015	15.480	0.010	15.371	0.008	15.079	0.003	14.856	0.005	14.519	0.003	14.440	0.003	14.250	0.002	14.141	0.003		
J20143504+0052087	17.407	0.014	16.820	0.013	16.735	0.017	16.473	0.011	16.331	0.011	16.101	0.010	15.533	0.003	15.283	0.006	14.739	0.002	14.582	0.002	14.302	0.003		
J20145209+010365	17.422	0.018	16.860	0.024	16.794	0.027	16.451	0.017	16.342	0.014	16.051	0.005	15.744	0.008	15.409	0.004	15.330	0.005	15.124	0.004	14.980	0.006		
J20154337+0030123	18.419	0.036	18.070	0.056	17.793	0.033	17.604	0.037	17.495	0.029	17.252	0.011	17.069	0.018	16.723	0.008	16.718	0.008	16.523	0.010	16.457	0.011		
J20160412+000254	16.935	0.011	16.412	0.012	16.166	0.015	15.832	0.014	16.011	0.010	15.869	0.009	15.546	0.004	15.300	0.006	14.947	0.007	14.878	0.003	14.667	0.007		
J20161414+0020139	16.119	0.007	15.466	0.007	15.314	0.015	15.047	0.007	14.876	0.007	14.545	0.004	14.313	0.004	13.900	0.002	13.815	0.002	13.576	0.002	13.436	0.002		
J2016211633+0113560	17.543	0.016	17.084	0.019	16.814	0.020	16.669	0.016	16.559	0.014	16.346	0.006	16.148	0.010	15.931	0.004	15.788	0.004	15.594	0.004	15.396	0.002		
J20261334+0058212	17.153	0.012	16.639	0.012	16.343	0.016	16.102	0.013	15.978	0.011	15.670	0.004	15.452	0.007	15.095	0.003	15.043	0.003	14.813	0.002	14.732	0.004		
J20265350+004																								

Table 2 (continued)

Star Name	uJAVA	σ	J0378	σ	J0395	σ	J0410	σ	J0430	σ	gSDSS	σ	J0515	σ	rSDSS	σ	J0660	σ	iSDSS	σ	J0861	σ	zSDSS	σ
J20422273+0045380	15.483	0.004	14.895	0.005	14.746	0.006	14.597	0.005	14.448	0.005	14.207	0.002	14.003	0.003	13.675	0.001	13.615	0.001	13.451	0.001	13.354	0.002	13.327	0.001
J20500458-0048444	17.679	0.015	17.222	0.016	17.030	0.020	16.781	0.014	16.649	0.013	16.304	0.005	16.104	0.009	15.721	0.001	15.682	0.004	15.457	0.007	15.395	0.007	15.324	0.004
J20514291+0104552	17.745	0.022	17.266	0.022	17.169	0.029	16.884	0.020	16.766	0.018	16.462	0.006	16.223	0.010	15.906	0.004	15.836	0.004	15.640	0.004	15.547	0.006	15.496	0.004
J20514829+0009230	17.199	0.011	16.673	0.012	16.494	0.015	16.303	0.011	16.134	0.010	15.848	0.004	15.619	0.007	15.251	0.003	15.198	0.003	14.988	0.002	14.863	0.006	14.836	0.003
J20531505-0016063	17.315	0.012	16.801	0.013	16.707	0.017	16.455	0.012	16.311	0.011	16.001	0.004	15.773	0.003	15.426	0.006	15.333	0.003	15.147	0.003	14.916	0.006	14.964	0.003
J20540726-013274	18.389	0.023	17.861	0.023	17.676	0.030	17.418	0.021	17.269	0.019	16.971	0.007	16.749	0.012	16.384	0.005	16.321	0.006	15.887	0.004	15.989	0.011	15.930	0.005
J20563226+0102264	16.613	0.008	16.247	0.010	16.075	0.012	15.911	0.009	15.779	0.008	15.571	0.003	15.356	0.006	15.094	0.004	15.056	0.003	14.852	0.002	14.812	0.004	14.803	0.003
J20574846-435671	16.024	0.006	15.564	0.007	15.387	0.010	15.176	0.007	15.033	0.006	14.789	0.002	14.576	0.004	14.284	0.002	14.228	0.002	14.046	0.002	13.964	0.002	13.945	0.002
J21025360-3721177	16.163	0.007	15.638	0.007	15.467	0.009	15.245	0.007	15.104	0.006	14.785	0.002	14.572	0.004	14.220	0.002	14.152	0.002	13.970	0.001	13.881	0.002	13.837	0.002
J21059595-5014054	17.836	0.017	17.356	0.019	17.213	0.027	16.978	0.019	16.845	0.018	16.533	0.006	16.346	0.011	15.987	0.004	15.913	0.005	15.737	0.004	15.628	0.006	15.617	0.005
J21080015-464154	16.164	0.007	15.642	0.008	15.443	0.010	15.213	0.008	15.082	0.007	14.771	0.003	14.536	0.004	14.199	0.002	14.126	0.002	13.923	0.002	13.819	0.002		
J21040930-4708238	17.379	0.019	16.941	0.020	16.787	0.023	16.607	0.020	16.481	0.018	16.269	0.006	16.075	0.011	15.820	0.004	15.739	0.005	15.614	0.004	15.544	0.006	15.527	0.005
J21041336-3019010	17.287	0.011	16.813	0.012	16.654	0.015	16.443	0.012	16.343	0.011	16.012	0.004	15.815	0.007	15.438	0.003	15.388	0.003	15.177	0.003	15.070	0.004	15.036	0.003
J21041365-3146396	16.712	0.008	16.151	0.011	15.932	0.011	15.724	0.009	15.578	0.008	15.288	0.003	15.080	0.005	14.734	0.002	14.678	0.002	14.468	0.002	14.333	0.003	14.323	0.002
J21041794-4105082	17.505	0.012	17.029	0.014	16.781	0.018	16.740	0.014	16.578	0.013	16.377	0.005	16.196	0.009	15.931	0.001	15.906	0.004	15.733	0.005	15.627	0.006	15.662	0.005
J210422739-0049341	15.832	0.003	15.257	0.004	15.072	0.005	14.900	0.004	14.729	0.004	14.440	0.001	14.223	0.002	13.861	0.001	13.779	0.001	13.590	0.001	13.491	0.001	13.450	0.001
J21045538-5054052	17.666	0.017	17.203	0.017	17.017	0.023	16.740	0.017	16.657	0.016	16.353	0.006	16.128	0.010	15.794	0.004	15.718	0.004	15.548	0.006	15.498	0.004		
J21054026-2527599	15.842	0.006	15.319	0.008	15.176	0.010	14.983	0.008	14.845	0.007	14.547	0.003	14.359	0.004	14.019	0.002	13.941	0.002	13.764	0.002	13.660	0.003	13.625	0.002
J21055882-4118416	16.417	0.011	15.920	0.011	15.729	0.015	15.514	0.011	15.384	0.010	15.125	0.003	14.918	0.006	14.620	0.002	14.458	0.003	14.379	0.002	14.284	0.004	14.264	0.002
J21074117+0106513	18.542	0.027	18.096	0.028	17.833	0.043	17.720	0.029	17.609	0.025	17.335	0.009	17.102	0.015	16.787	0.007	16.724	0.006	16.558	0.006	16.426	0.010	16.435	0.008
J21113775-2658131	16.073	0.007	15.535	0.008	15.351	0.010	15.190	0.008	15.031	0.006	14.731	0.002	14.552	0.004	14.219	0.002	14.134	0.002	13.969	0.002	13.867	0.002	13.835	0.002
J21115635-3708366	14.416	0.003	13.919	0.004	13.790	0.005	13.559	0.004	13.424	0.003	13.093	0.001	12.909	0.002	12.557	0.001	12.485	0.001	12.285	0.001	12.194	0.001	12.158	0.001
J21142351-2947778	16.795	0.019	16.394	0.010	16.168	0.013	16.018	0.010	15.659	0.004	15.659	0.004	15.483	0.004	15.195	0.003	15.140	0.003	14.994	0.002	14.922	0.004	14.904	0.003
J21152435-2635448	17.340	0.012	16.799	0.013	16.594	0.014	16.262	0.012	16.069	0.005	15.894	0.008	15.603	0.003	15.677	0.004	15.412	0.003	15.323	0.005	15.309	0.004		
J211622790-3504557	17.529	0.014	17.067	0.016	16.930	0.021	16.686	0.016	16.557	0.015	16.260	0.005	16.059	0.009	15.714	0.004	15.637	0.004	15.454	0.003	15.371	0.005	15.333	0.004
J21213312+0004251	17.444	0.014	17.127	0.018	16.374	0.020	16.427	0.015	16.331	0.014	16.013	0.004	15.842	0.008	15.537	0.003	15.543	0.004	15.466	0.003	15.386	0.006	15.342	0.004
J21254198-0120151	18.034	0.019	17.551	0.021	17.360	0.025	17.136	0.018	16.990	0.016	16.723	0.006	16.536	0.011	16.223	0.005	16.173	0.005	15.986	0.004	15.899	0.007	15.848	0.005
J21263701+0119228	18.324	0.024	18.118	0.038	17.228	0.024	17.121	0.018	16.942	0.015	16.423	0.005	16.285	0.009	15.679	0.003	15.603	0.004	15.407	0.003	15.303	0.005	15.262	0.004
J21304688+0046211	17.622	0.017	17.123	0.018	16.923	0.024	16.648	0.014	16.492	0.014	16.246	0.010	16.028	0.006	15.992	0.007	15.798	0.007	15.497	0.007	15.426	0.008		
J21341378-1545778	17.365	0.012	17.046	0.013	16.391	0.013	16.157	0.016	16.592	0.017	16.590	0.016	16.524	0.002	14.336	0.004	14.105	0.002	14.057	0.002	13.926	0.002	13.887	0.002
J21344068-0045199	17.633	0.010	17.014	0.010	16.866	0.016	16.630	0.010	16.507	0.009	16.142	0.003	15.918	0.006	15.561	0.002	15.478	0.002	15.298	0.002	15.176	0.003	15.149	0.002
J21430119+0058067	15.480	0.005	15.034	0.004	14.887	0.005	14.691	0.004	14.576	0.003	14.363	0.001	14.149	0.002	13.889	0.001	13.847	0.001	13.694	0.001	13.620	0.001	13.602	0.001
J214350571-2056106	16.663	0.008	16.280	0.009	15.680	0.010	15.809	0.009	15.727	0.009	15.553	0.003	15.378	0.006	15.196	0.003	15.203	0.003	15.089	0.003	15.078	0.005	15.062	0.003
J21510918+004279	15.079	0.005	14.694	0.007	14.505	0.009	14.255	0.005	14.172	0.005	13.905	0.003	13.766	0.003	13.512	0.002	13.523	0.002	13.359	0.001	13.285	0.002	13.253	0.001
J215537-014577	17.365	0.012	17.046	0.013	16.391	0.013	16.157	0.016	16.592	0.017	16.590	0.016	16.524	0.006	16.028	0.007	15.777	0.007	15.554	0.007	15.474	0.007		
J21562470-0233483	16.868	0.012	16.391	0.013	16.157	0.016	15.998	0.013	15.867	0.012	15.657	0.004	15.469	0.008	15.211	0.003	15.192	0.003	15.025	0.003	14.935	0.003		
J21570410-0025558	17.229	0.012	16.732	0.013	16.629	0.018	16.335	0.014	16.191	0.012	15.886	0.004	15.659	0.009	15.312	0.003	15.249	0.003	15.047	0.007	14.944	0.004		
J21590612+0029207	17.640	0.017	17.170	0.019	16.945	0.025	16.815	0.018	16.676	0.016	16.419	0.006	16.219	0.010	15.922	0.004	15.863	0.005	15.688	0.004	15.603	0.005	15.593	0.006
J21595072+0027368	16.553	0.009	16.022	0.010	15.862	0.013	15.696	0.010	15.589	0.009	15.265	0.003	15.048	0.006	14.707	0.002	14.642	0.002						

Table 2 (*continued*)

Star Name	uJAVA	σ	J0378	σ	J0395	σ	J0410	σ	J0430	σ	gSDSS	σ	J0515	σ	rSDSS	σ	J0660	σ	iSDSS	σ	J0861	σ	zSDSS	σ
J23131269-0036247	17.103	0.011	16.545	0.011	16.395	0.014	16.220	0.010	16.080	0.009	15.842	0.004	15.620	0.006	15.300	0.003	15.256	0.003	15.079	0.002	14.976	0.004	14.961	0.003
J23174221-0124338	17.720	0.021	17.250	0.024	17.055	0.028	16.877	0.022	16.755	0.020	16.476	0.007	16.269	0.012	15.971	0.004	15.921	0.006	15.758	0.004	15.684	0.007	15.653	0.005
J232333976-0048009	14.386	0.003	13.822	0.004	13.709	0.005	13.398	0.004	13.296	0.003	12.933	0.001	12.729	0.002	12.349	0.001	12.293	0.001	12.145	0.001	11.931	0.001	11.990	0.001
J23243811-0115388	15.242	0.005	14.819	0.006	14.700	0.008	14.393	0.006	14.284	0.006	14.006	0.002	13.795	0.004	13.496	0.002	13.424	0.002	13.289	0.001	13.203	0.002	13.149	0.001
J23271618+0008407	14.767	0.003	14.297	0.004	14.133	0.006	13.867	0.004	13.763	0.003	13.488	0.001	13.255	0.002	12.954	0.001	12.889	0.001	12.715	0.001	12.591	0.001	12.593	0.001
J23274511+0014400	18.405	0.027	18.037	0.031	17.826	0.050	17.735	0.036	17.643	0.031	17.330	0.009	17.153	0.019	16.871	0.007	16.828	0.008	16.682	0.007	16.598	0.012	16.588	0.009
J233400902-4205187	16.357	0.008	15.873	0.009	15.692	0.012	15.469	0.009	15.327	0.008	15.128	0.003	14.920	0.005	14.641	0.002	14.610	0.002	14.455	0.002	14.342	0.003	14.329	0.002
J23414363-0120203	15.850	0.006	15.051	0.006	14.777	0.007	14.540	0.006	14.424	0.005	14.175	0.002	13.962	0.003	13.675	0.001	13.620	0.001	13.458	0.001	13.371	0.002	13.337	0.001
J23433448+0042013	16.530	0.008	16.055	0.012	16.028	0.014	15.937	0.011	15.878	0.010	15.624	0.004	15.523	0.008	15.106	0.003	14.992	0.003	14.866	0.002	14.827	0.004	14.797	0.004

Table 3. Stellar Parameters and Abundances from the n-SSPP

Star Name (2MASS)	Teff (K)	$\log g$ (cgs)	[Fe/H]	[C/Fe]	$\Delta[\text{C}/\text{Fe}]$	a	b	c	α/Fe
J00044550+0101170	5227	2.56	-2.37	+0.85	+0.02	+0.87	+6.93	+0.30	
J00173643+0009215	4993	2.19	-2.63	+0.61	+0.01	+0.62	+6.42	+0.20	
J00255442-3050320	5186	1.72	-2.21	+0.05	+0.35	+0.40	+6.62	+0.31	
J00271209-3133515	5257	2.74	-2.27	+0.24	+0.01	+0.25	+6.41	+0.12	
J00271240+0100377	5394	3.41	-2.29	+0.21	0.00	+0.21	+6.35	+0.53	
J00355591-4204306	5645	3.38	-2.53	+0.51	0.00	+0.51	+6.41	+0.31	
J00503713-3154131	5384	3.06	-2.32	+0.26	+0.01	+0.27	+6.38	+0.15	
J00503717-3408167	4434	0.88	-2.71	+0.47
J00520900-0046092	5556	2.85	-2.99	+0.58	+0.01	+0.59	+6.03	+0.35	
J00542886-3001012	5497	3.53	-2.05	+0.14	0.00	+0.14	+6.52	+0.01	
J00552124-3031172	5047	1.41	-2.97	+0.68	+0.45	+1.13	+6.59	+0.30	
J01044308-3941159	4989	1.53	-3.16	+0.67	+0.34	+1.01	+6.28	+0.33	
J01062973-3030595	5007	1.51	-2.54	+0.13	+0.44	+0.57	+6.46	+0.35	
J01072229-3257031	5489	3.39	-2.38	+0.38	0.00	+0.38	+6.43	-0.07	
J01115530-3439512	4881	2.13	-2.27	+0.20	+0.01	+0.21	+6.37	+0.44	
J01115596-2924247	5014	2.23	-2.29	+0.36	+0.01	+0.37	+6.51	+0.10	
J01132882-3505175	4987	2.07	-2.50	+0.50	+0.03	+0.53	+6.46	+0.50	
J01142762-3229200	5600	3.42	-2.73	+0.37	0.00	+0.37	+6.07	+0.27	
J01153574-3148352	5454	2.47	-2.61	+0.53
J01153906-3234184	4815	1.75	-2.46	+0.11	+0.29	+0.40	+6.37	+0.48	
J01174900-3149004	5521	1.99	-3.39	
J01205304-3435456	5168	2.55	-2.50	+0.62	+0.01	+0.63	+6.56	+0.21	
J01232034-3218276	5759	2.42	-2.54	-0.03
J01252234-3158080	4704	2.29	-3.23	-0.10	+0.01	-0.09	+5.11	+0.35	
J01301783-2929538	5315	2.92	-2.68	+0.21
J01304113-2900179	4972	2.06	-2.54	+0.19	+0.02	+0.21	+6.10	+0.30	
J01335531-2912330	5080	2.65	-2.01	+0.18	+0.01	+0.19	+6.61	+0.39	
J01374941-3407505	4585	1.06	-3.29	-0.13	+0.76	+0.63	+5.77	+0.55	
J01383820-2740120	4980	3.59	-0.44	-0.17	0.00	-0.17	+7.82	+0.37	
J01384849-3123136	4955	2.12	-2.37	+0.23	+0.02	+0.25	+6.31	+0.15	
J01464720-0102503	5735	4.35	-0.65	+0.04	0.00	+0.04	+7.82	+0.41	
J01484480-2941171	5013	2.49	-2.37	+0.01	+0.01	+0.02	+6.08	+0.23	
J01530531-2748141	5496	2.40	-2.20	+0.78	+0.01	+0.79	+7.02	+0.24	
J01554444+0104512	4965	2.22	-2.48	+0.38	+0.01	+0.39	+6.34	+0.53	
J02180715-3049591	5497	3.18	-2.38	+0.28	0.00	+0.28	+6.33	+0.09	
J02284062-3025508	5183	2.35	-2.55	+0.55	+0.01	+0.56	+6.44	+0.51	
J02320469-3115085	4507	1.28	-3.14	-0.73	+0.61	-0.12	+5.17	+0.35	
J02325680+0019492	4869	2.20	-3.17	+0.08	+0.01	+0.09	+5.35	+0.19	
J02371447-4000452	5327	2.99	-2.05	+0.23	+0.01	+0.24	+6.62	+0.16	
J02441085-5009042	4844	1.72	-2.42	+0.16	+0.33	+0.49	+6.50	+0.22	
J02480029+0042038	5094	2.12	-2.26	+0.26	+0.02	+0.28	+6.45	+0.16	
J02480538-3316558	5309	2.64	-2.07	+0.48	+0.01	+0.49	+6.85	+0.49	
J03060042-3336317	5174	2.61	-2.32	+0.19	+0.01	+0.20	+6.31	+0.17	
J03060937-3308292	5043	2.26	-2.69	+0.26	+0.01	+0.27	+6.01	+0.26	
J03063076+0017480	5426	2.19	-1.89	-0.48	+0.01	-0.47	+6.07	+0.20	
J03093503-3300063	4845	1.66	-2.47	-0.07	+0.36	+0.29	+6.25	+0.17	
J03110634+0058038	6470	3.65	-2.17	+0.33
J03120419-3054279	5282	2.75	-2.42	+0.25	+0.01	+0.26	+6.27	+0.22	
J03144847+0110166	5743	4.27	-2.41	+0.07	0.00	+0.07	+6.09	+0.42	
J03145801-3236489	5073	2.67	-2.01	+0.19	+0.01	+0.20	+6.62	+0.25	
J03160457+0004038	5455	2.46	-2.03	-0.25	+0.01	-0.24	+6.16	+0.42	
J03170771-3243481	4655	0.83	-2.62	-0.00	+0.70	+0.70	+6.51	+0.37	
J03193648+0049320	6166	3.84	-2.14	+0.41
J03203189-5525405	5202	2.67	-2.51	+0.45	+0.01	+0.46	+6.38	+0.23	
J03250464-0039506	5818	3.28	-2.04	+0.22
J03255861+0107414	5528	4.66	-2.35	+0.01	0.00	+0.01	+6.09	+0.35	
J03272930-0100042	5347	3.11	-2.34	+0.33	+0.01	+0.34	+6.43	+0.45	
J03332804-0016148	5301	2.80	-1.95	+0.21	+0.01	+0.22	+6.70	+0.22	
J03370237-3458142	4802	1.61	-3.03	+0.07	+0.28	+0.35	+5.75	+0.32	
J03384463-0047295	5869	3.70	-1.98	+0.31
J03384871-0058248	5574	3.19	-1.97	+0.16	0.00	+0.16	+6.62	+0.04	
J03391097-0046039	5270	1.90	-1.96	-1.01	+0.15	-0.86	+5.61	+0.26	
J03394540+0111082	5688	4.45	-0.07	-0.15	0.00	-0.15	+8.21	+0.37	

Table 3 *continued*

Table 3 (*continued*)

Star Name	T_{eff}	$\log g$	[Fe/H]	[C/Fe]	$\Delta[\text{C}/\text{Fe}]^a$	$[\text{C}/\text{Fe}]_{\text{cor}}^b$	$A(\text{C})_{\text{cor}}^c$	$[\alpha/\text{Fe}]$
(2MASS)	(K)	(cgs)						
J03412634+0053306	5463	2.38	-1.79	-0.16	+0.01	-0.15	+6.49	+0.23
J03441353+0033004	5944	4.09	-0.49	+0.18	0.00	+0.18	+8.12	+0.31
J03443568+0045022	5755	4.24	-0.39	-0.03	0.00	-0.03	+8.01	+0.39
J03445171+0054107	5125	2.34	-1.61	+0.05	+0.02	+0.07	+6.89	+0.19
J03465824-0009150	6444	4.24	-2.36	+0.33
J03471548+0049366	5996	3.65	-0.23	+0.08	0.00	+0.08	+8.28	+0.29
J03473639+0049039	6283	3.72	-1.82	+0.39	0.00	+0.39	+7.00	+0.02
J03474822+0122390	6385	3.05	-1.00	+0.87	+0.02	+0.89	+8.32	+0.76
J03482415+0101192	6243	4.20	-0.36	+0.17	0.00	+0.17	+8.24	+0.10
J03483507+0003027	5635	4.34	-0.72	+0.30	0.00	+0.30	+8.01	+0.44
J03530888-0002590	5443	2.82	-2.37	+0.45	+0.01	+0.46	+6.52	+0.03
J03532457-0009297	6162	3.60	-1.30	+1.26	0.00	+1.26	+8.39	+0.17
J03540382+0026534	6357	3.72	-0.62	+0.20	0.00	+0.20	+8.01	+0.28
J03540459+0114066	5943	4.10	-2.15	+0.30	0.00	+0.30	+6.58	+0.19
J03540956+0033304	5691	3.52	-0.39	+0.40	0.00	+0.40	+8.44	+0.50
J03541889+0111247	6470	3.75	-0.31	+0.07	0.00	+0.07	+8.19	-0.01
J03543044+0052026	6106	3.92	-0.32	+0.15	0.00	+0.15	+8.26	+0.17
J03543348+0038140	6122	4.11	-0.26	+0.10	0.00	+0.10	+8.27	+0.29
J03543771+0046406	6316	3.25	-0.34	+0.37	+0.02	+0.39	+8.48	+0.34
J03544342-0017209	5830	4.08	-0.68	+0.19	0.00	+0.19	+7.94	+0.47
J03544466+0031400	5996	3.56	-0.59	+0.39	0.00	+0.39	+8.23	+0.66
J03544663+0040139	6051	2.53	-0.97	+1.16	+0.02	+1.18	+8.64	+0.64
J03545635-0025496	5856	3.39	-0.06	+0.13	0.00	+0.13	+8.50	+0.24
J03550876+0014345	5964	3.42	-2.53	+0.17
J03552342+0016535	6217	3.71	-0.97	+0.39	0.00	+0.39	+7.85	+0.53
J03552487+0024132	6296	3.54	-0.06	+0.14	0.00	+0.14	+8.51	+0.15
J03552546+0030381	5574	4.34	-0.45	+0.10	0.00	+0.10	+8.08	+0.53
J03554412+0025099	6400	3.63	-0.12	+0.47	0.00	+0.47	+8.78	+0.33
J03554671+0028063	5985	3.72	-0.42	+0.20	0.00	+0.20	+8.21	+0.32
J03555316+0033071	5263	2.66	-1.64	+0.38	+0.02	+0.40	+7.19	+0.30
J03560990+0037133	6247	3.88	-0.30	+0.65	0.00	+0.65	+8.78	+0.12
J03563384+0025258	6445	3.71	-0.31	+0.24	0.00	+0.24	+8.36	+0.25
J03563495+0017457	6019	3.21	-1.03	+0.66	+0.01	+0.67	+8.07	+0.74
J03565939-0056148	5306	2.91	-1.73	+0.30	+0.02	+0.32	+7.02	+0.34
J03565954+0008420	6606	3.56	-0.73	+0.54	0.00	+0.54	+8.24	+0.34
J03574129+0122357	5495	3.36	-1.43	+0.13	0.00	+0.13	+7.13	+0.19
J03574260+0115214	6079	3.43	-2.28	+0.51
J03582339-3438018	5005	2.28	-2.96	+0.48	+0.01	+0.49	+5.96	+0.33
J03582979-3841492	5243	2.85	-2.56	+0.34	+0.01	+0.35	+6.22	...
J03583937-3739179	4980	2.53	-2.60	+0.57	+0.01	+0.58	+6.41	+0.46
J03585338+0007050	6374	4.18	-0.19	+0.08	0.00	+0.08	+8.32	+0.41
J03590482+0046515	6231	4.22	-2.16	+0.48
J03592020+0034443	5502	4.02	-1.16	+0.85	0.00	+0.85	+8.12	+1.05
J03592418-3651140	4992	2.35	-2.77	+0.16	+0.01	+0.17	+5.83	+0.20
J03592423+0043021	6364	3.92	+0.07	+0.02	0.00	+0.02	+8.52	+0.22
J03592681+0022272	6084	3.98	-0.02	-0.09	0.00	-0.09	+8.32	+0.15
J03592803+0036543	5930	4.07	-0.59	+0.05	0.00	+0.05	+7.89	+0.32
J03593987+0106448	6148	3.46	-0.43	+0.38	0.00	+0.38	+8.38	+0.47
J03594115+0043429	6744	3.75	-0.04	+0.16	0.00	+0.16	+8.55	+0.20
J04003943-3513394	4921	1.90	-2.76	+0.51	+0.09	+0.60	+6.27	...
J04085456-3948262	4608	1.48	-3.02	-0.30	+0.43	+0.13	+5.54	+0.36
J04095416-4007327	4920	1.95	-2.16	+0.11	+0.10	+0.21	+6.48	+0.09
J04105455-3321498	4740	1.64	-2.46	-0.32	+0.35	+0.03	+6.00	+0.23
J04115568-3341064	4923	2.06	-2.14	+0.04	+0.03	+0.07	+6.36	+0.29
J04140591-3727559	5134	1.90	-3.01	+0.98	+0.07	+1.05	+6.47	+0.53
J04145894-3255389	4968	1.44	-2.95	+0.58	+0.42	+1.00	+6.48	+0.21
J04162964-4110418	5541	3.11	-2.02	-0.11	+0.01	-0.10	+6.31	+0.24
J04165229-3817335	5514	2.40	-2.18	+0.38
J04180140-3841420	5406	2.76	-2.73	+0.56	+0.01	+0.57	+6.27	+0.04
J04203417-3430458	4940	2.03	-2.16	+0.17	+0.03	+0.20	+6.47	+0.35
J04213793-3343353	5032	1.99	-2.57	+0.28	+0.05	+0.33	+6.19	+0.22
J04220661-4111088	4900	1.83	-3.02	+0.06	+0.08	+0.14	+5.55	+0.34
J04253919-3814243	5374	2.66	-3.06	+0.30
J04254177-3640132	5496	3.13	-2.49	+0.41	+0.01	+0.42	+6.36	+0.52
J04271588-4113523	5135	2.42	-2.38	+0.23	+0.01	+0.24	+6.29	+0.41
J04315718-4354175	5101	1.59	-2.34	-0.31	+0.41	+0.10	+6.19	+0.32

Table 3 *continued*

Table 3 (*continued*)

Star Name (2MASS)	T_{eff} (K)	$\log g$ (cgs)	[Fe/H]	[C/Fe]	$\Delta[\text{C}/\text{Fe}]^a$	$[\text{C}/\text{Fe}]_{\text{cor}}^b$	$A(\text{C})_{\text{cor}}^c$	[α/Fe]
J04322488-4639409	5038	2.48	-2.24	+0.11	+0.01	+0.12	+6.31	+0.13
J04322908-3947519	5140	2.47	-2.84	+0.33	+0.01	+0.34	+5.93	+0.21
J04323909-4634270	5576	4.37	-2.04	-0.13	0.00	-0.13	+6.26	+0.28
J04324431-3445588	4565	1.55	-2.71	-0.28	+0.42	+0.14	+5.86	+0.28
J04351543-4250160	4808	1.49	-2.48	+0.27
J04352215-4704488	5192	2.12	-3.57
J04354512-4350225	5567	3.41	-1.75	+0.14	0.00	+0.14	+6.82	+0.20
J04355217-4203517	4902	2.29	-2.90	+0.53	+0.01	+0.54	+6.07	+0.23
J04371974-4254147	5212	2.69	-2.44	+0.74	+0.01	+0.75	+6.74	+0.57
J04375734-3337240	5259	2.56	-2.64	+0.41	+0.01	+0.42	+6.21	+0.42
J04380295-4736337	5143	2.41	-2.65	+0.56	+0.01	+0.57	+6.35	+0.46
J04382497-4215130	5317	3.08	-1.59	+0.11	+0.01	+0.12	+6.96	+0.28
J04402161-3549473	5087	2.17	-2.64	+0.31	+0.01	+0.32	+6.11	+0.41
J04404847-4214219	4808	1.51	-2.61	+0.41
J04424308-3630571	5226	2.48	-2.58	+0.40	+0.01	+0.41	+6.26	+0.39
J04425689-4627403	5430	2.49	-2.45	+0.47	+0.01	+0.48	+6.46	+0.03
J04441395-3356317	6044	3.77	-0.23	+0.10	0.00	+0.10	+8.30	+0.22
J04484727-3945309	4995	2.10	-2.78	+0.56	+0.01	+0.57	+6.22	+0.06
J04485242-3709099	5276	3.02	-2.69	+0.59	+0.01	+0.60	+6.34	+0.35
J04495212-3210361	5162	1.80	-3.00	+0.34	+0.14	+0.48	+5.91	+0.24
J04504685-3946382	5147	2.29	-2.42	+0.32	+0.01	+0.33	+6.34	+0.35
J04512454-3139582	5074	2.18	-2.27	+0.19	+0.01	+0.20	+6.36	+0.30
J04543666-4754298	5056	3.16	-3.14	+0.33	0.00	+0.33	+5.62	+0.49
J04545976-4212485	5288	2.50	-2.71	+0.53	+0.01	+0.54	+6.26	+0.44
J04551021-3249438	4765	1.50	-2.40	-0.03	+0.49	+0.46	+6.49	+0.10
J04590976-4632284	4953	2.47	-2.23	0.00	+0.01	+0.01	+6.21	+0.34
J04592454-4518477	5110	2.74	-2.78	+0.30	+0.01	+0.31	+5.96	+0.28
J09580012-1803531	5534	2.35	-1.82	+0.27
J09595158-0822008	4713	1.47	-2.70	+0.27
J10003629-1725512	5225	2.80	-2.39	+0.12	+0.01	+0.13	+6.17	+0.15
J10005938-1800599	4912	2.82	-3.24
J10011607-1747125	5167	2.58	-2.28	+0.28	+0.01	+0.29	+6.44	-0.12
J10021099-0030092	5180	1.85	-2.07	+0.35	+0.17	+0.52	+6.88	+0.30
J10024495-1716153	4909	1.50	-2.03	+0.24
J10040075+0134108	5724	3.76	-1.60	+0.48	0.00	+0.48	+7.31	+0.84
J10040252-0917128	5302	2.81	-2.17	+0.37	+0.01	+0.38	+6.64	+0.09
J10040553+0235484	5203	1.72	-2.64	+0.03
J10040693-1138417	5690	3.90	-2.40	+0.20
J10043854-0939488	5155	2.36	-2.46	+0.45	+0.01	+0.46	+6.43	+0.33
J10050873+0025517	5815	3.73	-1.91	+0.72
J10052824-0911423	4784	1.56	-2.35	-0.55	+0.45	-0.10	+5.98	+0.34
J10052863-1433198	5068	2.66	-2.03	+0.24	+0.01	+0.25	+6.65	+0.24
J10053549-0924326	5570	1.85	-3.27
J10054690-1226387	4804	1.95	-2.47	-0.02	+0.08	+0.06	+6.02	+0.15
J10062477-1950366	5553	3.49	-2.14	+0.28	0.00	+0.28	+6.57	+0.31
J10072392-1317186	4995	1.93	-2.40	+0.16	+0.09	+0.25	+6.28	+0.31
J10081117-1918306	5564	3.17	-2.19	-0.06
J10092998-2057477	5503	2.35	-2.85	+0.50
J10093999-1641194	5474	2.81	-2.04	+0.30	+0.01	+0.31	+6.70	+0.05
J10105387-1754549	4433	1.15	-2.75	-0.79	+0.72	-0.07	+5.61	+0.22
J10113371-1342160	4598	1.06	-2.50	+0.30
J10154250-1611132	5043	2.22	-2.65	+0.52	+0.01	+0.53	+6.31	+0.31
J101653359-1937168	5421	2.90	-2.02	+0.25	+0.01	+0.26	+6.67	+0.13
J10174646-2106150	5921	2.56	-2.93	+0.85
J10184004-2031276	5269	2.65	-2.83	+0.17
J10184162-1729364	4976	1.28	-2.99	+0.58	+0.52	+1.10	+6.54	+0.31
J10192807-2020499	5210	1.85	-3.55	-0.08
J10193237-1638584	5106	1.90	-2.04	+0.35
J10254045-1622201	6131	2.79	-1.96
J10255315-1635461	5294	2.52	-2.14	+0.13	+0.01	+0.14	+6.43	-0.10
J10261897-1459502	5304	3.53	-2.74	+0.64	0.00	+0.64	+6.33	0.00
J10264356-1425080	6504	4.09	-2.90	-0.02	0.00	-0.02	+5.51	+0.31
J10285881-1527074	5662	1.65	-1.80	+0.26	+0.27	+0.53	+7.16	+0.73
J10292435-1859548	4900	1.86	-2.64	+0.62	+0.13	+0.75	+6.54	+0.59
J10315059-1914338	5239	3.67	-3.13	+0.77	0.00	+0.77	+6.07	+0.45
J10320298-1650547	5434	2.12	-2.22	-0.23	+0.01	-0.22	+5.99	+0.41

Table 3 *continued*

Table 3 (*continued*)

Star Name (2MASS)	T_{eff} (K)	$\log g$ (cgs)	[Fe/H]	[C/Fe]	$\Delta[\text{C}/\text{Fe}]^a$	$[\text{C}/\text{Fe}]_{\text{cor}}^b$	$A(\text{C})_{\text{cor}}^c$	$[\alpha/\text{Fe}]$
J10323970–2044339	5332	2.75	−2.88	+0.27	+0.01	+0.28	+5.83	+0.33
J10341301–1753472	5375	2.71	−2.51	+0.30	+0.01	+0.31	+6.23	+0.32
J10362492–1900221	5226	3.13	−2.57	+0.46	+0.01	+0.47	+6.33	+0.49
J10371207–1855498	5227	2.44	−2.21	+0.12	+0.01	+0.13	+6.35	+0.15
J10394834–1719284	5603	3.21	−2.40	+0.44	0.00	+0.44	+6.47	+0.20
J10414658–1827443	5157	3.17	−3.18	+0.82	0.00	+0.82	+6.07	+0.37
J10414788–1715518	4251	0.57	−3.13	−0.43	+0.75	+0.32	+5.62	+0.56
J10434103–1712132	5336	2.77	−2.76	+0.37
J10482732–1707224	5092	2.25	−2.13	+0.41	+0.01	+0.42	+6.72	+0.32
J10485833–2143574	5968	3.85	−2.57	+0.55
J10511281–2136425	5133	2.51	−2.34	0.00	+0.01	+0.01	+6.10	+0.25
J10512357–2121108	5283	2.41	−2.60	+0.35	+0.01	+0.36	+6.19	+0.54
J10570497–2215021	5355	3.06	−2.22	−0.01	+0.01	0.00	+6.21	+0.07
J10572425–2110418	4932	1.38	−2.87	+0.12	+0.50	+0.62	+6.18	+0.09
J10573193–2223341	5376	1.74	−2.60	+1.20	+0.16	+1.36	+7.19	+0.10
J10580923–2144147	4907	2.28	−2.25	+0.08	+0.01	+0.09	+6.27	+0.25
J11001243–2111286	4533	1.02	−3.04	+0.33
J11002053–1833151	4888	1.17	−2.83	+0.21	+0.63	+0.84	+6.44	+0.44
J11022646–2342494	5387	2.80	−2.08	+0.31	+0.01	+0.32	+6.67	+0.31
J11030563–2231467	5109	1.93	−2.16	−0.65	+0.09	−0.56	+5.71	+0.19
J11081009–1944043	5297	2.83	−2.77	+0.83	+0.01	+0.84	+6.50	...
J11083127–2235143	5234	2.64	−2.39	+0.37	+0.01	+0.38	+6.42	+0.35
J11120172–2212075	5360	2.90	−2.75	+1.04	+0.01	+1.05	+6.73	+0.37
J11124929–2357161	4969	1.89	−2.85	+0.21	+0.07	+0.28	+5.86	+0.48
J11135686–2041051	4781	1.76	−2.48	−0.06	+0.25	+0.19	+6.14	+0.08
J11135726–2222091	5354	3.44	−2.40	+0.33	0.00	+0.33	+6.36	+0.08
J11144560–2212214	5400	3.12	−2.38	+0.31	+0.01	+0.32	+6.37	+0.30
J11162403–1843000	5132	1.32	−2.39	+0.46
J11171192–1911211	5577	4.59	−2.56	+0.05	0.00	+0.05	+5.92	+0.54
J11190308–1846350	4876	1.66	−2.01	−0.69	+0.37	−0.32	+6.10	+0.11
J11194427–2308401	5282	3.13	−2.90	+0.73	0.00	+0.73	+6.26	+0.78
J11194933–2317327	5128	2.35	−2.17	+0.35	+0.01	+0.36	+6.62	+0.37
J11201142–1933447	5167	2.37	−2.48	+0.42	+0.01	+0.43	+6.38	+0.26
J11203812–2356163	4680	1.84	−2.65	+0.41	+0.14	+0.55	+6.33	+0.25
J11220137–2330358	4959	1.64	−2.09	+0.08	+0.35	+0.43	+6.77	+0.15
J11222244–1818163	5301	4.31	−3.11	+0.18	0.00	+0.18	+5.50	+0.23
J11225058–2243447	4781	1.43	−2.47	−1.07	+0.53	−0.54	+5.42	+0.12
J11225672–1902327	5374	2.55	−2.35	+0.67	+0.01	+0.68	+6.76	+0.11
J11230328–2126276	5589	2.45	−2.99	+1.83	+0.02	+1.85	+7.29	+0.01
J11241118–2115149	5486	2.62	−3.46
J11254036–2034269	5971	4.63	−2.55	+0.27	0.00	+0.27	+6.15	+0.29
J11254158–2449096	5488	4.12	−2.15	+0.05	0.00	+0.05	+6.33	...
J11300605–2138213	5456	2.40	−2.89	+0.23
J11304517–2347312	5876	3.04	−3.11	+0.50
J11312025–1957045	5618	3.43	−3.24	+0.42	0.00	+0.42	+5.61	...
J11312204–2148119	5324	2.46	−2.38	+0.57	+0.01	+0.58	+6.63	+0.14
J11325195–1228109	5270	1.98	−2.55	+0.71	+0.05	+0.76	+6.64	+0.42
J11345006–2056390	5115	2.31	−2.07	+0.21	+0.01	+0.22	+6.58	+0.08
J11363130–1945100	4712	1.54	−2.26	−0.40	+0.46	+0.06	+6.23	+0.07
J11373260–2257565	5461	3.83	−2.75	+0.32	0.00	+0.32	+6.00	+0.70
J11383060–1825588	5264	2.06	−2.70	+0.27	+0.03	+0.30	+6.03	+0.56
J11403793–2013014	5951	4.21	−2.19	+0.52
J11404863–0231525	5962	3.57	−1.54	+0.66	0.00	+0.66	+7.55	...
J11420747–2236055	4934	1.98	−2.16	+0.10	+0.05	+0.15	+6.42	+0.20
J11434535–1852575	5356	2.49	−2.88	+0.47	+0.01	+0.48	+6.03	+0.30
J11440387–1658068	5296	2.62	−2.21	+0.49	+0.01	+0.50	+6.72	+0.32
J11443172–2122152	4998	1.33	−3.50	+1.43	+0.45	+1.88	+6.81	...
J11445275–2030317	4821	2.09	−2.28	−0.02	+0.01	−0.01	+6.14	+0.21
J11445318–1958567	5649	2.57	−2.57	+0.52
J11464483–1936295	5567	3.19	−2.78	+0.40
J11464646–2216104	4670	1.25	−3.02	+0.21
J11464903–2105098	4558	1.40	−2.49	−0.43	+0.57	+0.14	+6.08	+0.23
J11482911–2109456	5205	1.97	−2.82	+0.46	+0.06	+0.52	+6.13	−0.17
J11493550–2101315	5507	2.87	−2.60	−0.08
J11500693–1943013	5259	2.32	−2.62	+0.36	+0.01	+0.37	+6.18	+0.18
J11503041–2209074	5899	3.70	−2.28	+0.50	0.00	+0.50	+6.65	+0.25

Table 3 *continued*

Table 3 (*continued*)

Star Name (2MASS)	T_{eff} (K)	$\log g$ (cgs)	[Fe/H]	[C/Fe]	$\Delta[\text{C}/\text{Fe}]^a$	$[\text{C}/\text{Fe}]_{\text{cor}}^b$	$A(\text{C})_{\text{cor}}^c$	$[\alpha/\text{Fe}]$
J11511408-2159328	5731	3.22	-1.94	+0.27	0.00	+0.27	+6.76	+0.13
J11514550-1834578	5220	2.57	-2.15	+0.22	+0.01	+0.23	+6.51	+0.15
J11525640-2035404	5963	3.60	-2.14	+0.16
J11562039-1936572	5223	3.34	-3.06	+0.56	0.00	+0.56	+5.93	+0.41
J12023299-1931447	5173	2.56	-2.54	+0.26	+0.01	+0.27	+6.16	+0.34
J12023816-1957058	5263	2.59	-2.24	+0.22	+0.01	+0.23	+6.42	+0.22
J12040768-0234051	4926	3.25	-4.01	+0.86	0.00	+0.86	+5.28	+0.77
J12064282+0004032	4518	1.87	-2.96	-0.16	+0.09	-0.07	+5.40	+0.23
J12090903-1508048	4983	2.21	-2.47	+0.32	+0.01	+0.33	+6.29	+0.40
J12112971-0212276	5296	3.12	-2.64	+0.38	+0.01	+0.39	+6.18	+0.30
J12141957-0036482	5348	2.19	-3.09	+0.91	+0.01	+0.92	+6.26	+0.44
J12184512+0051359	4886	1.93	-2.88	+0.30	+0.05	+0.35	+5.90	+0.26
J12203518-0057582	5527	3.25	-2.14	+0.22	0.00	+0.22	+6.51	+0.42
J12233624-1522120	5761	3.67	-1.96	+0.20	0.00	+0.20	+6.67	+0.23
J12234076-0131031	5267	1.86	-3.21	+0.97	+0.07	+1.04	+6.26	...
J12253942-1452401	5568	2.22	-1.64	-0.46	+0.02	-0.44	+6.35	+0.59
J12290963-0059118	5099	2.79	-2.40	+0.91	+0.02	+0.93	+6.96	+0.24
J12292867+0115087	5818	3.66	-2.44	+0.38	0.00	+0.38	+6.37	+0.21
J12381720-1503087	5142	3.05	-2.38	+0.27	+0.01	+0.28	+6.33	+0.14
J12413337-1318137	4876	1.60	-3.10	+1.00	+0.29	+1.29	+6.62	+0.16
J12543883-1440173	5671	3.88	-2.53	+1.39	0.00	+1.39	+7.29	...
J12551524-1533478	5022	2.33	-2.67	+0.30	+0.01	+0.31	+6.07	+0.33
J12581969-1423114	4864	2.49	-3.40	+0.36	+0.01	+0.37	+5.40	+0.09
J13011453-1455403	5220	2.72	-2.42	+0.40	+0.01	+0.41	+6.42	+0.33
J13012016-1442042	5188	2.42	-2.47	+0.47	+0.01	+0.48	+6.44	+0.32
J13070601-1452022	5462	3.65	-2.51	+0.69	0.00	+0.69	+6.61	+0.10
J13073449-1327258	5083	1.55	-2.58	-0.27	+0.43	+0.16	+6.01	+0.21
J13073627-1158131	5236	2.77	-2.70	+0.11	+0.01	+0.12	+5.85	+0.07
J13080410-1327591	4678	1.53	-2.55	-0.61	+0.43	-0.18	+5.70	+0.12
J13083350-1313027	5413	3.18	-2.13	+0.58	+0.01	+0.59	+6.89	+0.18
J13091852-1528133	5096	2.33	-2.16	+0.33	+0.01	+0.34	+6.61	+0.10
J13092690-1513172	5038	2.48	-2.32	+0.16	+0.01	+0.17	+6.28	+0.20
J13103235-1257092	4842	1.85	-2.86	+0.02	+0.11	+0.13	+5.70	+0.20
J13115341-1352295	5237	2.77	-2.93	+0.62	+0.01	+0.63	+6.13	+0.42
J13131774-1148370	6185	3.25	-2.45	+0.65	0.00	+0.65	+6.63	+0.31
J13162234-1439423	4788	1.69	-2.56	-0.11	+0.29	+0.18	+6.05	+0.11
J13175379-0017126	4907	2.70	-2.72	+0.29	+0.01	+0.30	+6.01	+0.52
J13202007-0850032	5233	2.71	-2.27	+0.22	+0.01	+0.23	+6.39	+0.28
J13202534-1405312	5236	2.96	-2.69	+0.67	+0.01	+0.68	+6.42	+0.32
J13224728+0027099	5507	2.15	-2.40	+0.91
J13230218-1401407	5002	1.94	-2.59	+0.63	+0.07	+0.70	+6.54	+0.11
J13234665-1456070	5276	2.47	-2.74	+1.02	+0.02	+1.04	+6.73	...
J13255973-1331509	5535	3.23	-2.39	+0.30	0.00	+0.30	+6.34	+0.11
J13260147-1420519	5569	3.40	-1.99	+0.08	0.00	+0.08	+6.52	+0.24
J13263400-0751220	5101	2.39	-2.37	+0.30	+0.01	+0.31	+6.37	+0.25
J13263837-1351343	6524	2.86	-1.30	+0.55
J13273793-0736314	5203	2.41	-2.71	+0.28
J13285008-0753313	5070	2.30	-2.70	+0.44	+0.01	+0.45	+6.18	+0.48
J13285225-1453128	5409	2.28	-2.40	+0.51
J13285822-1428027	5828	3.73	-2.49	+0.89	0.00	+0.89	+6.83	-0.15
J13302081-1053210	4989	2.29	-2.47	+0.28	+0.01	+0.29	+6.25	+0.15
J13303025-1445223	5471	3.38	-2.55	+0.73	0.00	+0.73	+6.61	...
J13304241-1258149	5161	1.70	-2.70	+0.29
J13305370-0812151	5074	2.11	-2.60	+0.13	+0.01	+0.14	+5.97	+0.02
J13305807-1524301	5149	2.39	-2.55	+0.54	+0.01	+0.55	+6.43	+0.17
J13330549-1143314	5287	2.88	-2.29	+0.26	+0.01	+0.27	+6.41	+0.21
J13331559-1032347	5288	2.83	-2.36	+0.52	+0.01	+0.53	+6.60	+0.08
J13334281-0635309	5001	1.56	-3.27	+0.52	+0.35	+0.87	+6.03	...
J13334161-1231003	4844	1.09	-3.00	+0.48	+0.63	+1.11	+6.54	+0.17
J13354927-1013160	5065	2.26	-2.69	+0.33	+0.01	+0.34	+6.08	+0.47
J13363905-1148292	5214	2.90	-2.82	+0.33	0.00	+0.33	+5.94	+0.31
J13374402-1217279	4804	1.67	-2.56	-0.00	+0.36	+0.36	+6.23	+0.22
J13382471-0958520	5510	3.35	-2.37	+0.30	0.00	+0.30	+6.36	+0.03
J13390885-1305334	4994	1.79	-3.02	+0.63	+0.14	+0.77	+6.18	+0.46
J13392436-0847090	4809	2.04	-2.92	-0.35	+0.01	-0.34	+5.17	+0.38
J13394057-0636508	5269	3.10	-2.30	+0.15	+0.01	+0.16	+6.29	+0.23

Table 3 *continued*

Table 3 (*continued*)

Star Name (2MASS)	T_{eff} (K)	$\log g$ (cgs)	[Fe/H]	[C/Fe]	$\Delta[\text{C}/\text{Fe}]^a$	$[\text{C}/\text{Fe}]_{\text{cor}}^b$	$A(\text{C})_{\text{cor}}^c$	$[\alpha/\text{Fe}]$
J13404551-0633557	5264	2.84	-2.39	+0.26	+0.01	+0.27	+6.31	+0.29
J13410860-1232133	5221	2.76	-2.53	+0.41	+0.01	+0.42	+6.32	+0.24
J13420799-1157040	6267	4.48	-2.19	+0.29	0.00	+0.29	+6.53	+0.15
J13430545-0807438	4992	2.75	-2.64	+0.13	+0.01	+0.14	+5.93	+0.26
J13431375-0948485	5075	2.25	-2.46	+0.34	+0.01	+0.35	+6.32	+0.28
J13432075-1113168	4847	2.83	-2.72	+0.40	+0.01	+0.41	+6.12	+0.01
J13432477-0922116	5255	2.73	-1.98	+0.22	+0.01	+0.23	+6.68	+0.22
J13440121-0910128	5340	3.57	-2.14	+0.19	0.00	+0.19	+6.48	+0.11
J13442905-0831492	4851	1.35	-2.71	+0.48	+0.47	+0.95	+6.67	+0.90
J13444602-1445281	5062	1.30	-3.38
J13450057-0640371	4784	2.09	-2.43	-0.11	+0.01	-0.10	+5.90	+0.28
J13452554-0746249	5015	2.50	-1.95	+0.29	+0.01	+0.30	+6.78	+0.22
J13460151-0819059	5268	2.83	-2.62	+0.28	+0.01	+0.29	+6.10	-0.09
J13462090-1507098	5355	2.82	-2.48	+0.44	+0.01	+0.45	+6.40	-0.06
J13481357-0615460	4477	1.27	-3.28	-0.24	+0.61	+0.37	+5.52	+0.26
J13482307-0731330	5355	2.40	-2.06	-0.19	+0.01	-0.18	+6.19	+0.19
J13490050-1404170	5321	3.01	-2.30	+0.23	+0.01	+0.24	+6.37	+0.33
J13501035-1423065	5034	2.13	-3.04	+0.53	+0.01	+0.54	+5.93	-0.02
J13504014-1044541	5045	2.25	-2.11	+0.17	+0.01	+0.18	+6.50	+0.14
J13505366-0750034	5724	3.51	-2.16	+0.29	0.00	+0.29	+6.56	+0.17
J13510296-1324579	5219	2.60	-2.28	+0.17	+0.01	+0.18	+6.33	+0.04
J13511758-0214080	4786	1.28	-2.93	-0.29	+0.60	+0.31	+5.81	+0.65
J13521214-1256228	5802	3.25	-2.78	+0.92	+0.01	+0.93	+6.58	...
J13533510-0617040	5094	2.83	-2.14	+0.12	+0.01	+0.13	+6.42	+0.10
J13542102-0748421	5176	2.45	-3.13	+0.79	+0.01	+0.80	+6.10	...
J13544697-0056033	5320	2.90	-2.19	+0.34	+0.01	+0.35	+6.59	+0.20
J13550907-0101322	4999	2.23	-2.94	-0.22	+0.01	-0.21	+5.28	+0.20
J13552684-1533012	5520	2.07	-1.79	+0.01	+0.04	+0.05	+6.69	+0.37
J13552725-0226158	5022	1.66	-3.05	+0.76	+0.27	+1.03	+6.41	+0.37
J13554812-1421502	4980	2.39	-1.12	-0.43	+0.02	-0.41	+6.90	+0.25
J13554903-1024575	5375	3.03	-2.26	+0.25	+0.01	+0.26	+6.43	+0.11
J13555260-1202077	5095	2.38	-2.04	+0.14	+0.01	+0.15	+6.54	+0.17
J13562879-0651334	4991	2.41	-3.01	+0.55	+0.01	+0.56	+5.98	+0.32
J13563597-1406119	5616	3.71	-2.30	+0.49	0.00	+0.49	+6.62	...
J13563913-1031441	5263	2.87	-2.14	+0.35	+0.01	+0.36	+6.65	+0.33
J13565864-0452027	4714	1.85	-2.23	-0.25	+0.18	-0.07	+6.13	+0.15
J13570105-1533313	5788	4.32	-1.37	+0.12
J13573148-1529155	5281	2.59	-2.53	+0.43	+0.01	+0.44	+6.34	+0.07
J13575322-0635347	5304	2.82	-2.28	+0.40	+0.01	+0.41	+6.56	+0.29
J13575436+0138509	5391	2.50	-2.89	+0.61	+0.01	+0.62	+6.16	+0.20
J13580211-1147193	4999	2.72	-3.19	+0.12	+0.01	+0.13	+5.37	...
J13590545-1331507	5283	2.87	-1.78	+0.17	+0.01	+0.18	+6.83	+0.14
J14000698-0724400	4631	1.16	-2.62	-0.66	+0.72	+0.06	+5.87	+0.31
J14004719-1323003	5367	4.60	-2.01	-0.17	0.00	-0.17	+6.25	+0.43
J14005144-1052395	5359	3.46	-2.32	+0.05	0.00	+0.05	+6.16	+0.31
J14013381-0702242	5199	2.69	-2.20	+0.46	+0.01	+0.47	+6.70	+0.07
J14014158-0653325	4988	2.10	-2.73	+0.14	+0.01	+0.15	+5.85	+0.15
J14021343-0620160	5217	2.94	-2.31	+0.19	+0.01	+0.20	+6.32	+0.16
J14135326-2528368	6064	2.95	-3.33
J14151573-2527453	5250	2.87	-2.20	+0.12	+0.01	+0.13	+6.36	+0.12
J14184988-2520449	5333	2.93	-2.66	+0.40	0.00	+0.40	+6.17	+0.27
J14233651-2537324	4978	2.03	-2.76	+0.87	+0.03	+0.90	+6.57	+0.39
J14244532-2542471	4700	1.48	-3.82	-0.03	+0.32	+0.29	+4.90	+0.30
J14271500+0600227	5052	2.26	-2.63	+0.37	+0.01	+0.38	+6.18	+0.47
J14502910-2526048	5229	2.31	-2.51	-0.26	+0.01	-0.25	+5.67	+0.13
J14511827-2055451	5637	3.77	-2.63	+0.75	0.00	+0.75	+6.55	+0.32
J14513033-2512253	4998	1.69	-2.71	+0.46
J14521073-2106049	5233	2.75	-2.86	+0.35	+0.01	+0.36	+5.93	+0.04
J14523635-2139456	5173	2.71	-2.67	+0.54	+0.01	+0.55	+6.31	+0.08
J14523952+0505565	4896	2.28	-3.82
J14532817-2239567	5236	2.92	-2.28	-0.08	+0.01	-0.07	+6.08	+0.08
J14533245-2110176	6284	3.93	-1.30	+0.12
J14533615+0526514	4925	2.34	-3.31	+0.09	+0.01	+0.10	+5.22	...
J14541347-2336512	5363	1.99	-1.99	+0.34
J14550579-2505475	5534	3.31	-2.47	+0.46	0.00	+0.46	+6.42	...
J14551208-2232367	5420	2.85	-2.29	+0.25	+0.01	+0.26	+6.40	...

Table 3 *continued*

Table 3 (*continued*)

Star Name (2MASS)	T_{eff} (K)	$\log g$ (cgs)	[Fe/H]	[C/Fe]	$\Delta[\text{C}/\text{Fe}]^a$	$[\text{C}/\text{Fe}]_{\text{cor}}^b$	$A(\text{C})_{\text{cor}}^c$	$[\alpha/\text{Fe}]$
J14561699–2059219	5866	4.43	−2.14	+0.16	0.00	+0.16	+6.45	+0.13
J14561723–2202397	4996	1.82	−2.85	+0.76	+0.14	+0.90	+6.48	+0.39
J14563893+0459229	5618	3.37	−3.04	+0.48	0.00	+0.48	+5.87	+0.26
J14564274–2310276	6097	3.70	−2.95	+0.19
J19584551+0054253	5201	2.68	−3.39	−0.06	+0.01	−0.05	+4.99	+0.50
J19585614+0047295	5159	2.82	−2.24	+0.11	+0.01	+0.12	+6.31	+0.12
J19590382+0119513	5382	2.72	−2.25	−0.16	+0.01	−0.15	+6.03	+0.33
J19590543–0105589	6051	4.15	−1.49	+0.20	0.00	+0.20	+7.14	+0.40
J19593741+0058058	5355	2.84	−1.52	+0.21	+0.02	+0.23	+7.14	+0.47
J19595905+0113391	5477	2.54	−2.15	+0.50	+0.01	+0.51	+6.79	+0.30
J20002309+0035205	5634	4.67	−1.39	+0.03	0.00	+0.03	+7.07	+0.43
J20002987+0114169	5928	3.72	−0.87	+0.47	0.00	+0.47	+8.03	+0.61
J20003435–0021415	5595	3.31	−2.54	+0.81	0.00	+0.81	+6.70	+0.05
J20004079+0058381	5082	1.55	−2.36	−0.51	+0.45	−0.06	+6.01	+0.28
J20005889+0041324	6095	4.17	−1.42	+0.43	0.00	+0.43	+7.44	+0.54
J20010859+0056428	6116	3.93	−1.68	+0.16	0.00	+0.16	+6.91	+0.22
J20011680–0116257	6638	3.62	−0.10	+0.13	0.00	+0.13	+8.46	+0.23
J20012799–0023095	5442	2.45	−1.46	−0.30	+0.02	−0.28	+6.69	+0.19
J20013415–0058565	6152	2.93	−2.02	+0.83	+0.01	+0.84	+7.25	...
J20014181–0019202	6473	4.60	−2.84	+0.50
J20015964–0015327	5797	3.54	−1.31	+0.22	0.00	+0.22	+7.34	+0.17
J20021702–0005218	5370	2.09	−1.83	−0.09	+0.02	−0.07	+6.53	...
J20023118+0104018	5774	2.60	−1.25	+0.05	+0.02	+0.07	+7.25	+0.74
J20023405+0021449	6344	4.02	−1.47	+0.16	0.00	+0.16	+7.12	+0.20
J20035721–0116184	5785	3.26	−0.48	+0.28	+0.02	+0.30	+8.25	+0.44
J20051837+0001271	5736	4.12	−2.35	−0.16	0.00	−0.16	+5.92	−0.12
J20052052–0120319	5985	4.20	−1.79	+0.26	0.00	+0.26	+6.90	+0.49
J20053795+0017075	5314	1.95	−2.54	+0.96	+0.07	+1.03	+6.92	+0.39
J20054459–0055530	5356	3.13	−2.28	+0.54	+0.01	+0.55	+6.70	+0.33
J20061788–0013289	5401	3.12	−2.39	+0.46	+0.01	+0.47	+6.51	+0.05
J20073634+0057150	5244	2.85	−2.72	+0.61	+0.01	+0.62	+6.33	+0.40
J20075027–0020098	5463	3.13	−2.61	+0.66	+0.01	+0.67	+6.49	−0.11
J20085488+0057297	5823	3.02	−2.32	+0.65	+0.01	+0.66	+6.77	+0.32
J20090004+0105370	5520	3.64	−2.00	+0.36	0.00	+0.36	+6.79	+0.08
J20090076–0036452	6271	3.83	−2.63	+0.48
J20091617–0048192	5292	2.93	−2.81	+0.73	+0.01	+0.74	+6.36	+0.20
J20092146+0051002	5892	2.36	−2.48
J20095425–0007011	5188	2.45	−2.71	+0.22	+0.01	+0.23	+5.95	+0.21
J20101610–0014480	5357	3.56	−2.67	+0.57	0.00	+0.57	+6.33	+0.24
J20114178+0122331	5547	3.33	−3.05	+0.99	0.00	+0.99	+6.37	+0.32
J20121125–0005105	6269	4.00	−2.47	+0.69	0.00	+0.69	+6.65	+0.27
J20122497+0113575	5457	2.86	−2.18	+0.56	+0.01	+0.57	+6.82	+0.39
J20123247+0101043	5590	3.65	−2.50	+0.56	0.00	+0.56	+6.49	+0.48
J20133793+0116431	5213	2.64	−2.49	+0.37	+0.01	+0.38	+6.32	+0.22
J20141258+0056212	5515	3.37	−2.14	+0.30	0.00	+0.30	+6.59	+0.22
J20143504–0052087	4841	1.56	−2.35	+0.05	+0.44	+0.49	+6.57	+0.24
J20145209+0101365	5262	3.27	−2.25	+0.60	0.00	+0.60	+6.78	+0.20
J20154337+0030123	5342	2.87	−2.62	+0.37	+0.01	+0.38	+6.19	+0.27
J20160412–0056393	5503	4.58	−2.58	+0.12	0.00	+0.12	+5.97	...
J20185694+0118567	5609	4.38	−1.74	+0.03	0.00	+0.03	+6.72	+0.55
J20200678–0021468	5021	2.17	−2.96	+0.40	+0.01	+0.41	+5.88	+0.07
J20231520+0120002	5841	3.53	−1.66	+0.24	0.00	+0.24	+7.01	+0.36
J20232142–0000254	5490	2.41	−3.04	+1.84	+0.02	+1.86	+7.25	+0.55
J20244141+0020139	5450	2.94	−2.49	−0.19	+0.01	−0.18	+5.76	+0.31
J20251633–0113560	6610	4.34	−3.12
J20261334+0058212	5386	2.96	−2.49	+0.03	+0.01	+0.04	+5.98	+0.26
J20265350+0041583	5470	3.04	−2.51	+0.29	+0.01	+0.30	+6.22	+0.21
J20275057+0045295	5434	3.05	−2.71	+0.52	+0.01	+0.53	+6.25	+0.20
J20311940+0045509	6381	4.23	−2.34	+0.36	0.00	+0.36	+6.45	+0.29
J20321142+0102056	5354	3.40	−2.32	+0.33	0.00	+0.33	+6.44	+0.25
J20334782–0107490	6030	3.32	−2.28	+0.73	0.00	+0.73	+6.88	+0.70
J20343070+0027091	5636	3.49	−2.33	+0.44	0.00	+0.44	+6.54	+0.04
J20381130+0038211	5089	2.00	−3.51
J20422273+0048380	5416	2.85	−3.34	+0.78	+0.01	+0.79	+5.88	...
J20500458–0048444	5464	3.25	−2.91	+0.34	0.00	+0.34	+5.86	+0.08
J20514291+0104552	5630	2.49	−2.58	+0.84	+0.02	+0.86	+6.71	+0.13

Table 3 *continued*

Table 3 (*continued*)

Star Name (2MASS)	T_{eff} (K)	$\log g$ (cgs)	[Fe/H]	[C/Fe]	$\Delta[\text{C}/\text{Fe}]^a$	$[\text{C}/\text{Fe}]_{\text{cor}}^b$	$A(\text{C})_{\text{cor}}^c$	[α/Fe]
J20514829+0000230	5321	2.15	-3.66	+1.05	+0.01	+1.06	+5.83	...
J20531505-0016063	5622	3.81	-2.77	+1.14	0.00	+1.14	+6.80	+0.97
J20540726-0113274	4748	1.46	-3.83	+0.81	+0.42	+1.23	+5.83	+0.56
J20563226+0102264	5500	3.74	-3.43	+0.58	0.00	+0.58	+5.58	+0.80
J20574846-4356271	5300	2.76	-2.83	+0.53	+0.01	+0.54	+6.14	+0.29
J21025360-3721177	5264	2.87	-2.87	+0.53	+0.01	+0.54	+6.10	+0.23
J21025985-5014054	5133	2.46	-2.76	+0.62	+0.01	+0.63	+6.30	+0.09
J21030015-4641514	5172	2.85	-3.01	+0.76	+0.01	+0.77	+6.19	+0.32
J21040930-4708338	5300	2.50	-2.89	+1.05	+0.01	+1.06	+6.60	+0.59
J21041356-3019010	5621	3.31	-2.89	+0.63	0.00	+0.63	+6.17	+0.21
J21041365-3146396	5474	3.11	-2.81	-0.73	+0.01	-0.72	+4.90	+0.24
J21041794-4105082	5313	3.35	-3.66	+0.52	0.00	+0.52	+5.29	+0.54
J21042799-0049341	5056	3.18	-4.29	+0.67	0.00	+0.67	+4.81	+0.37
J21045538-5054052	5157	2.54	-2.74	+0.20	+0.01	+0.21	+5.90	+0.06
J21054026-2527599	5168	2.27	-3.20	+0.46	+0.01	+0.47	+5.70	+0.43
J21055882-4118416	5354	1.99	-2.76	+0.97
J21074117+0100513	5360	2.74	-3.38	+1.15	+0.01	+1.16	+6.21	+0.91
J21113775-2658131	5277	2.73	-3.51	+0.47	+0.01	+0.48	+5.40	+0.38
J21115655-3708366	5430	3.00	-2.26	+0.55	+0.01	+0.56	+6.73	-0.00
J21142351-2947278	5931	3.29	-2.77	+0.49	0.00	+0.49	+6.15	+0.08
J21152435-2635448	5522	2.99	-2.80	-0.42	+0.01	-0.41	+5.22	+0.69
J21162790-3504557	5002	2.76	-3.75	+0.78	+0.01	+0.79	+5.47	+0.35
J21213312+0002451	5925	3.84	+0.20	-0.32	0.00	-0.32	+8.31	-0.08
J21254198-0120151	5175	2.13	-3.06	+0.79	+0.01	+0.80	+6.17	+0.36
J21263701+0119228	4952	4.57	-0.67	-0.24	0.00	-0.24	+7.52	+1.06
J21304688+0046211	5440	2.93	-2.37	+0.19	+0.01	+0.20	+6.26	+0.20
J21341378-2932056	5689	3.34	-2.48	-0.25	0.00	-0.25	+5.70	+0.42
J21344068-0045499	4909	1.93	-3.19	+0.71	+0.02	+0.73	+5.97	+0.08
J21430119+0058067	5431	2.88	-2.82	+0.47	+0.01	+0.48	+6.09	+0.15
J21435071-2056106	6319	4.05	-0.90	+0.29	0.00	+0.29	+7.82	+0.28
J21510918+0004279	6251	3.73	-1.51	+0.35	0.00	+0.35	+7.27	+0.21
J21551357-0114578	5611	4.37	-3.41	+1.03	0.00	+1.03	+6.05	+1.05
J21562470-0233483	6309	3.65	-2.03	+0.53	0.00	+0.53	+6.93	-0.07
J21570410-0025558	5494	3.28	-2.52	+0.37	0.00	+0.37	+6.28	+0.17
J21590612+0029207	5476	3.26	-3.01	+0.72	0.00	+0.72	+6.14	+0.11
J21595072+0027368	5188	2.22	-3.37	+1.69	+0.01	+1.70	+6.76	+0.21
J22024068-0112054	5727	4.57	-3.23	+1.10	0.00	+1.10	+6.30	+1.18
J22093470+0047105	5388	3.39	-2.83	+0.12	0.00	+0.12	+5.72	+0.19
J22165605+0013206	5232	2.93	-3.09	+0.78	+0.01	+0.79	+6.13	+0.50
J22174445-0107091	5127	2.31	-2.56	+0.38	+0.01	+0.39	+6.26	-0.01
J22223335-2934216	5135	4.45	-0.62	-0.28	0.00	-0.28	+7.53	+0.33
J22245762-0059071	5283	4.72	-2.90	+0.18	0.00	+0.18	+5.71	+0.62
J22302534-0055095	5357	3.10	-3.14	+0.77	0.00	+0.77	+6.06	+0.25
J22390604-0102356	5233	2.86	-3.31	+0.66	+0.01	+0.67	+5.79	...
J22430733+0103384	5092	2.12	-2.34	+0.57	+0.02	+0.59	+6.68	-0.02
J22460189+0052078	5404	4.49	-3.19	+0.26	0.00	+0.26	+5.50	+0.58
J22481036+0006493	5993	4.77	-2.22	+0.19	0.00	+0.19	+6.40	+0.19
J23073186-0115408	5282	3.09	-3.00	+0.67	0.00	+0.67	+6.10	+0.48
J23131269-0036247	5280	3.63	-3.42	+0.13	0.00	+0.13	+5.14	+0.18
J23174221-0124338	5402	3.43	-2.58	+0.66	0.00	+0.66	+6.51	+0.09
J23233976-0048009	5001	1.90	-2.39	+0.21	+0.13	+0.34	+6.38	+0.18
J23243811-0115388	5276	2.71	-2.21	+0.16	+0.01	+0.17	+6.39	+0.35
J23271618+0008407	5156	2.58	-2.82	+0.40	+0.01	+0.41	+6.02	+0.49
J23274511+0014400	5551	3.78	-2.22	+0.47	0.00	+0.47	+6.68	+0.47
J23400902-4205187	5308	3.24	-2.60	-0.28	0.00	-0.28	+5.55	+0.12
J23414363-0122023	5523	2.64	-2.16	+0.56	+0.01	+0.57	+6.84	+0.45
J23433448+0042013	5797	2.97	-2.04	+0.35	+0.01	+0.36	+6.75	+0.09

^a Carbon correction from [Placco et al. \(2014\)](#).^b Corrected carbon-to-iron ratio.^c Corrected absolute carbon abundance.